Modelling cumulus convection over the eastern escarpment of South Africa

Z Dedekind

24277037

Thesis submitted for the degree *Magister Scientiae* in Geography and Environmental Management at the Potchefstroom Campus of the North-West University

Supervisor: R Burger

Co-supervisor: Dr FA Engelbrecht

October 2015

Table of Contents

Abstract

The complex and coupled physical processes taking place in the atmosphere, ocean and land surface are described in Global Circulation Models (GCMs). These models have become the main tools to simulate climate variability and project future climate change. GCMs have the potential to give physically reliable estimates of climate change at global, continental or regional scales, but their projections are currently of too course horizontal resolution to capture the smaller scale features of climate and climate change. This situation stems from the fact that GCM simulations, which are effectively three-dimensional simulations of the coupled atmosphere-ocean-land system, are computationally extremely expensive. Therefore, downscaling techniques are utilised to do perform simulations over preselected areas that are of sufficiently detailed to represent the climate features at the meso-scale. Dynamic regional climate models (RCMs), based on the same laws of physics as GCMs but applied at high resolution over areas of interest, have become the main tools to project regional climate change.

The research presented here utilises the Conformal-Cubic Atmospheric Model (CCAM), a variable-resolution global atmospheric model that can be applied in stretched-grid mode to function as a regional climate model. As is the case with RCMs, CCAM has the potential to improve climate simulations along rough topography and coastal areas when applied at high spatial resolution, whilst side-stepping the lateral boundary condition problems experienced by typical limited-area RCMs**.** CCAM has been developed by the Commonwealth Scientific and Industrial Research Organisation (CSIRO) in Australia**.** The objective in the study is to test capability of a regional climate model, CCAM, to realistically simulate cumulus convection at different spatial scales over regions with steep topography, such as the eastern escarpment of South Africa.

Since both GCMs and RCMs are known to have large biases and shortcomings in simulating rainfall over the steep eastern escarpment of southern Africa and in particular Lesotho, the paper ***"Model simulations of rainfall over southern Africa and its eastern escarpment"*** (Chapter 3) has a focus on verifying model performance over this region. In the paper the CCAM simulations include six 200 km resolution Atmospheric Model Intercomparison Project (AMIP) simulations that are forced with sea surface temperatures and one 50 km resolution National Centre for Environmental

Prediction (NCEP) reanalysis simulation that is forced with sea surface temperatures and synoptic scale atmospheric forcings. These simulations are verified against rain gauge data sets and satellite rainfall estimates. The results reveal that at these resolutions the model is capable of simulating the key synoptic-scale features of southern African rainfall patterns. However, rainfall totals are often drastically overestimated.

A key aspect of model performance is the representation of the diurnal cycle in convection. For the case of South Africa, the realistic representation of the complex patterns of rainfall over regions of steep topography is also of particular importance. At a larger spatial scale, the model also needs to be capable of representing the west-east rainfall gradient found over South Africa. The ability of CCAM to simulate the diurnal cycle in rainfall as well as the complex spatial patterns of rainfall over eastern South Africa is analysed in ***"High Resolution Rainfall Modelling over the Eastern Escarpment of South Africa"*** (Chapter 4). The simulations described in the paper have been performed at 8km resolutions in the horizontal and span a thirty-year long period. These are the highest resolution climate simulations obtained to date for the southern African region, and were obtained through the downscaling reanalysis data of the European Centre for Medium-range Weather Forecasting (ECMWF). The simulations provide a test of the robustness of the CCAM convective rainfall parameterisations when applied at high spatial resolution, in particular in representing the complex rainfall patterns of the eastern escarpment of South Africa.

Keywords: Dynamical Downscaling, Conformal-Cubic Atmospheric Model, Diurnal cycle, southern Africa, eastern escarpment, west-east rainfall gradient.

Acknowledgements

First and foremost I would like to thank my supervisor and colleague Dr. F.A. Engelbrecht (*Council for Scientific and Industrial Research, Pretoria*) for guiding me and for the support and the “unwritten” open door policy that you have and to my other supervisor R. Burger thanks for ideas and development of the Master’s degree (*North-West University, South Africa*).

A Special thanks to the Applied Centre for Climate and Earth System Studies (ACCESS) for the funding the research through the Master’s degree and for several training sessions that was also fully funded by you for my development.

I would also like to thank my colleagues, Willem, Mary-Jane and Koos, at the Council for Scientific and Industrial Research for the support, development opportunities and encouragement.

A special thanks to the Centre for High Performance Computing (CHPC) for supplying the computational resources for model setup and model simulations.

Preface

The work presented in the thesis, conducted by the author from 2012 to 2014, is original work and has never been published or previously submitted for any degree purposes. The author was personally involved in the development, research and the writing of the thesis and the journal articles.

The format and reference style in the thesis is in accordance with the specifications supplied by the North-West University in the Manual for Post-graduate Students. The articles in Chapters 3 and 4 retained the original work as described in the paper even though it was reformatted to the thesis style. That is, the thesis includes two manuscripts, of which Manuscript 1 is in the proses of being peer review by Water SA.

Manuscript 1 (Chapter 3):

Dedekind, Z, F.A. Engelbrecht and J. van der Merwe, 2014: Model simulations of rainfall over southern Africa and its eastern escarpment

All the authors gave permission that manuscript 1 to be submitted for degree purposes (see Addendums).

Manuscript 2 (Chapter 4):

Dedekind, Z and F.A. Engelbrecht, 2014: High Resolution Modelling over the Eastern Escarpment of South Africa

Glossary

ACCESS:	Applied Centre for Climate and Earth System Studies
AMIP:	Atmospheric Model Intercomparison Project
CCAM:	Conformal-Cubic Atmospheric Model
CGCM:	Coupled Global Circulation Model
CHPC:	Centre for High Performance Computing
COL:	Cut-Off Low
CORDEX:	Coordinated Regional Downscaling Experiment
CRCM5:	Canadian Regional Climate Model 5
CRU:	Climatic Research Unit
CSIRO:	Commonwealth Scientific and Industrial Research Organisation
DARLAM:	Division of Atmospheric Research Limited Area Model
DJF:	December-January-February
ENSO:	El Niño Southern Oscillation
ESA:	Eastern South Africa
GCM:	Global Circulation Model
GFDL:	Geophysical Fluid Dynamics Laboratory
IOH:	Indian Ocean High
IPCC:	Inter-governmental Panel on Climate Change
ITCZ:	Inter Tropical Convergence Zone
JJA:	June-July-August
KZN:	Kwa-Zulu Natal
LES:	Lesotho
NCEP:	National Centre for Environmental Prediction
NESA:	North-Eastern South Africa
NWP:	Numerical Weather Prediction
MCS:	Meso-scale Convective System
MCC:	Meso-scale Convective Complex
RCM:	Regional Climate Model
RMSE:	Root Mean Square Error
SAWS:	South African Weather Service
SD:	Standard Deviation
SRC:	Spearman Rank Correlation
SST:	Sea Surface Temperature
SWC:	South Western Cape

TRMM:	Tropical Rainfall Measuring Mission
TTT:	Tropical temperate trough
WRF:	Water Research and Forecasting

List of Tables and Figures

Tables:

Figures:

Chapter 1: Introduction and Literature Review

1.1 Introduction

The eastern escarpment of South Africa, consisting of the Drakensberg Mountain range, has attributes such as a significant meridional extent, high altitudes and steep topographic gradients, which all provide challenges to rainfall modelling. Rainfall over the eastern escarpment results from a variety of circulation patterns. Of key importance are the synoptic types that result in moist easterly winds being forced to rise against the mountain slopes, or that facilitate warm air from the mountainous region to rise in response to surface heating in an unstable environment. Rainfall over the eastern escarpment occurs not only in the form of orographically-induced thunderstorms and heat thunderstorms, but also as a result of, or in combination with synoptic-scale systems such as cut-off lows, tropical temperate troughs and cold fronts (Taljaard, 1986; Lyons, 1991; D'Abreton and Tyson, 1996). In order to realistically simulate rainfall patterns over the eastern escarpment, regional climate models (RCMs) therefore need to accurately describe the atmospheric dynamics of all the mentioned rainfall producing systems over the region. It is essential for the models to be integrated at sufficiently high spatial resolution to capture the complex interactions between steep topography, moisture-laden winds and atmospheric convection over the region (e.g. Engelbrecht *et al.,* 2002). Two key processes to represent in RCMs, towards the realistic simulation of moist convection, are the release of potential available energy and the destabilisation of the atmosphere to the state of convection (Cerlini *et al*., 2005). With the strong advance in super-computing technologies, which enable simulating the weather at high spatial resolutions, simulations resolving convection to some extent have become a reality (e.g. Engelbrecht *et al.*, 2007; Pearson *et al.,* 2014; Hohenegger *et al.,* 2015) – particularly for the cases of regional climate modelling and short-range numerical weather prediction. However, in the case of global climate modelling, it is plausible that model resolutions will remain well within the hydrostatic limit for at least a decade to come. That is, global circulation models (GCMs) are likely to be applied at relatively low spatial resolutions over the eastern escarpment in the foreseeable future. To gain insight into the effect that resolution has on rainfall simulations over the eastern escarpment of South Africa, simulations of 200 km resolution in the horizontal (typical of GCMs (IPCC, 2013)) are compared to simulations of 50km resolution (typical of RCMs (Nikulin *et al.*, 2012)). These simulations were analysed as part of Chapter 3 (manuscript 1: Model simulations of

rainfall over southern Africa and its eastern escarpment). At a resolution of 50km the hydrostatic approximation is still valid, and convection is simulated through the use of parameterisation schemes. Currently there are no examples where models have been applied beyond the hydrostatic limit, which is at resolutions of about 10 km in the horizontal or finer, over the eastern escarpment of South Africa. It is thought that at resolutions higher than 10km in the horizontal the nonhydrostatic dynamics, such as those occurring within thunderstorms or mountain waves can at least be partially resolved (Janjic *et al.*, 2001; Engelbrecht *et al*., 2007). Models can still be applied at these resolutions using the hydrostatic primitive equations and suitable parameterisations for the nonhydrostatic flow features (e.g. Ohfuchi *et al.*, 2005; Shen *et al.*, 2006). However, nonhydrostatic models that partially or fully resolve these dynamics should in principle provide superior simulations. The research described here provides the first example of nonhydrostatic simulations over a large part of South Africa – simulations have been performed at an 8 km resolution in the horizontal to explore potential benefits gained in simulation interaction of airflow with topography, and atmospheric convection, over the eastern escarpment region (from Chapter 4 (manuscript 2: High Resolution Modelling over the Eastern Escarpment of South Africa)). Also of interest, in the analysis, is the ability of the high-resolution simulations to realistically represent the diurnal cycle in rainfall over the eastern escarpment region. This Chapter proceeds to provide a brief overview of southern African climate, with an emphasis on weather systems bringing rainfall to the eastern escarpment region of South Africa. This is followed by a discussion of the status quo of regional climate modelling over the subcontinent and the eastern escarpment region. Finally, the objectives of the research are listed.

1.2 The climate of southern Africa

1.2.1 Orography of southern Africa

Steep gradients in orography are known to induce steep gradients in climate, and the realistic representation of these gradients in climate models require the use of detailed regional climate models (e.g. Giorgi and Mearns, 1991; McGregor, 1997; Engelbrecht *et al.* 2002). The orography of southern Africa exhibits some particularly steep gradients, which require careful consideration in the design of climate simulations over the region. The coastal plain is generally narrow, with an elevated escarpment (generally reaching altitudes of 1000 – 2000 m) separating the coastal regions from the interior plateau (Van der Beek *et al.*, 2002). The eastern escarpment of South Africa

and Lesotho (the Drakensberg Mountains) is particularly steep and high, with the eastern escarpment of Lesotho peaking at altitudes of more than 3000 m. The country has a pronounced upwelling system along its west coast, generally known as the Benguela current (Andrews and Hutchings, 1980), whilst the fast-flowing, narrow Agulhas current has a pronounced influence on the climate of the east coast (e.g. Rouault *et al.,* 2002).

1.2.2 Southern African Rainfall

The climate of southern Africa is highly variable and the region frequently experiences the impacts of severe droughts and floods (e.g. Tyson, 1986; Mason and Jury, 1997; Rouault and Richard, 2003; Reason *et al.*, 2005; Reason and Jagadheesha, 2005). The El Niño Southern Oscillation (ENSO) and regional sea surface temperatures (SST) are thought to be the most important driving factors for southern African climate variability (Nicholson and Kim, 1997; Reason and Mulenga, 1999; Washington and Preston, 2006). Seasonal rainfall patterns across the region are affected by the Intertropical Convergence Zone (ITCZ) that migrates from the north to the south as the South African summer (Desember-January-February, DJF) sets in (and vice versa when the South African winter sets in). The meridional movement of the ITCZ causes two rainfall maxima (in time) over tropical Africa whereas the largest part of southern Africa (Africa south of 10 °S) only experience one rainfall peak annually (e.g. Taljaard, 1986; Nikulin *et al*., 2012). The ITCZ moves far to the south during the South African summer as the Angola low and the Indian Ocean High induce the occurrence of tropical-temperate cloud bands over southern Africa. These cloud bands have a northwest to southeast alignment, with low-level flow of moisture around the Indian Ocean High acting as a primary source of moisture for convection and rainfall originating from these cloud bands (Taljaard 1986; D'Abreton and Tyson, 1995; Reason *et al*., 2006; Engelbrecht *et al.*, 2009; Hart *et al.*, 2010). Tropical-temperate cloud bands are estimated to be the leading rain-producing synoptic type system over South Africa and they represent an import mechanism of poleward transport of energy, water vapour and momentum (Harrison, 1984; Todd and Washington, 1999; Palmer *et al.,* 2004; Todd *et al.*, 2004). During the summer a prominent heat low is found over the interior of southern Africa aiding in rainfall, but the rainfall is suppressed by large scale subsidence in winter as the Southern Hemisphere high pressure system is situated over the region (Taljaard, 1986; Rouault *et al.*, 2013). The net result of easterly flow as the primary source of moisture for the southern African region, in combination with the

topographic forcing of rainfall by the eastern escarpment, results in the southern Africa region having a pronounced west-east gradient in rainfall. The western parts of South Africa are semi-arid or arid, with annual rainfall totals gradually increasing over the central interior, peaking over the east coast and the eastern escarpment where rainfall totals can exceed 1500mm per year (Nel and Sumner, 2006, Engelbrecht *et al.*, 2009; Jury, 2012). This west-east gradient in rainfall is slightly diminished over the southern parts of Botswana and Zimbabwe where a dry slot is present annually (e.g. Engelbrecht *et al.*, 2002; Engelbrecht *et al*., 2009).

1.2.3 Seasonality of rainfall producing systems over southern Africa

The South African winter (June-July-August, JJA) is a dry season for the largest part of southern Africa as high-pressure systems block most cold fronts from moving into the interior, whilst suppressing cloud formation over the interior through enhanced subsidence (e.g. Taljaard, 1986). However, cold fronts regularly make landfall over the southern tip of South Africa. As a result, the south-western Cape of South Africa receives the bulk of its rainfall in winter, whilst the Cape south coast to the east also receives winter rainfall. The prevailing pattern in summer is very different as this high-pressure belt is shifted southwards and the broad continental trough deepens at lower levels (Tyson and Preston-Whyte, 2000). When a tropical disturbance in the lower atmosphere is coupled with a mid-latitude trough, it leads to the formation of tropical temperate troughs (TTT) (Lyons, 1991) and these synoptic-scale systems are responsible for the bulk of southern Africa's rainfall (Palmer *et al.,* 2004; Todd *et al.*, 2004). TTTs mainly occur during the summer half-year (October-March) and are rooted in the south Indian Ocean convergence zone (Cook, 2000). An important mechanism for the development of these systems are the Botswana/Angola low and heat low over the Kalahari that develop during summer and enhances low-level moisture flux from the tropical south-eastern Atlantic (Hart *et al.,* 2012). Another system that brings widespread rainfall to southern Africa is the cut-off low (COL) that occurs mainly during the transition seasons of spring and autumn (Taljaard, 1986; D'Abreton and Tyson, 1996; Singleton and Reason, 2007). COLs are defined as cold-cored depressions that start out as a trough in the upper westerlies and deepen into a closed circulation extending to the surface (Tyson and Preston-Whyte, 2000). They are categorised as heavy rain and flood producing systems, especially over the central interior toward the south and east coast (Tyson, 1986). The eastern side of southern Africa is susceptible to tropical cyclone downpours even though these systems do not occur frequently

(Malherbe *et al.,* 2013). Annually about 3 tropical cyclones make landfall over Mozambique and/or Madagascar (Mavume *et al.*, 2009). In the event of such a system making landfall large amount of rainfall occur over southern Africa and specifically over the Limpopo River Basin (Malherbe *et al.,* 2013).

1.2.4 Rainfall over the eastern escarpment

Thunderstorms occur as a result of the complex interactions between cloud dynamics, cloud microphysical processes, mesoscale forcing (e.g. topographic forcing), diurnal heating and the synoptic-scale conditions. The convective substructures that are in the order of 1 to 50 km in horizontal scale are part of larger meso-scale convective systems that are typically hundreds of kilometres in horizontal dimension and have lifespans in the order of 10 hours (Houze *et al.,* 1989). Generally, the eastern escarpment north-east of Lesotho is responsible for producing a positive correlation between altitude and rainfall (Tyson *et al.*, 1976), although this relationship seems to break down at altitudes of 2100m (Nel and Sumner, 2006). The occurrence of the thunderstorms over the eastern interior is mostly later in the day from mid- to late afternoon over the continental interior with a night-time maximum in mountainous regions (Rouault *et al.*, 2013). Nel and Sumner (2006) showed that the total rainfall measured at Sani Pas and Sentinel, 40.1% and 30.8% respectively fall between 15h00 and 20h00. The diurnal cycle in rainfall is an expression of land surface response to solar radiation and is made more complex by a number of dynamical and physical processes (Rouault *et al.*, 2013). Larger amplitudes of the diurnal cycle are experienced by the land rather than the ocean. Over the eastern escarpment anabatic flows in valleys and highland areas may play a role in forcing the region's unique diurnal cycle (e.g. McGregor and Nieuwolt, 1998). The most prominent rainfall producing system that occurs over the eastern escarpment of South Africa and Lesotho in summer is the orographically-induced line thunderstorm (Tyson *et al.,* 1976). Once convective systems are present over the eastern escarpment, they can potentially trigger meso-scale convective vortices as a result of the changes in topography on the eastern escarpment (Blamey and Reason, 2009).

1.3 Modelling

1.3.1 A brief history of the application and development of atmospheric models in South Africa

The first South African Numerical Weather Prediction (NWP) model, a quasi-geostrophic barotropic model applied at the 500-hPa level in the southern hemisphere (Triegaardt, 1965a), was developed in the 1960s (Triegaardt, 1965b). A more complex model that consisted of 5 levels in the vertical, based on the hydrostatic primitive equations solved with a split-explicit method and which had nesting capabilities, was developed by the Council for Scientific and Industrial Research (CSIR) in the 1980s, and was further enhanced by a semi-Lagrangian advection scheme (Riphagen, 1984; Riphagen and Van Heerden, 1986). In South Africa atmospheric model development ceased in the 1980s. In continued international research in atmospheric modelling, the hydrostatic equations that made use of the hydrostatic approximation (assuming a balance of forces in the vertical, such that the product of density and gravitational acceleration is equal to the magnitude of the vertical pressure gradient) was replaced by the quasi-hydrostatic (White and Bromley, 1995) or fully elastic nonhydrostatic equations (Davies *et al.*, 2005). When applied at high spatial resolution, nonhydrostatic models can resolve the dynamics of small-scale and mesoscale circulations such as sea breeze and cumulus convection. In South Africa a number of hydrostatic and nonhydrostatic models developed by international institutions have been applied over the last two decades. The Division of Atmospheric Research Limited Area Model (DARLAM) and the Conformal-Cubic Atmospheric Model (CCAM) of the Commonwealth Scientific and Industrial Research Organisation (CSIRO) were applied for climate simulations over southern and tropical Africa at the University of Pretoria (Engelbrecht *et al*., 2002; Engelbrecht, 2005; Engelbrecht *et al.*, 2009). More recently CCAM has been applied at the CSIR across time-scales ranging from short-range weather prediction to seasonal forecasting to the projection of future climate change (e.g. Engelbrecht *et al.*, 2011; Landman *et al.*, 2012; Malherbe et al., 2013). These applications of CCAM have been at both hydrostatic and nonhydrostatic spatial resolutions. At the University of Cape Town the Mesoscale Community Level Model Version Five (MM5) and the Weather Forecasting and Research model (WRF), both developed in the United States, have similarly been applied for regional climate modelling (Tadross *et al.*, 2006) as well as the study of meso-scale weather systems at resolutions beyond the hydrostatic limit (Lennard *et al.*, 2014). The South African Weather Service also has a long history of the application of international models, mostly for purposes of NWP. Examples are the ETA model of the United States which was used in the 1990s for hydrostatic NWP and the Unified Model (UM) of the United Kingdom, which is currently applied at resolutions ranging from 15 km (Landman *et al.*,

2012) to about 4 km in the horizontal. The recent development of nonhydrostatic modelling capacity in South Africa may also be noted. A new nonhydrostatic atmospheric model with a dynamic kernel based on novel, split semi Langrangian formulation of a set of quasi-elastic equations in a terrain-following vertical coordinate based on the full pressure field, was developed at the University of Pretoria (Engelbrecht, 2006; Engelbrecht *et al.*, 2007). More recently a model capable of explicitly simulating moist convection was configured at the CSIR (Bopape *et al.*, 2013, 2014).

1.3.2 Seamless forecasting and multi-scale models

The advantage of using a nonhydrostatic model is that it can in principle be applied at spatial resolutions of 100-200 km in the horizontal, as is typical for global simulations, up to resolutions as high as 1km to simulate meso-scale flow (e.g. Davies *et al.*, 2005; Engelbrecht *et al.*, 2011). Also, the application of models that are normally used for the projection of future climate change to short-range weather forecasting and seasonal forecasting provides the opportunity to test the model's physical robustness on a regular basis. For example, NWP provides the opportunity to regularly test a model's capability to simulate the occurrence of convective rainfall, whilst seasonal forecasting provides a test for a model to simulate the teleconnections associated with the El Niño Southern Oscillation (ENSO) (Engelbrecht *et al.,* 2011) to models that can be applied to over a range of time and spatial scales. However, very few global models that are applied for the projection of future climate change and seasonal forecasting are also applied for high resolution short-range forecasting. In South Africa and over the southern African domain it is only CCAM that has been applied seamlessly across spatial and time scales (e.g. Engelbrecht *et al.*, 2011).

1.3.3 Regional climate models and their most recent application over Africa

1.3.3.1 Advantages of RCMs

Since GCMs are computationally expensive, RCMs provide a great alternative to GCMs to obtain very high resolution runs over areas of interest. For example, RCMs are currently routinely applied at 50 km resolution over Africa (e.g. Hewitson *et al.,* 2012; Kalognomou *et al.*, 2013; Kim *et al.*, 2014). Over smaller areas applications beyond the nonhydrostatic limit are feasible (e.g. Engelbrecht *et al.*, 2011; Nickless *et al.*, 2015). The relatively high resolution of RCMs provide these models with the opportunity to improve climate simulations along areas with complex topography and

along coastal regions (McGregor, 1997), compared to GCM simulations in which these features are poorly resolved. Most RCMs are forced with GCMs at their lateral boundaries, a methodology that is associated with a number of problems (e.g. McGregor, 1997; Giorgi and Bi, 2000). An advantage of variable resolution global models such as CCAM is that the stretched-grid approach avoids the traditional lateral boundary value problems. RCM has the ability improve climate simulations along areas with rough topography and along coastal regions (McGregor, 1997).

1.3.3.2 Simulating rainfall totals over eastern South Africa

Most of the individual RCMs used by Nikulin *et al.* (2012) show a significant overestimation in summer rainfall over the eastern escarpment of South Africa and Lesotho that describes the current challenges there are in resolving rainfall over mountainous regions like the Drakensberg (Nikulin *et al.* 2012; Pohl *et al.*, 2014). The challenge, however, in the individual RCMs arise from the large biases in the boundary condition datasets, producing large overestimations in rainfall over Madagascar even though these RCMs do improve the precipitation climate over Africa (Nikulin *et al.*, 2012). General overestimations of rainfall over eastern South Africa has also been reported in the modelling studies of Engelbrecht *et al.* (2002), Engelbrecht *et al.* (2009) and Engelbrecht *et al.* (2011).

1.3.3.3 Simulations of the diurnal cycle

Of particular interest with regards to model simulations over southern Africa is the representation of the diurnal cycle in convection and convective rainfall. Generally the simulation of the amplitude and phase of the diurnal cycle offers a good check for model parameterizations and for the representation of land-atmosphere feedbacks (Yang and Slingo, 2001 and Wang *et al.*, 2007). The verification of model simulations performed at hydrostatic resolutions has indeed revealed systematic errors over the summer rainfall region. In the simulations of Hernadez-Diaz *et al.* (2012), rainfall peaks too early in the day over the eastern parts of South Africa and Lesotho. The current inadequate simulations seem to be largely the result of the convection parameterisation schemes not realistically representing the convective cycle. In a study with a range of different RCMs applied over Africa, it was found that problems with the phase (timing) of precipitation most probably result from the formulation of the convective parameterizations used in models (Nikulin *et al.*, 2012). Tadross *et al.* (2006) also showed inconsistencies, with models either peaking rainfall too early or too late during the day in terms of convective rainfall.

Along the eastern escarpment of South Africa, the diurnal amplitude of surface moisture fluxes has been shown to be important for the diurnal cycle in rainfall as daytime surface latent heat fluxes increase steeply toward the east compared to the almost non-existent night time fluxes that exhibit little east-west gradient (Jury, 2012). Correctly simulating all the variables that contribute to the diurnal cycle is of utmost importance, because it influences rainfall on a variety of time scales such as monthly, seasonal, annual, intra-annual and inter-annual rainfall scales.

Pohl *et al.* (2014) set up an experiment to show how the nonhydrostatic weather research and forecasting (WRF) model simulates the diurnal and annual cycles over southern Africa using four alternative parameterization schemes for deep convection at a spatial resolution of roughly 55 km. That is, although the model is nonhydrostatic, these simulations were performed at resolutions where nonhydrostatic dynamics are not resolved. The timing of the simulated diurnal cycle is shifted to be 2-3 hours earlier against observations showing that rainfall peaks during the first half of the night over the inland regions. A trigger function for moisture convection, that is used with one of these convection schemes, the Kain-Fritch scheme, significantly reduced the rainfall biases associated with the other three convection schemes that are applied (Dai and Trenberth, 2004; Pohl *et al.*, 2014). Earlier applications of the Kain-Fritch scheme in WRF produced too unstable atmospheric conditions and too much moisture convergence over the southern African region (e.g. Ratna *et al.*, 2013).

1.3.3.4 Simulating weather systems over southern Africa

The realistic simulation of synoptic-scale weather patterns such as tropical cyclones and COLs are important. RCM simulations need to realistically represent the present-day rainfall patterns. Malherbe *et al.*, (2013) demonstrated that RCMs can simulate warm-cored closed lows realistically over the south western Indian Ocean, and also over the southern African continent after landfall. However, the track placement of the tropical cyclone-like vortices is systematically placed northwards of the ideal westward path seen in the observations. In general RCMs simulate closed-lows over the Mozambique Channel well, but closed-lows frequencies are overestimated especially over the Mozambique Channel during summer and over the central interior of South Africa (Engelbrecht *et al.*, 2012).

1.4 Simulations of inter-annual variability

An important measure of model performance (both GCMs and RCMs) is found in whether the model possesses the ability to capture the inter-annual variability in precipitation, especially the variability that is associated large scale modes such as ENSO. ENSO influences the rainfall variability over southern Africa as the region typically experiences anomalously dry weather during El Niño years and anomalously wet weather during La Niña years (e.g. Mason, 1995; Reason *et al.*, 2006; Landman and Beraki, 2012). The multi-model setup used by Landman and Beraki, (2012) distinguishes between above-normal and below-normal rainfall categories during ENSO years. Besides only capturing droughts during El Niño years and floods during La Niña years the multi-model possesses the skill in predicting wet El Niño and dry La Niña seasons (Landman and Beraki, 2012). However, earlier verification work does indicate that the predictability of the middle category, that includes half of the climatological data, is low (Landman *et al.*, 2012). RCMs have the highest summer prediction skill in the northwestern and central parts of southern Africa, but the northeastern parts of South Africa yield lower prediction skill that is most probably related to ENSO teleconnections biases within RCMs (Yuan *et al.*, 2014). This can likely be explained by the coarse resolution of models that are not able to resolve complex topography over the eastern escarpment (Garstang *et al.*, 1987; Yuan *et al.*, 2014).

1.5 Nonhydrostatic simulations in South Africa

Only a few studies where regional climate models have been applied beyond the hydrostatic limit (~ 10 km resolution in the horizontal, see Janjic and Gerrity, (2001) and Engelbrecht *et al.* (2007)) have been performed for the southern African region to date (e.g. Engelbrecht *et al.*, 2011). At the Council for Scientific and Industrial Research, the CCAM has been applied at resolutions of 1 km to simulate the transport of carbon dioxide over the Cape Peninsula (Nickless *et al.*, 2015). In these simulations, the domain sizes were relatively small, in the order of 150 x 150 km^2, and the simulations were nudged in 8 km resolution CCAM simulations performed over a larger area. The simulations performed spanned only a few years for each of these studies. The 8 km simulations were nudged within ERA reanalysis data. At both the CSIR and SAWS routine weather forecast systems also exist where numerical weather prediction models are applied at resolutions finer than 10 km. No study has to date, however, verified model simulations beyond the nonhydrostatic limit within the context of the

representation of convective rainfall over the region. It is thought that such simulations, that may partially resolve storm dynamics, may provide a substantial improvement over typical simulations performed at hydrostatic resolutions, where convection is parameterised.

1.6 Problem statement and purpose of this study

It is clear from subsection 1.1 to 1.5 that GCMs and RCMs are known to have shortcoming in simulating rainfall over steep topography. Large rainfall biases are often associated with steep topography over the eastern escarpment of southern Africa and in particular Lesotho. The aim of Chapter 3, ***"Model simulations of rainfall over southern Africa and its eastern escarpment"***, is to evaluate the performance of the variable-resolution atmospheric model CCAM in representing rainfall totals over southern and tropical Africa and in particular the eastern escarpment region of South Africa and Lesotho. This model is currently applied as a GCM and RCM at the Council for Scientific and Industrial Research (CSIR) in South Africa. The evaluations are therefore based on simulations where the model is applied at typical GCM resolutions, with alternative simulations exploring the performance of the model at higher RCM resolutions. Of particular interest is the model's ability to simulate rainfall totals, the seasonal cycle of rainfall and inter-annual variability.

The representation of the diurnal cycle in convection is another key aspect in model performance. The diurnal amplitude of surface moisture fluxes has been shown to be important for the diurnal cycle in rainfall over the eastern escarpment of South Africa. RCMs applied over Africa have shown to have precipitation phase (timing) problems most probably as a result from the formulation of the convective parameterizations used in models (Section 1.3.3.3). Nonhydrostatic models applied over resolutions where nonhydrostatic dynamics are not resolved trigger convection schemes too early causing models to simulate rainfall earlier in the day compared against observations over southern Africa. The aim of Chapter 4, ***"High Resolution Rainfall Modelling over the Eastern Escarpment of South Africa"***, is to evaluate the most extensive models simulation performed to date beyond the hydrostatic limit over eastern South Africa. The model simulations presented are downscaling's of ERA reanalysis data over the steep topography region of the eastern South Africa. The model simulations of a range of convective rainfall attributes, including the diurnal cycle, are verified against observations. Correctly simulating all the variables that contribute to the diurnal

cycle is of utmost importance, because it influences rainfall on a variety of time scales such as monthly, seasonal, annual, intra-annual and inter-annual rainfall scales.

1.7 Research Objectives

Given the background described above on the application of GCMs and RCMs over southern Africa, and known model biases, this study aims to model convective rainfall using a variable resolution global atmospheric model. The objectives include:

1) Verify the ability of the CCAM to simulate the synoptic-scale rainfall patterns over southern Africa (Chapter 3).
2) Evaluate the CCAM simulations of rainfall over complex orography (Chapter 3)
3) Use the CCAM to perform high resolution (8km) rainfall simulations over the eastern escarpment of South Africa (Chapter 4)
4) Evaluate the high resolution simulations over the eastern escarpment in terms of the spatial patterns of rainfall and the diurnal cycle in rainfall (Chapter 4)

Chapter 2: Data and Methods

2.1 CCAM

The dynamic regional climate model applied in this research is the CCAM of the Commonwealth Scientific and Industrial Research Organisation (CSIRO) in Australia (McGregor, 1996, 2005a, 2005b; McGregor and Dix, 2001; 2008). CCAM is a variable-resolution global atmospheric model that functions as a regional climate model when applied in stretched-grid mode. A semi-implicit semi-Lagrangian method is used to solve the either the hydrostatic primitive equations or the quasi-elastic equations cast in an σ-coordinate based on the full pressure field (e.g. Engelbrecht *et al.*, 2007). The GFDL parameterisations for long-wave and short-wave radiation and the stability-dependent boundary layer scheme and cumulus convection scheme are employed. A canopy scheme is included that has 6 soil temperature layers, 6 soil moisture layers and 3 snow layers. Sea-ice and bias-corrected SSTs of 6 Coupled Global Circulation Models (CGCMs) are used as lower-boundary forcing in CCAM quasi-uniform horizontal resolution simulations as the first step in the downscaling process to better capture present day trade winds and circulations (Thatcher and McGregor, 2011). These CGCMs include CSIRO Mk 3.5, GFDL2.1, GFDL2.0, HadCM2, ECHAM5 and Miroc-Medres from the AR4 of the Inter-governmental Panel on Climate Change (IPCC).

The CCAM simulations analysed in Journal Article 1 include; 6 Atmospheric Model Intercomparison Project (AMIP) (Gates, 1992) stretched-grid 24-hourly rainfall simulations (200km 1979-2005) performed by forcing the model with observed SSTs to investigate the influence that resolution has on the model's ability to correctly simulate the features of convection over the region, 1 National Centre for Enviromental Prediction (NCEP) stretched-grid 6-hourly simulations (50km from 1979-2012) performed by forcing the model with observed SSTs and synoptic scale atmospheric circulation.

The 8 km high resolution in the horizontal simulation in Journal Article 2 over Lesotho CCAM was applied in stretched-grid mode using a Schmidt transformation factor of 0.133. Each panel of the cube projected onto the sphere contained 160 x 160 grid points. The 8 km resolution simulations were nudged within ERA reanalysis, using a digital filter technique to preserve large-scale patterns of the ERA data (Thatcher and McGregor, 2009; 2010). The model simulations were performed for the period 1979-

2005. At its lower boundary, the model was forced with SSTs and sea-ice from the ERA reanalysis data.

2.2 Observed data

Rainfall station data from around Lesotho were selected based on completeness of the records. The rainfall stations acquired from the South African Weather Service (SAWS) were required to have more than 80 % of their entries to be complete (hourly and daily data, for the case of automatic stations (data record from 1993-2012) and manual stations (data record for 1979-2012). Additionally, extreme and missing value tests were performed using 14 daily rainfall stations and 5 separate hourly rainfall stations (Table 1 and Table 2). The hourly stations are used to create the 6-hourly datasets ranging from 02-08h, 08-14h, 14-20h and 20-02h. This insight into the diurnal cycle is used to evaluate the 6-hourly CCAM simulations, to see if the convection scheme used in CCAM is robust and can describe the diurnal rainfall cycle.

The spatial patterns and magnitude of the simulated monthly and seasonal rainfall totals were verified against rain gauge based data from the Climatic Research Unit (CRU) for the period 1979-2004 (New *et al.*, 1999) and against satellite sensor based data of the Tropical Rainfall Measuring Mission (TRMM) at a resolution of 0.5 degrees for the period 1998-2011 (Dinku *et al.*, 2007). The CRU and TRMM data sets will from now on be referred to as the observational data sets. The CCAM simulations were designed and carried out to fit the CRU dataset exactly so that no further interpolation methods was needed for comparison beyond the latitude, longitude and elevation interpolation using thin plate splines that is originally done to get the CRU data on a grid. The TRMM dataset that is captured using a sensor on board the satellite is, however, interpolated using a box-averaging function within the Grid Analysis and Display System from a resolution of 0.25 to 0.5 degrees for analysis against the CCAM simulations.

2.3 Simulation evaluation objectives

The model data and TRMM data are interpolated to the CRU TS3.1 0.5 degree resolution grid to facilitate quantitative inter-comparisons (the CRU data represents only land points). Bi-cubic interpolation was applied in the case of the model data, whilst the 2 dimensional box-averaging method within the Grid Analysis and Display System was used in the case of the TRMM data. For both the cases of the model and TRMM data this approach implies that some ocean points have been applied to obtain estimates of land-based precipitation for those CRU TS3.1 grid points close to the

coast line. A mask is fitted to all the fields so that analyses are carried out over land areas (used in manuscript 1 and 2). An ensemble-average is used for the 6 CCAM-AMIP members to evaluate the rainfall totals as well as the seasonal cycle in rainfall. The pattern-correlation, root mean square error (RMSE), standard deviation (SD) and bias are used to evaluate accuracy and average uncertainty (used in manuscript 1 and 2). The pattern correlation is calculated between the simulations and observed fields (Walsh and McGregor, 1995). It is a correlation of two spatial fields, x_i and o_i, applied in this paper to monthly, seasonal or annual rainfall averages, as i range from 1 to N, where N is the number of grid points in the model domain:

$$\rho = \frac{\sum(x_i - \bar{x})(o_i - \bar{o})}{\sqrt{(\sum(x_i - \bar{x})^2)(\sum(o_i - \bar{o})^2)}}$$

Here $\bar{x}$ and $\bar{o}$ are the domain averages of x_i and o_i. The root mean square error (RMSE) used here measures the accuracy between a specific forecasted variable, in this case rainfall, from the CCAM simulations and the same observed variable since it is scale dependent (Hyndman and Koehler, 2006). Another measurement, the standard deviation, for the CCAM and observed fields are calculated and is an estimate of average uncertainty of the rainfall. An important measure for a model performance is found in the ability of the model to capture the inter-annual variability. The Spearman rank correlation is applied for the inter-annual variability (time series data) from CCAM, on the premise that there are no tied ranks within the data, to test for a statistically significant correlation with the corresponding observations. This data is then also subjected to significance testing.

Station data, 6-hourly and daily, from the SAWS are used as one of the observational datasets as a direct measure of rainfall at a particular point on a monthly, seasonal and annual time-scale. This also aids as a benchmark test to see how the CRU and TRMM observational dataset compare to a specific rainfall station. The diurnal cycle is calculated and verified on a 6-hourly basis against the SAWS rainfall stations that measure hourly rainfall (used only in manuscript 2).

Chapter 3 (Journal Article): Model simulations of rainfall over southern Africa and its eastern escarpment

Authors:

Zane Dedekind

CSIR Natural Resources and the Environment – Climate Studies, Modelling and Environmental Health, Pretoria, 0001, South Africa

Francois A. Engelbrecht

CSIR Natural Resources and the Environment – Climate Studies, Modelling and Environmental Health, Pretoria, 0001, South Africa

Jacobus H. van der Merwe

CSIR Natural Resources and the Environment – Climate Studies, Modelling and Environmental Health, Pretoria, 0001, South Africa

Model simulations of rainfall over southern Africa and its eastern escarpment

Zane Dedekind[1], Francois A. Engelbrecht[1] and Jacobus Van der Merwe[1]
1. CSIR Natural Resources and the Environment – Climate Studies, Modelling and Environmental Health, Pretoria, 0001, South Africa

Abstract

Rainfall simulations over southern and tropical Africa in the form of low resolution Atmospheric Model Intercomparison Project (AMIP) simulations and higher resolution National Centre for Environmental Prediction (NCEP) reanalysis downscalings are presented and evaluated in this paper. The model used is the conformal-cubic atmospheric model (CCAM), a variable-resolution global atmospheric model. The simulations are evaluated with regards to rainfall totals, spatial distribution, seasonality and inter-annual variability. Since both Global Circulation Models (GCMs) and Regional Climate Models (RCMs) are known to have large biases and shortcomings in simulating rainfall over the steep eastern escarpment of southern Africa and in particular Lesotho, the paper has a focus on evaluating model performance over these regions. It is shown that in the reanalysis simulations the model realistically represents the seasonal cycle in rainfall. However, the AMIP simulations are prone to the model overestimating rainfall totals in spring. The spatial distribution of rainfall is simulated realistically; however rainfall totals are significantly overestimated over the escarpment areas of both southern Africa and East Africa. When nudged within the observed circulation patterns, the model is capable of realistically simulating inter-annual rainfall variability over the eastern parts of southern Africa.

Keywords: CCAM; Conformal-Cubic Atmospheric Model; inter-annual rainfall; model simulations; eastern escarpment

3.1 Introduction

Rainfall over southern and tropical Africa

Southern and tropical Africa (STA) are prone to the occurrence of droughts and floods (e.g. Mason and Joubert, 1997; Rouault and Richard, 2003; Lyon and DeWitt, 2012), which constitutes a highly variable climate. The driving mechanisms of this variability include the El Niño Southern Oscillation (ENSO) and regional sea surface temperatures (SSTs) (e.g. Reason and Mulenga, 1999; Landman and Beraki, 2010). STA are also marked by pronounced seasonality in rainfall. Tropical West Africa receives up to 7.5 mm/day during August, but for the November-April period yields are as low as 1mm/day. Over Central Africa two rainfall peaks occur, one during November (7.5 mm/day) and another during March (6 mm/day). East Africa's rainfall peaks during January at 6mm/day (Nikulin *et al*., 2012). The seasonality of rainfall in tropical Africa is driven by the meridional displacements of the Inter Tropical Convergence Zone (ITCZ). During the austral summer when the ITCZ is displaced to the south of the equator, north-easterly flow of low-level moisture takes placed around the Indian Ocean High (IOH) into southern Africa (here defined as Africa south of 15 ºS), forming a convergence zone in combination with the Angola Low (Reason *et al*., 2006). To this

region is referred to as the South Indian Convergence Zone, and it is associated with the formation of tropical-temperate cloud bands (Taljaard 1986; Walker and Lindesay, 1989; D'Abreton and Tyson, 1995; Todd *et al*., 2004, Hart *et al*., 2010). This results in southern Africa being largely a summer rainfall region, with the exception of the south-western Cape and the Cape south coast regions. Moreover, the southern African region exhibits a strong west to east rainfall gradient, especially in South Africa from the Northern Cape in the west to Lesotho in the east (Jury, 2012). Another key feature of the southern African rainfall climatology is the dry slot that extends zonally from southern Namibia over Botswana into the Limpopo river basin of Zimbabwe, South Africa and Mozambique (e.g. Engelbrecht *et al.*, 2002; Engelbrecht *et al*., 2009; fig. 3.1).

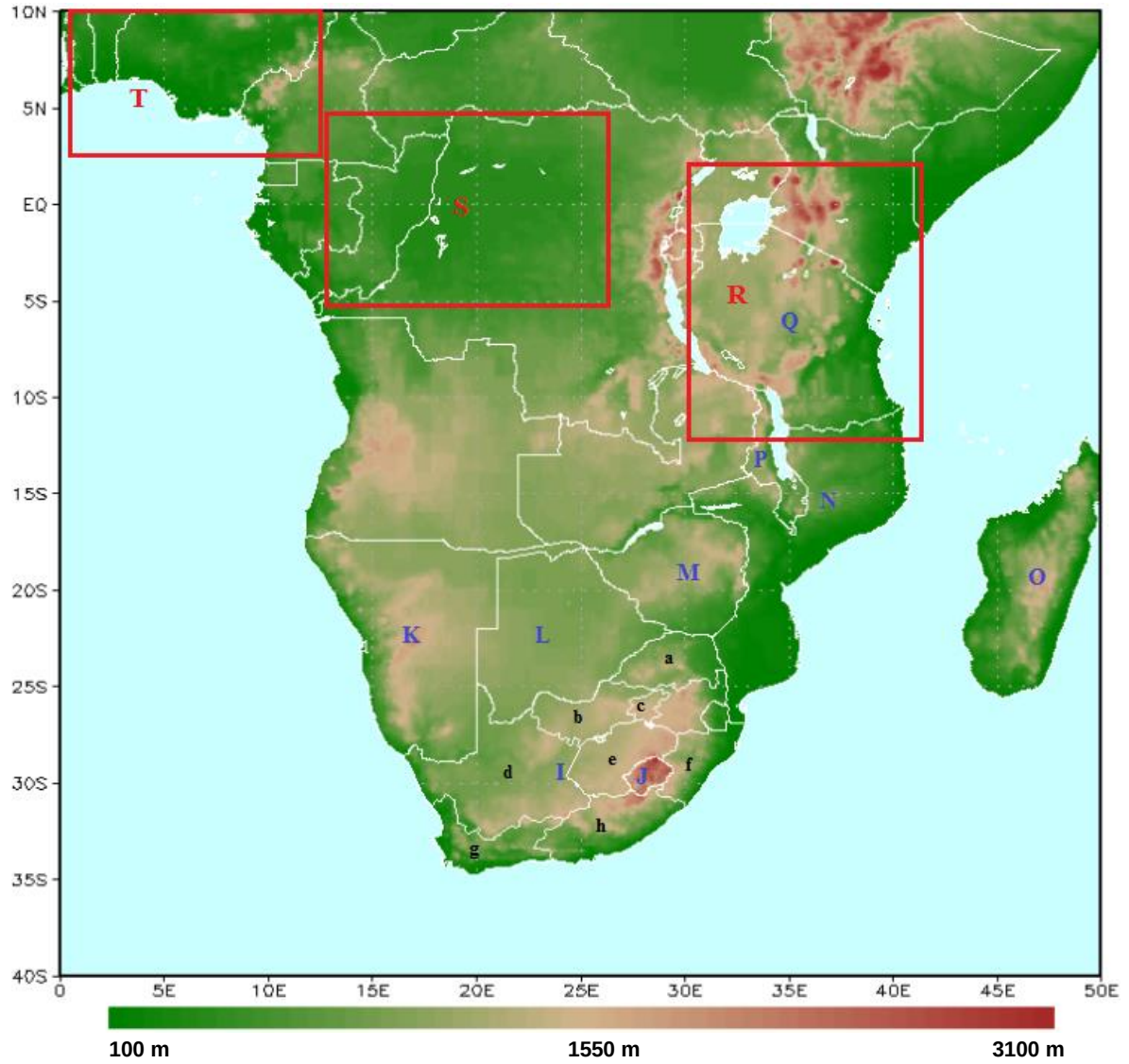

Figure 3.1. Topographical map showing provinces, countries and sub-regions. a) Limpopo, b) North West, c) Gauteng, d) Northern Cape, e) Free State, f) Kwa-Zulu Natal, g) Western Cape, h) Eastern Cape, I) South Africa, J) Lesotho, K) Namibia, L) Botswana, M) Zimbabwe, N) Mozambique, O) Madagascar, P) Malawi, Q) Tanzania, R) East Africa, S) Central Africa and T) West Africa

Rainfall-producing systems of southern Africa

During the austral winter months (June-August) the subtropical high-pressure belt is situated over southern Africa, enforcing large-scale subsidence and suppressing rainfall. This high-pressure belt has a blocking effect on cold fronts, preventing these systems from sweeping over the biggest part of the subcontinent. It is only the southern extremes of the south-western Cape and Cape south coast of South Africa where cold fronts regularly bring winter rainfall. The prevailing pattern in summer is very different as the high-pressure belt is shifted southward and a broad continental trough deepens in lower levels (Tyson and Preston-Whyte, 2000). It is during the summer half-year (October to March) that southern Africa receives the bulk of its rainfall. Most of the rain (about 80%) occurs from tropical-temperate troughs (TTTs) (Harrison, 1984), between spring and autumn. Another important rainfall-producing system is the cut-off low (COL). These systems also receive the bulk of their moisture from the tropics (D'Abreton and Tyson, 1996, Taljaard, 1986), even though they are defined as cold-core depressions of the upper westerlies that deepen to form closed circulations extending to the surface (Tyson and Preston-Whyte, 2000). COLs are often heavy rain and flood producing systems, especially over the central interior of South Africa and the south and east coast. They peak in frequency during the transition seasons of autumn and spring (Tyson, 1986; Mason and Jury, 1997). The reader is referred to Reason *et al*. (2006) and Hart *et al*. (2010) for more comprehensive discussions of the different synoptic types occurring over southern Africa, including maps showing their typical geographical locations (fig. 3.1).

Rainfall over the eastern Escarpment of South Africa and Lesotho

In southern Africa cumulus convection is the foremost rainfall producing process. The dynamics of severe storms are very complicated as it is controlled by the interactions of cloud microphysical processes, meso-scale forcing, diurnal heating and synoptic conditions. Southern Africa has a steep eastern escarpment that peaks in the Maluti Mountains of Lesotho, reaching altitudes of more than 3 km (Engelbrecht *et al*., 2002). The eastern escarpment region exhibits high annual rainfall totals and often sees the occurrence of deep convection. This in turn, is the result of complex meso-scale circulation patterns that occur over the region in response to synoptic-scale circulation forcing and topographic forcing.

The development of meso-scale convective complexes (MCCs) occurs under conditions of high moisture content and instability from the surface up to 700hPa, warm advection and strong surface convergence. MCCs, which is one of several types of meso-scale convective systems (MCSs), around the world are linked to large mountain ranges such as the Rockies

in the United States (e.g. Ashley *et al*., 2003) and the Andes in South America (e.g. Durkee and Mote, 2009). Over the eastern escarpment MCCs are often triggered by the topographical gradients, while already existing MCSs have the potential to create meso-scale convective vortices over the region (Laing and Fritsch, 1993a; Blamey and Reason, 2009).

At larger spatial scales the eastern escarpment of South Africa and Lesotho interacts with westerly wave propagation and its associated low-level flow. The latter typically consists of a ridging high-pressure system and south-easterly flow (Tyson and Preston-Whyte, 2000), which through topographic lift along the eastern escarpment and westerly wave dynamics lead to the strong ascent of moist air. This synoptic-scale pattern often leads to the development of strong convective storms along the escarpment (Garstang *et al*., 1987) and contributes to this region being the location of the rainfall maximum over southern Africa (de Coning *et al*., 1998). That is, the steep topographic gradients induce a steep west-east gradient in rainfall over eastern South Africa (Engelbrecht and Rautenbach, 2000).

Rainfall modelling

Simulating rainfall still proves to be a challenge for Global Circulation Models (GCMs) and Regional Climate Models (RCMs) especially with regards to the diurnal cycle in convective rainfall, due to biases in the intensity, timing and frequency of precipitation during the day (e.g. Shin *et al*., 2007; da Rocha *et al*., 2009; Jeong *et al*., 2010). An important reason for this situation is that models are generally still applied at relatively course resolutions where convection is not explicitly resolved. This forces models to use convective parameterisation schemes, that is, the statistical treatment of convection, which currently seems to be inadequate to represent the diurnal cycle and even convective rainfall totals (e.g. Liang *et al*., 2004).

Through the Coordinated Regional Downscaling Experiment (CORDEX) the simulations of African precipitation using 10 RCMs on various temporal resolutions have been analysed (Nikulin *et al*., 2012). Consistent with the findings described above, the realistic representation of the diurnal cycle of precipitation was identified as a major challenge for the RCMs applied over Africa. The currently inadequate simulations seem to be largely the result of the convection parameterisation schemes not realistically representing the convective cycle. However, the RCMs are capable to represent key aspects of the seasonal cycle in rainfall over Africa well (Nikulin *et al.,* 2012), although some models simulate the

onset of summer rainfall over southern Africa too early (Nikulin *et al*., 2012; Sylla *et al.*, 2010).

Zang *et al.* (2012) showed the differences between reanalyses data sets obtained using different convection schemes and different spatial resolutions over STA. These simulations yielded large overestimations of rainfall over the Great Rift Valley (compared to observations). In fact, models generally overestimate rainfall totals over East Africa and the eastern parts of southern Africa (e.g. Engelbrecht *et al*., 2009). All ten CORDEX RCMs of Nikulin *et al*. (2012) overestimate rainfall over the eastern escarpment region of southern Africa.

A noteworthy point from Zang *et al*. (2012) is that the model that had the highest horizontal resolution, (about 38 km), shows the best resemblance to the observed data. The higher resolution also aided in capturing land-based convergence zones over Lake Malawi and Madagascar, and the representation of the intra-annual rainfall cycle was also improved. Models applied at 50 km resolution over Africa show increased biases over Madagascar and countries between the equator and 10 °S during summer (Hernandez-Diaz *et al*., 2013). Thus, the simulation of a number of attributes of the rainfall climatology over southern Africa may be improved through increased model resolution.

The biases exhibited in representing rainfall totals over southern Africa are not limited to RCMs but also occur in numerical weather prediction models. Recent studies show that for the summer months (December to February – DJF) the Conformal Cubic Atmospheric Model (CCAM) have a modest but general wet bias when predicting rainfall over South Africa at short-range time scales. This wet bias is as large as 2 mm per day over the eastern Free State of South Africa (Engelbrecht *et al.*, 2011). The model generally is skilful in predicting the occurrence of rainfall events larger than 10 mm/day in magnitude, but skill is reduced or is absent over the eastern escarpment region of South Africa (Landman *et al*., 2012). GCMs also exhibit pronounced wet biased over the eastern escarpment region of southern Africa. Jury (2012) analysed the summer climatology of the zonal gradient in the vertical atmospheric humidity profile over the maize belt (25-30 °S) in South Africa and found a wet bias in most of the simulations over the eastern escarpment. In some models, this bias extends well to the west over the South African plateau. The causes for such overestimations may be found in the moist layer depth (that is affected by the amount of humid southwest Indian Ocean air drawn from the east), the rate of evapotranspiration over

the eastern escarpment and the deposition of vertical uplift in the continent-heated air (Jury, 2012).

In summary, the steep topography of the eastern escarpment is known for creating problems for climate models as rainfall totals are generally overestimated (Joubert *et al.*, 1999; Engelbrecht *et al*., 2002; Giorgi, 2005; Christensen *et al*., 2007; Liang *et al.*, 2008; Engelbrecht *et al*., 2009; Nikulin *et al*., 2012; Jury, 2012; Sylla *et al*., 2012; Hernandez-Diaz *et al*., 2013). The purpose of this paper is to evaluate the performance of the variable-resolution atmospheric model CCAM in representing rainfall totals over STA and in particular the eastern escarpment region of South Africa and Lesotho. This model is currently applied as a GCM and RCM at the Council for Scientific and Industrial Research (CSIR) in South Africa. Our evaluations are therefore based on simulations where the model is applied at typical GCM resolutions, with alternative simulations exploring the performance of the model at higher RCM resolutions. Of particular interest is the model's ability to simulate rainfall totals, the seasonal cycle of rainfall and inter-annual variability.

3.2 Data & Methods

The model applied in this research is the variable-resolution global atmospheric model CCAM, developed by the Commonwealth Scientific and Industrial Research Organisation (CSIRO) in Australia (MgGregor, 2005). CCAM may be applied at quasi-uniform horizontal resolution globally, to function as a GCM, or alternatively in stretched-grid mode as an RCM to provide high resolution over an area of interest (see Engelbrecht *et al.*, 2009). Variable-resolution global modelling avoids the problems caused by the reflections of atmospheric waves at the lateral boundaries of limited-area models (McGregor and Dix, 2001; Wang *et al*., 2004). When applied in stretched-grid mode, CCAM may be forced only at its lower boundary through the provision of sea-surface temperatures and sea-ice fields of a host model/analysis or, alternatively, may also be nudged within the three dimensional dynamic and thermodynamic forcing fields (Thatcher and McGregor, 2009; 2010).

CCAM It employs a semi-implicit semi-Langrangian method to solve the hydrostatic primitive equations (McGregor, 1996). It contains a comprehensive range of physical parameterisations, including the CSIRO mass-flux cumulus convection scheme (which includes downdrafts and the evaporation of rainfall) (McGregor, 2003), the GFDL parameterisation for long- and short-wave radiation (interactive cloud distributions diagnosed from liquid and ice-water content) (Schwarzkopf and Fels, 1991) and gravity wave drag (Rotstayn, 1997). The model is a highly flexible dynamic downscaling tool for obtaining

detailed simulations of present-day climate, and projected future climates, at the sub-continental and continental scale (e.g. Engelbrecht *et al.* 2009; Engelbrecht *et al.*, 2011; Engelbrecht and Engelbrecht, 2015). Two different types of CCAM simulations are analysed here. Firstly, an ensemble of 6 Atmospheric Model Intercomparison Project (AMIP) simulations was performed for the period 1979-2005. The AMIP experimental design (Gates, 1992) implies that the model is forced at its lower boundary with observed SSTs and sea-ice, but is free to develop its own atmospheric circulation patterns. In these simulations the model was applied at a quasi-uniform resolution of about 200 km in the horizontal. Each of the six ensemble members was initialised using different initial conditions obtained from reanalysis data, using a lagged-average forecasting approach. A main purpose of CCAM-AMIP simulations is to determine whether the model can realistically represent inter-annual variability in response to the prescribed lower-boundary forcing. The second experiment performed is a so-called reanalysis downscaling. The National Centre for Environmental Prediction (NCEP) reanalysis data was used to force CCAM simulations performed in stretched-grid mode. The modestly stretched grid provided a resolution of about 50 km over southern and tropical Africa, with the resolution decreasing to about 400 km in the far-field. The model was nudged towards the NCEP reanalysis fields every 6-hours, through the application of a digital filter using a 600 km length scale. The filter was applied from 900 hPa upwards.

The simulated monthly and seasonal rainfall totals, (rainfall totals and rainfall spatial patterns), intra-annual and inter-annual rainfall variability are compared against the station-based rainfall data of the Climatic Research Unit (CRU). The CRU TS3.1 data has a resolution of 0.5 degrees in latitude and longitude and span the period 1901-2012 (New *et al.*, 1999). The Tropical Rainfall Measuring Mission (TRMM) remotely sensed precipitation estimates, at a resolution of 0.25 degrees for the period 1998-2012, is also used (Dinku *et al.*, 2007). The CRU and TRMM will collectively be referred to as “observed data” in the remainder of this paper. It may be noted that no observational data set is a perfect representation of reality – the quality of the CRU data depends on the quality and density of station data. This is a particular concern in the Lesotho region where the density of station data is low. TRMM data is of higher spatial resolution, but the remote sensing of rainfall is also suffering from a range of errors, particularly in regions of steep topography. There is therefore value in assessing more than one observational data set towards estimating reality and to obtain some description, at least qualitatively, of the uncertainty in observing reality. Model biases are therefore calculated separately for each of the observational data sets in the evaluation section of this paper. The simulations are analysed as follows:

1) Only rainfall values over the land are used in the analyses.
2) The model data and TRMM data are interpolated to the CRU TS3.1 0.5 degree resolution grid to facilitate quantitative inter-comparisons (the CRU data represents only land points). Bi-cubic interpolation was applied in the case of the model data, whilst the 2 dimensional box-averaging method within the Grid Analysis and Display System was used in the case of the TRMM data. For both the cases of the model and TRMM data this approach implies that some ocean points have been applied to obtain estimates of land-based precipitation for those CRU TS3.1 grid points close to the coast line.
3) For the CCAM-AMIP simulations the ensemble-average of the six ensemble members is used in the evaluation of rainfall totals and the seasonal cycle in rainfall.
4) The pattern correlation is calculated between the simulations and observed fields (Walsh and McGregor, 1995). It is a correlation of two spatial fields, x_i and o_i, applied in this paper to monthly, seasonal or annual rainfall averages, as *i* ranges from 1 to N, where N is the number of grid points in the model domain:

$$\rho = \frac{\sum(x_i - \bar{x})(o_i - \bar{o})}{\sqrt{(\sum(x_i - \bar{x})^2)(\sum(o_i - \bar{o})^2)}} \quad (1)$$

   Here $\bar{x}$ and $\bar{o}$ are the domain averages of x_i and o_i.
5) The Root Mean Square Error (RMSE) is a measure of the accuracy between a specific forecasted variable from a model and the same observed variable since it is scale dependent (Hyndman and Koehler, 2006).
6) The Standard deviation (SD) is calculated as the measurements for the simulated and observed fields and is an estimate of average uncertainty of those measured values.
7) The Spearman rank correlation (SRC) is applied in the research to determine whether model simulation of inter-annual variability (time series data) has a statistically significant correlation with the corresponding observations. The SRC is calculated on the premise that there are no tied ranks within the data and is then subjected to significance testing.

With the CCAM-AMIP simulations only available for the period 1979-2005, the evaluation of both the CCAM-AMIP simulations and the CCAM-NCEP downscaling are performed for this period. The TRMM data is available only from 1998 onwards, and as a result, model evaluation data against TRMM data is confined to the period 1998-2005.

3.3 Results and Discussion

Annual rainfall totals

The CCAM simulated annual rainfall totals for both the CCAM-AMIP simulations and CCAM-NCEP downscaling (figs. 3.3a and 3.3b) realistically represent the observed synoptic-scale rainfall features of STA. These include the dry slot (dry conditions in a zonal band) located over Botswana stretching to the Limpopo River basin of South Africa and Zimbabwe, the relatively high rainfall over the tropics that occur in association with the ITCZ (extending from Angola over Zambia into Mozambique) and the west-east rainfall gradient over South Africa. A pronounced rainfall maximum is evident over the Great Rift Valley in both the CCAM-AMIP and CCAM-NCEP simulations, in relation to the complex topography found in this region (e.g. Zhang *et al*., 2012). This feature is present in the TRMM observations (fig. 3.3d), but not in the CRU data (fig. 3.3e). One shortcoming of the CRU data is that rainfall patterns may be misrepresented in areas with a low density of weather station data. The higher resolution CCAM-NCEP downscaling have a higher pattern correlation with both the CRU and TRMM observed data sets, compared to the CCAM-AMIP simulations. This can probably be attributed to the higher resolution of the CCAM-NCEP downscaling, which leads to a more realistic representation of complex patterns of topography across the continent. A wet bias is present in the simulations for the biggest part of southern Africa, for both the CCAM-AMIP and CCAM-NCEP simulations (figs. 3.3e and 3.3f). This wet bias is the biggest in amplitude over the eastern escarpment region of South Africa, and exceeds 400 mm in some locations. The magnitude of the overall negative bias is largest for the CCAM downscaling of NCEP reanalysis, compared to the CCAM-AMIP simulations. The SD portrayed in the CRU (603 mm) and TRMM (338 mm) has two distinct differences in the climate variability over the whole domain. In both the simulation setups the model climate is less variable than CRU and more variable than TRMM with CCAM-NCEP having the highest variable and the driest climate.

Seasonal rainfall totals

The meridional movement of the ITCZ is a feature that is well represented in the CCAM-AMIP and CCAM-NCEP simulations. The ITCZ is displaced to its most southerly location during DJF, reaching about 20 °S (figs. 3.3c and 3.3d). It is during this time of the year that southern Africa receives the bulk of its rainfall from tropical-temperate cloud bands. Many of the other regional features of observed DJF rainfall are captured in the simulations, such as the dry slot extending eastward at 20 °S from eastern Botswana to Limpopo and southern Zimbabwe. Zimbabwe has very high spatial summer rainfall variability, with totals exceeding 400 mm in the north and 160 mm in south (fig. 3.4). Both the CCAM-AMIP and CCAM-NCEP

simulations capture this south-north gradient rainfall, but underestimate the ITCZ-induced rainfall over northern Zimbabwe.

The area of high summer rainfall over the eastern escarpment is captured in the model simulations. However, rainfall totals are overestimated, particularly so in the higher resolution CCAM-NCEP simulation. Apart from the wet bias over the Lesotho the simulations have a high spatial correlation to the observations (higher than for the annual rainfall totals). Rainfall is underestimated in general across the domain as is evident from the overall negative biases of the simulations (figs. 3.4e to 3.4h). The CCAM-NCEP downscaling exhibits a large dry bias over East Africa, which is a recurring shortcoming, also for the other seasons. These reanalysis simulation for DJF has a less variable climate than the observations and is also the driest that is mainly due to the tropics not being as wet as the

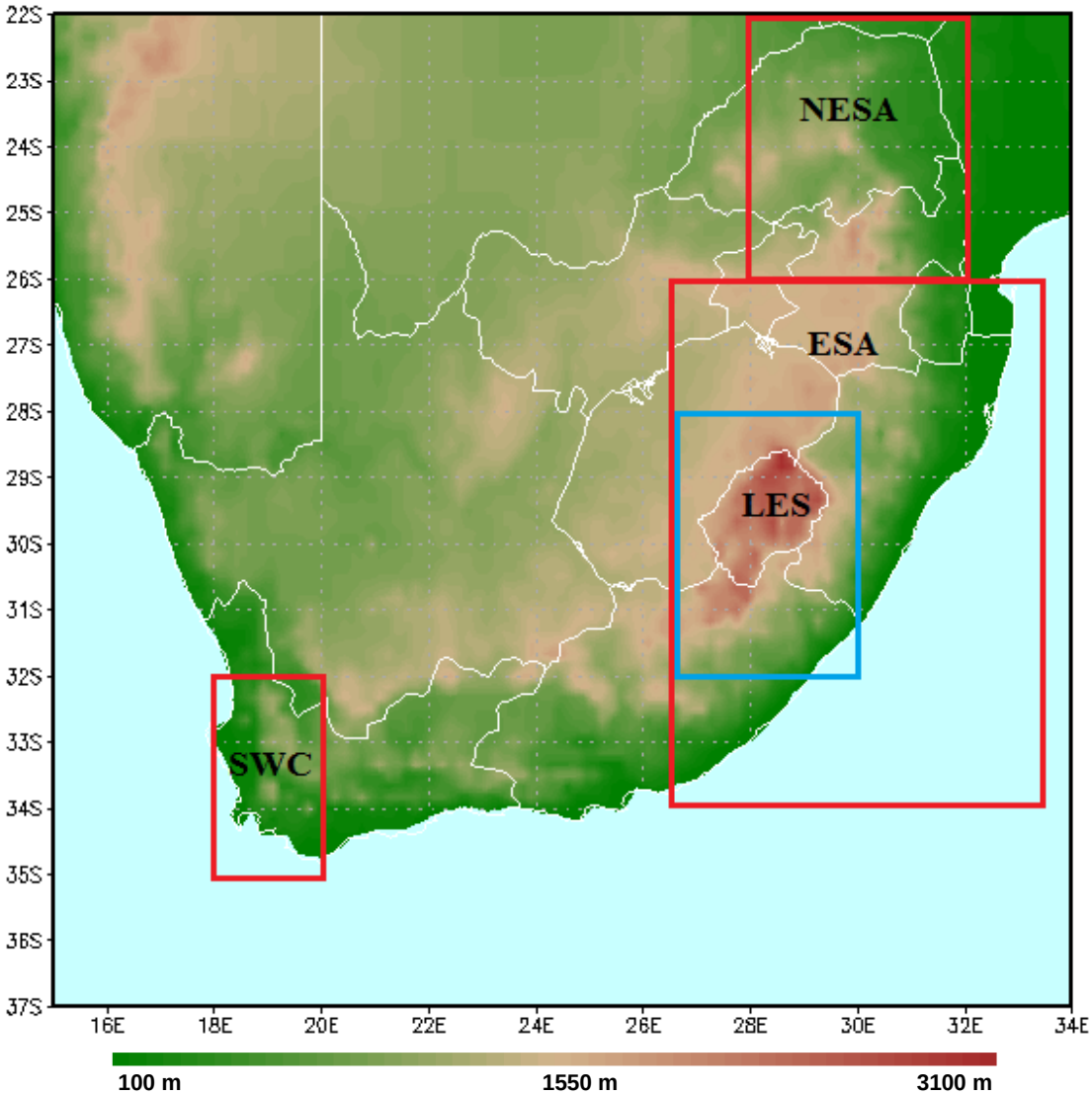

Figure 3.2. Locations of sub-regions in southern Africa. It is the South Western Cape (SWC), Lesotho (LES), Eastern South Africa (ESA) and North-Eastern South Africa (NESA). Ocean-areas are masked out

CCAM-AMIP or the observations.

Winter (JJA) rainfall is strongly controlled by the strengthening of the sub-tropical high pressure belt in the lower and mid-levels over southern Africa. This circulation change is associated with sinking air and supressed rainfall over the region. Simultaneously, the ITCZ shifts to Africa north of the equator. Rainfall over southern Africa during this season results mostly from cold fronts and cut-off lows that move in over the subcontinent from the south (figs. 3.5c and 3.5d). Both the CCAM-AMIP and CCAM-NCEP simulations underestimate winter rainfall over the Cape coast region, with totals represented somewhat more realistically in the higher resolution reanalysis simulations (figs. 3.5a and 3.5b). However, over the eastern parts of the Free State a large wet bias is present in the CCAM-NCEP simulations. One of the reasons for the extreme dry bias over the south-western Cape (SWC, fig. 3.2) in the CCAM-AMIP simulations is that the regional topographic features are very smooth at 200 km horizontal resolution, implying that the interaction between low level flow and steep topography can't be realistically represented.

Monthly rainfall totals

The November rainfall patterns, including the zonal rain band associated with the ITCZ are represented well in both the CCAM-AMIP and reanalysis simulations. There are a number of areas where the model displays noticeable biases in rainfall totals, with overestimations over the complex topography regions of the Great Rift Valley and the eastern escarpment of South Africa and Lesotho in particular. These biases are also present in the December and January rainfall simulations (figs. 3.6a, 3.6b, 3.7a, 3.7b, 3.8a, 3.8b). The CCAM-AMIP simulations are indicative of too strong tropical-temperate linkages during November that contributes to the large RMSE and weaker pattern correlation. Rainfall totals in excess of 100 mm are simulated across the southern African interior, whereas the observed rainfalls are less than 60 mm. Rainfall totals over the eastern escarpment of South Africa are also drastically overestimated compared to the CRU and TRMM observations. These overestimations are also evident from the area-averaged intra-annual rainfall cycles simulated for Lesotho (LES), eastern South Africa (ESA) and north-eastern South Africa (NESA) (figs. 3.2, 3.9a, 3.9b and 3.9c). Over much of the summer rainfall region the model incorrectly simulates the peak of the summer rain to occur in November rather than January. The relatively drier Western and Eastern Cape coastline regions are captured well in the CCAM-AMIP and reanalysis data. However, the inland areas over the Western Cape and the biggest part of Namibia are drier than what the simulations are indicating. The CCAM-NCEP has a more variable climate (for November, December and January) that correlates well with

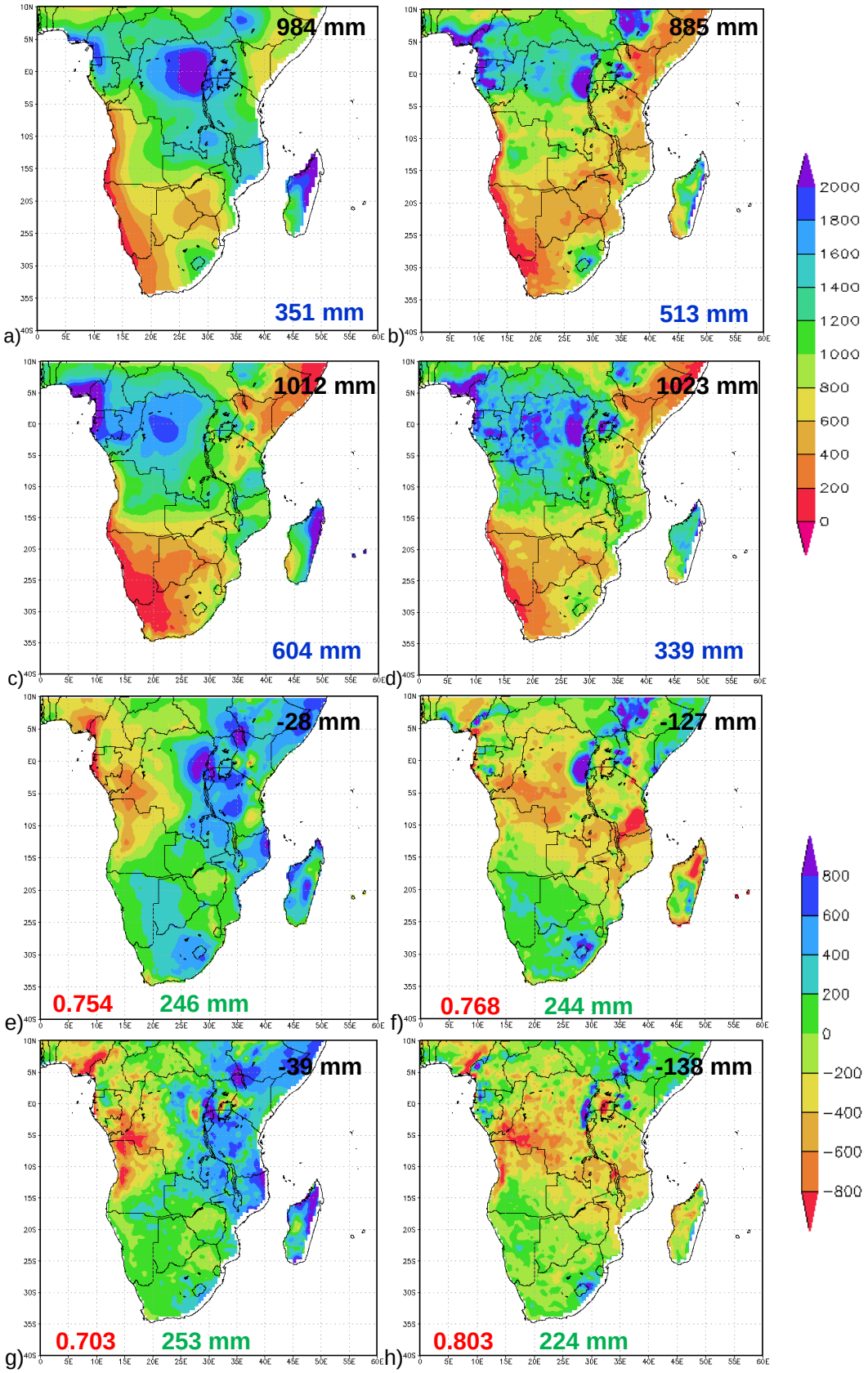

Figure 3.3. Annual rainfall totals (mm) for a) CCAM-AMIP (1979-2005), b) CCAM-NCEP (1979-2005), c) CRU (1979-2005) and d) TRMM (1998-2012). Bias (mm) for e) AMIP-CRU (1979-2005), f) NCEP-CRU (1979-2005), g) AMIP-TRMM (1998-2005) and h) NCEP-TRMM (1998-2005). Also shown is the average rainfall per grid point (a-d, top right), bias (e-h, top right), pattern correlation (bottom left), RMSE (bottom middle) and STDEV (bottom right)

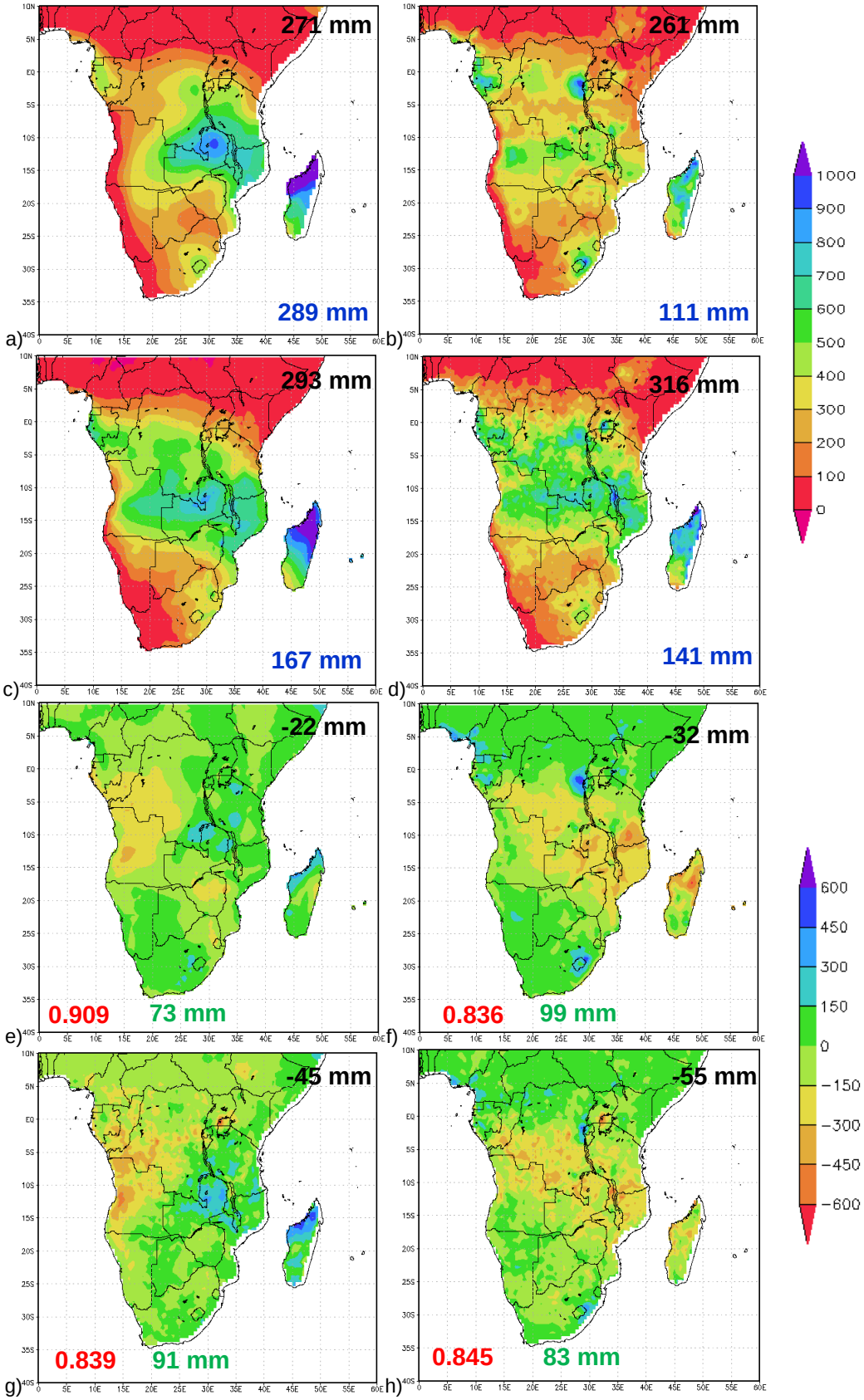

Figure 3.4. December-January-February (DJF) rainfall totals (mm) for a) CCAM-AMIP (1979-2005), b) CCAM-NCEP (1979-2005), c) CRU (1979-2005) and d) TRMM (1998-2012). Bias (mm) for e) AMIP-CRU (1979-2005), f) NCEP-CRU (1979-2005), g) AMIP-TRMM (1998-2005) and h) NCEP-TRMM (1998-2005). Also shown is the average rainfall per grid point (a-d, top right), bias (e-h, top right), pattern correlation (bottom left), RMSE (bottom middle) and STDEV (bottom right)

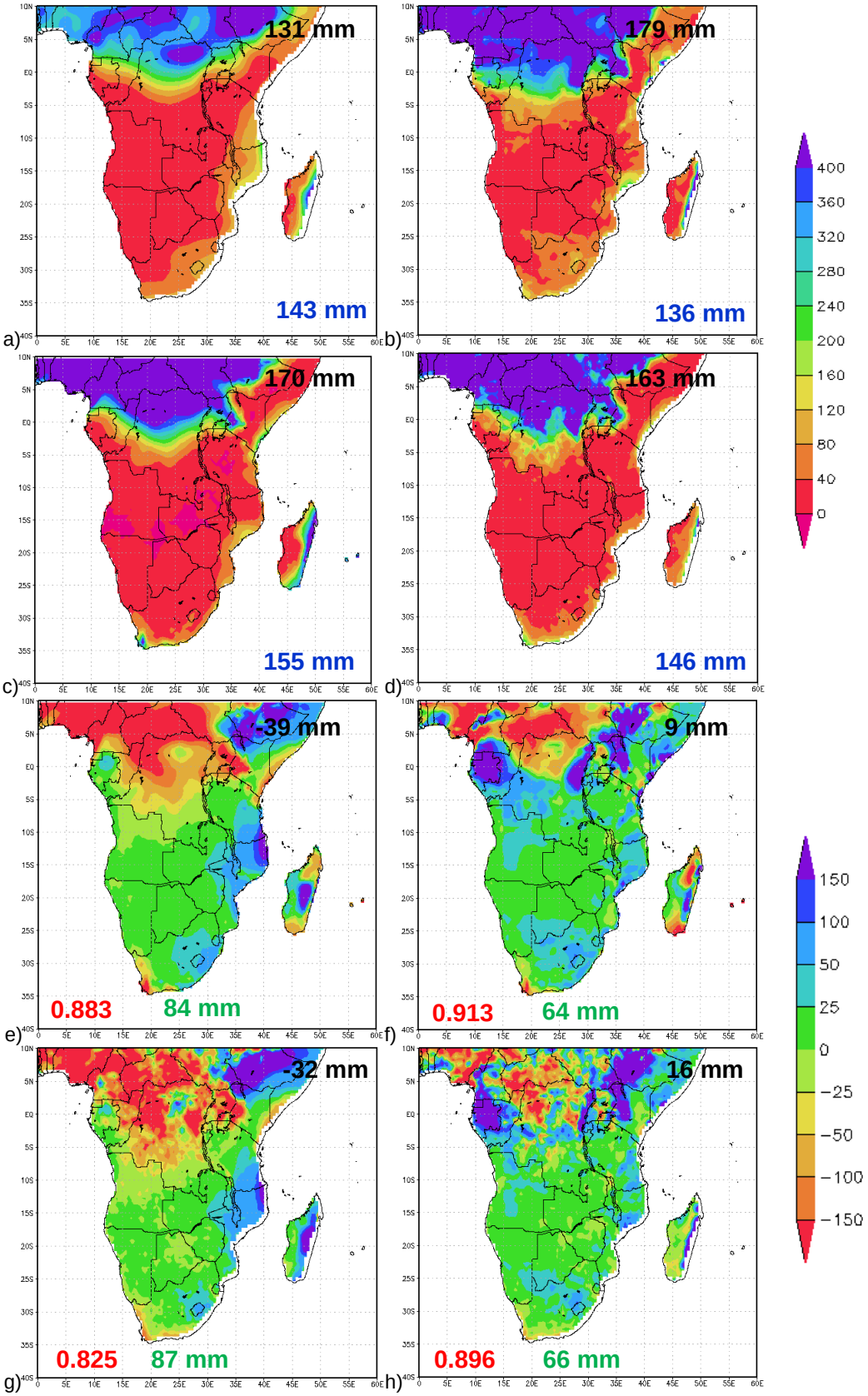

Figure 3.5. June-July-August (JJA) rainfall totals (mm) for a) CCAM-AMIP (1979-2005), b) CCAM-NCEP (1979-2005), c) CRU (1979-2005) and d) TRMM (1998-2012). Bias (mm) for e) AMIP-CRU (1979-2005), f) NCEP-CRU (1979-2005), g) AMIP-TRMM (1998-2005) and h) NCEP-TRMM (1998-2005). Also shown is the average rainfall per grid point (a-d, top right), bias (e-h, top right), pattern correlation (bottom left), RMSE (bottom middle) and STDEV (bottom right)

observations especially during January, but the steeper topographic regions such as the eastern escarpment yields very large overestimations. During December the ITCZ is displaced more towards the south with a general increase in rainfall over much of southern Africa, especially over the eastern parts of southern Africa and Madagascar (figs. 3.7c and 3.7d). For this month the CCAM-AMIP runs have a stronger pattern correlation than the CCAM-NCEP simulations. The observed rainfall band linking southern Africa and the tropics, indicative of the occurrence of TTT induced rainfall, is present in the model simulations, albeit overestimated in intensity. Rainfall is underestimated by the reanalysis run over Mozambique. The same spatial features found in November are again seen in December regarding the severe over estimation of rainfall over complex topography (figs. 3.7a and 3.7b). According to the CRU observations there is a slight increase in rainfall over the eastern escarpment of South Africa compared to November. TRMM rainfall shows a larger increase of about 40 mm in Lesotho and to the north east of Lesotho in Kwazulu-Natal from November to December. This increase is overestimated in the model simulations - a steady increase of 20-40 mm is found over the Gauteng, North-West and eastern Free State from the previous month in both the CCAM-AMIP and CCAM-NCEP simulations. The over estimation of rainfall for the western part of South Africa and Namibia is still present in the December simulations. These increases in rainfall from November to December show up in the regions for LES, ESA and NESA, where the reanalysis simulations are generally producing smaller pattern correlations than the CCAM-AMIP simulations (figs. 3.9a, 3.9b and 3.9c).

During January the rainfall totals associated with the ITCZ are higher than earlier in the season, reaching values of 200 mm. The band is narrower than for the November and December months (fig. 3.8c). This pattern and change is well represented in the CCAM-AMIP simulations. The CCAM-NCEP runs capture the increase in ITCZ related rainfall totals more realistically, and exhibits a high pattern correlation with observations (figs. 3.8a and 3.8b). There is an increase in rainfall over the biggest part of South Africa indicating that January is the month in which LES, ESA and NESA gets the bulk of their rain annually (figs. 3.9a, 3.9b and 3.9c). This is in direct contrast to the simulations that peaks rainfall too early. In the model simulations rainfall totals are incorrectly simulated to decrease relative to December, possibly in response to a weakening in the simulated link between the tropics and mid-latitudes (fig. 8a). This simulation is also a feature of the CCAM reanalysis runs, although to a lesser extent (fig. 3.8b).

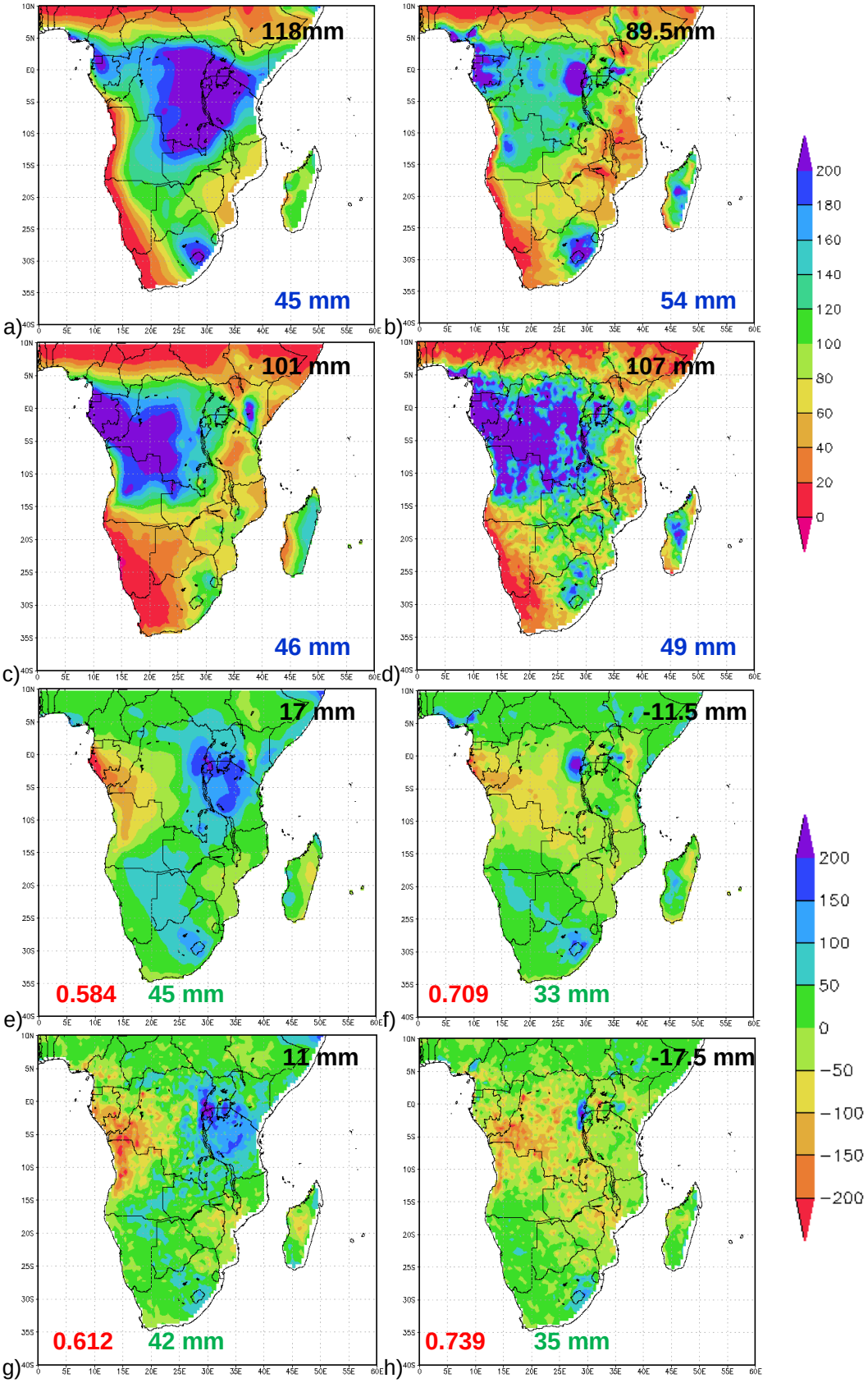

Figure 3.6. November rainfall totals (mm) for a) CCAM-AMIP (1979-2005), b) CCAM-NCEP (1979-2005), c) CRU (1979-2005) and d) TRMM (1998-2012). Bias (mm) for e) AMIP-CRU (1979-2005), f) NCEP-CRU (1979-2005), g) AMIP-TRMM (1998-2005) and h) NCEP-TRMM (1998-2005). Also shown is the average rainfall per grid point (a-d, top right), bias (e-h, top right), pattern correlation (bottom left), RMSE (bottom middle) and STDEV (bottom right)

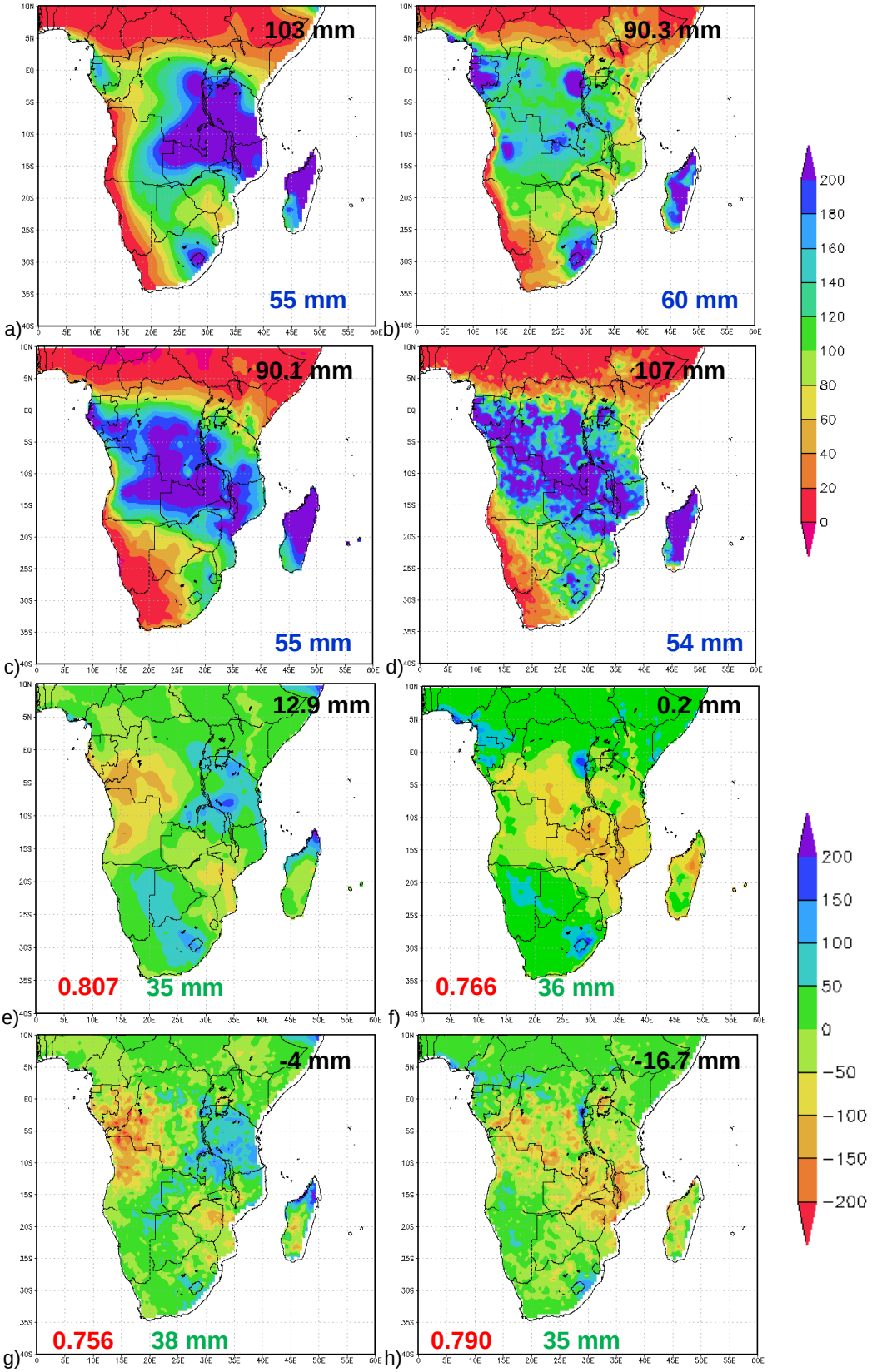

Figure 3.7. December rainfall totals (mm) for a) CCAM-AMIP (1979-2005), b) CCAM-NCEP (1979-2005), c) CRU (1979-2005) and d) TRMM (1998-2012). Bias (mm) for e) AMIP-CRU (1979-2005), f) NCEP-CRU (1979-2005), g) AMIP-TRMM (1998-2005) and h) NCEP-TRMM (1998-2005). Also shown is the average rainfall per grid point (a-d, top right), bias (e-h, top right), pattern correlation (bottom left), RMSE (bottom middle) and STDEV (bottom right)

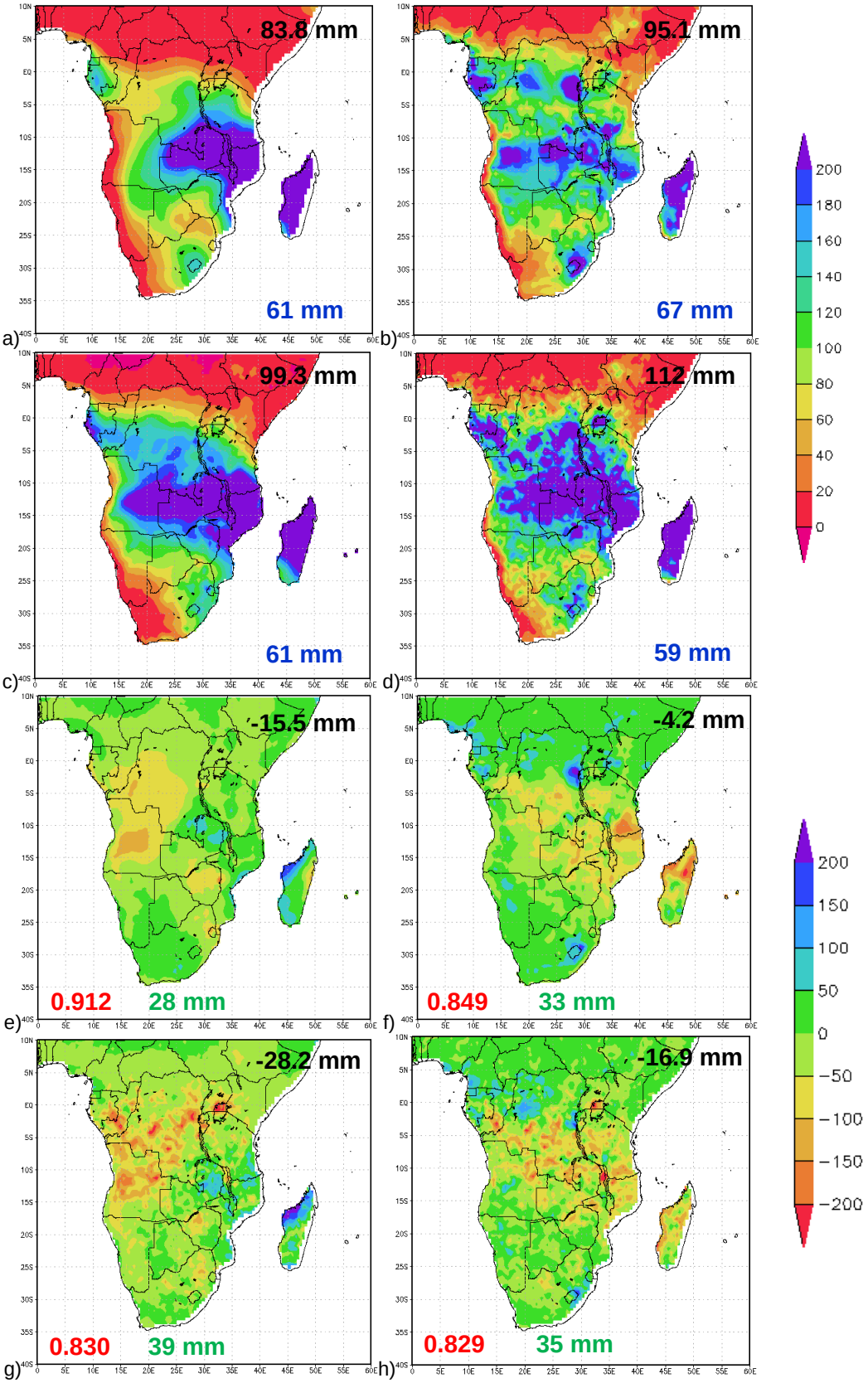

Figure 3.8. January rainfall totals (mm) for a CCAM-AMIP (1979-2005), b) CCAM-NCEP (1979-2005), c) CRU (1979-2005) and d) TRMM (1998-2012). Bias (mm) for e) AMIP-CRU (1979-2005), f) NCEP-CRU (1979-2005), g) AMIP-TRMM (1998-2005) and h) NCEP-TRMM (1998-2005). Also shown is the average rainfall per grid point (a-d, top right), bias (e-h, top right), pattern correlation (bottom left), RMSE (bottom middle) and STDEV (bottom right)

Intra-annual rainfall

A large positive bias in simulating annual, seasonal and monthly rainfall totals have been identified in both the CCAM-AMIP simulations and the CCAM-NCEP downscalings. Moreover, the ensemble of CORDEX RCMs evaluated to date over southern Africa all exhibit rainfall overestimations over this region (Nikulin *et al.*, 2012). For this reason the focus for the following section is the LES, ESA and NESA regions of eastern southern Africa. LES, ESA and NESA are all summer rainfall regions characterised by the low rainfall totals during April to August (figs. 3.9a, 3.9b and 3.9c). The CCAM-NCEP downscalings significantly overestimates the observed rainfall totals for the summer half-year (October to March). The CCAM-AMIP simulations exhibit similar overestimations, with a pronounced overestimation of rainfall totals during the early summer. This may be related to tropical-temperate linkages

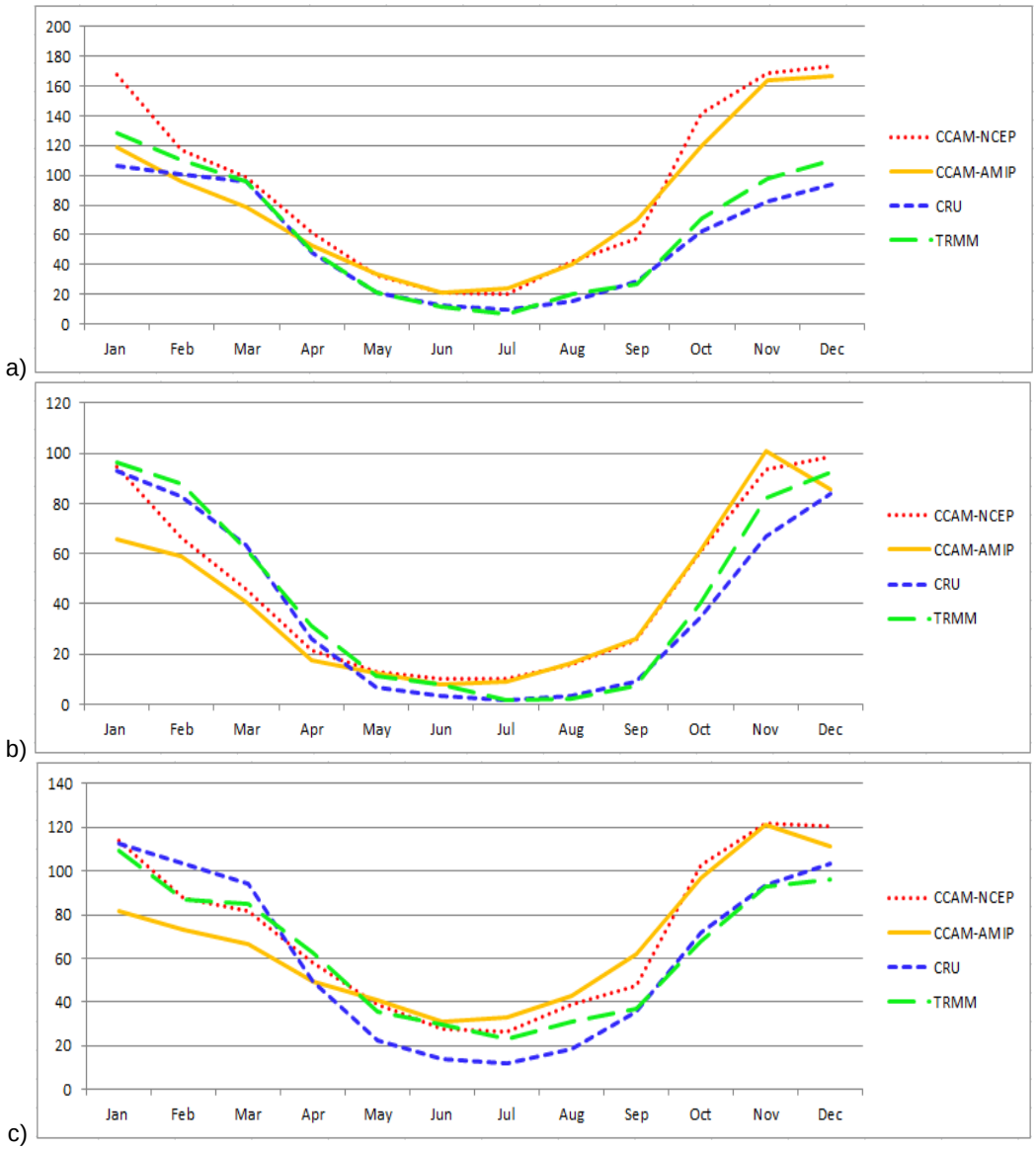

Figure 3.9. Intra-annual area-averaged rainfall totals (mm) for CCAM-AMIP (1979-2005), CCAM-NCEP (1979-2005), CRU (1979-2005) and TRMM (1998-2012) over the regions of a) LES, b) NESA and c) ESA

being overestimated during the early summer (see Figure 3.7 and the associated discussion, also see Tozuka et al (2013)). The largest over estimations occur over LES, which contains the steepest and most complex topography of the three sub-regions. One possible reason for the CCAM overstimations (and those of RCMs in general, when applied over LES), is the inadequate parameterisation of deep convection that occurs over the mountains in the presence of moist easterly low-level flow. It would be interesting to explore the hypothesis, by performing climate simulations at ultra-high resoltion over the region, well beyond the hydrostatic limit (e.g. Engelbrecht *et al.*, 2007). Although supercomputing capacity in South Africa is close to reaching the point of making feasible such simulations, they are beyond the scope of the current paper. The CCAM-NCEP simulations has a larger rainfall bias than the CCAM-AMIP simulations for most months, but the intra-annual rainfall cycle is greatly improved overall. That is, the CCAM-NCEP does show January to be the peak of the rainfall season in correspondence to observations. Note that in the CCAM-NCEP downscalings the model is forced with the synoptic-scale flow patterns every 6 hours, implying that no artifical overstimations or underestimations of tropical-temperate cloud band formation are allowed to occur, unlike in the AMIP simulations where the model is allowed to develop atmospheric circulation patterns freely in response to the lower-boundary forcing.

Inter-annual rainfall

The inter-annual area-averaged rainfall variability is analysed for summer rainfall (DJF) over the summer rainfall regions (LES, ESA and NESA) over southern Africa. The over estimation of rainfall by the CCAM- NCEP downscaling over the Lesotho region are a reoccurring feature from 1984 to 2007 (fig. 3.10a) even though the SRC calculated is 0.57 and significant at the 99.9% level. The latter result indicates that the CCAM-NCEP simulations have skill in representing inter-annual variability of summer rainfall over the Lesotho region. This is an important result. It implies that if the model simulations reflect the inter-annual variability in circulation realistically (this is forced to be the case in the CCAM-NCEP downscaling), the model's convection scheme is capable of realistically simulating the inter-annual variability in rainfall. The rainfall amounts for NESA and ESA are better fitted with the CRU rainfall in terms of amplitude (figs. 3.10b and 3.10c) compared to the LES area, and remains highly correlated to the corresponding observed time-series of inter-annual variability. This is an important result. It implies that if the model simulations reflect the inter-annual variability in circulation realistically (this is forced to be the case in the CCAM-NCEP downscaling through the 6-hourly nudging), the model's convection scheme is capable of

realistically simulating the inter-annual variability in rainfall over these three domains in eastern southern Africa.

In the CCAM-AMIP simulations, however, inter-annual rainfall variability is only represented skilfully for the NESA region (at the 95% level of significance). These results may stem from the synoptic-scale inter-annual variability in circulation not well-represented in the CCAM-AMIP runs, or alternatively that the relatively low resolution CCAM-AMIP runs are not skilful in representing rainfall totals over eastern South Africa. It may also be noted that in the case of the CCAM-AMIP simulations, the model is only forced at its lateral boundary with observed sea-surface temperatures and sea-ice distributions, and is initialised only once, at the beginning of the simulation. Internal model variability and natural variability are therefore

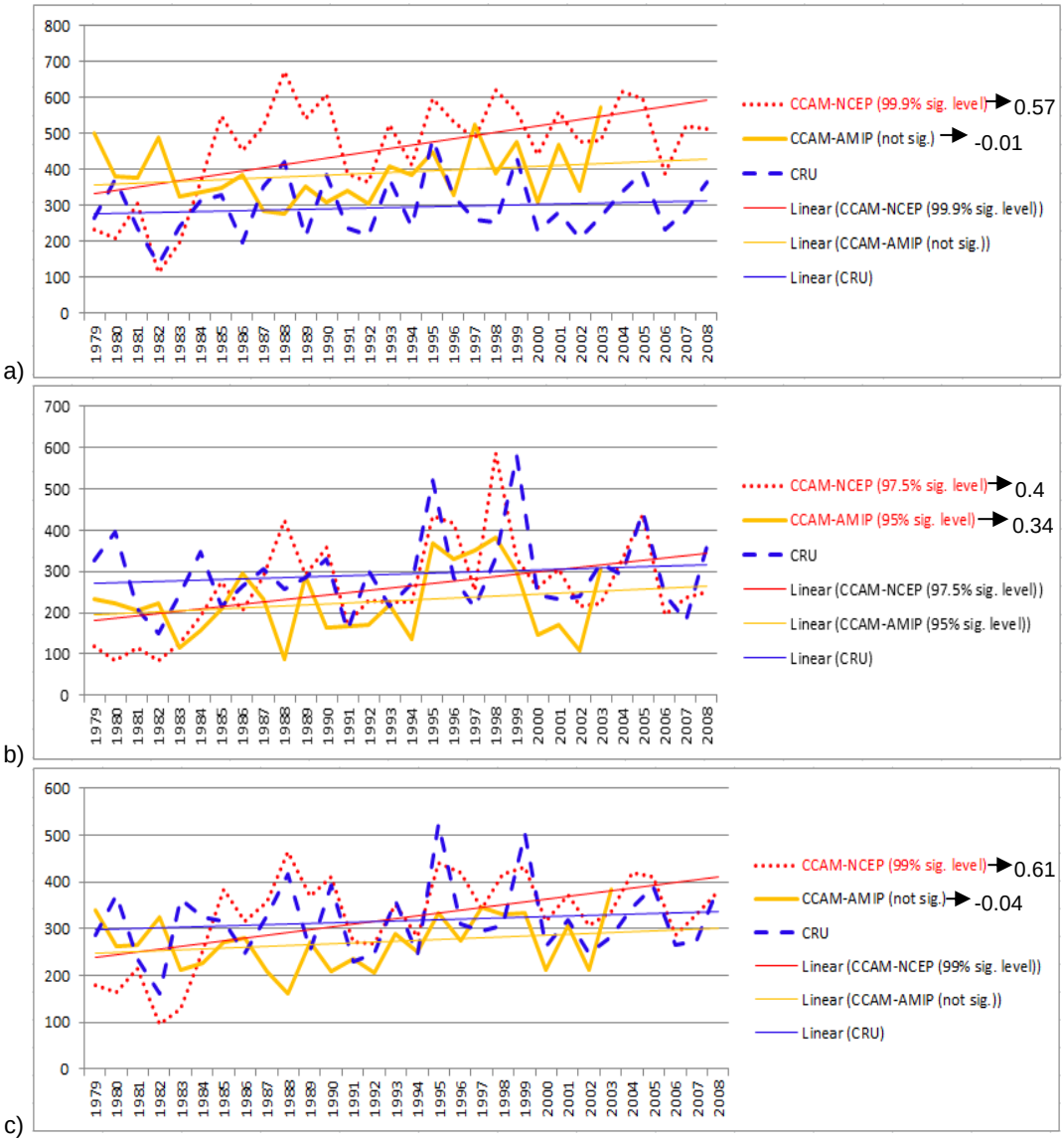

Figure 3.10. Inter-annual area-averaged DJF (December-January-February) rainfall totals (mm) for CCAM-AMIP (1979-2005), CCAM-NCEP (1979-2005) and CRU (1979-2005) over the regions of a) LES, b) NESA and c) ESA. Included is the Spearman rank correlation and in brackets is the Spearman rank correlation level of significance

also factors influencing the simulated inter-annual variability, and it is probably only during seasons of strong ENSO forcing the CCAM-AMIP runs may be expected to represent the observed circulation and rainfall anomalies realistically (see, for example, Landman and Beraki (2010)).

Although a detailed analysis of observed and simulations of trends in climate over southern Africa fall beyond the scope of this paper, it is interesting to note that an increasing rainfall trend over the three regions is present in both the observations and simulations (Fig. 3.10). This finding is consistent with the projections of future climate change for DJF of Engelbrecht et al. (2009) and Engelbrecht et al. (2011). Such a rainfall increase is plausible to occur in response to a deepening of the continental trough and the strengthening of the IOH in the low- and mid-levels over the Indian Ocean (Engelbrecht et al., 2009). An alternative reason for the upward trend in rainfall is that the 1982–1984 drought period created an artefact due to the specific time range, but because the previous finding is consistent with Engelbrecht et al. (2009) and Engelbrecht et al. (2011) the artefact creating the trend seems less likely.

3.4 Conclusions

Present-day CCAM-AMIP simulations and CCAM-NCEP downscaling were performed using a variable-resolution GCM, CCAM. Important synoptic-scale features of the observed rainfall climatology are well captured in the CCAM simulations, including the west-east gradient in rainfall over South Africa and the meridional movement of ITCZ-induced rainfall bands. The dry slot, extending eastward at 20 °S from eastern Botswana to Limpopo and southern Zimbabwe, found during the summer and annually is another important feature that both simulations captured remarkably well. A couple of shortcomings were also identified in the model simulations. Rainfall totals are significantly overestimated the eastern escarpment areas of southern Africa, despite of a general negative rainfall bias over the larger SAT region. The model simulations generally represent the seasonality of rainfall over southern Africa well, although spring rainfall is significantly overestimated in the CCAM-AMIP simulations, over the eastern parts of southern Africa. This leads to the peak in summer rainfall to be simulated to occur to early in the CCAM-AMIP simulations. The CCAM-NCEP simulations have a more variable climate (the SD being larger that for CCAM-AMIP and observations) and correlates well with observations in general. Furthermore, the CCAM-NCEP simulations tend to outperform the CCAM-AMIP simulations on most timescales. Significant SRC between the CCAM-NCEP rainfall simulations and observations indicate that inter-annual rainfall variability is skilfully simulated over the LES, ESA and NESA regions. This result implies that if the model simulations reflect the inter-annual variability in

circulation realistically (this is forced to be the case in the CCAM-NCEP downscaling through 6-hourly nudging), the model's convection scheme is capable of realistically simulating the inter-annual variability in rainfall. The CCAM-AMIP simulations represent the inter-annual variability with skill only over NESA. The difference in general between the CCAM-AMIP and CCAM-NCEP simulations can to some extent be attributed to the difference in resolution even though the CCAM-NCEP simulations were also forced with synoptic scale atmospheric circulations. In particular, the CCAM-AMIP simulations are only forced through SSTs and sea-ice at the model's lower boundary, and except for seasons of strong ENSO forcing, are unlikely to reflect the observed inter-annual variability (e.g. Landman and Beraki, 2012). These results imply that the relatively low-resolution AMIP simulations are not able to capture aspects of inter-annual variability over southern Africa. Improved results may be obtained through an ensemble of simulations and a probabilistic approach, the downscaling of the simulations using either dynamic or statistical methods, the inclusion of additional forms of radiative forcing such as stratospheric ozone, and the use of fully-coupled climate models. Further investigation is needed to understand the effect of increasing the resolution in the model and if the already large over estimations in rainfall seen in the coarse resolution simulations over strenuous topography can be improved. To this end, the authors foresee that improvements in supercomputing in South Africa, primarily through the supercomputers of the Centre for High Performance Computing (CHPC) of the CSIR, will over the next few years make feasible the first climate simulations performed beyond the hydrostatic limit, over the eastern escarpment areas of South Africa.

Acknowledgements

I would like to thank the Applied Centre for Climate and Earth System Studies (ACCESS) for funding the MSc research of the first author. Roelof Burger is thanked for his comments on the paper. The comments of two anonymous referees were also most valuable in improving the paper. All model simulations have been performed on the computer clusters of the Centre for High Performance Computing (CHPC) in South Africa.

3.5 References

Ashley, W.S., T.L. Mote, P.G. Dixon, S.L. Trotter, E.J. Powell, J.D. Durkee, and A.J. Grundstein, 2003: Distribution of mesoscale convective complex rainfall in the United States. *Mon. Weather Rev.,* **131,** 3003-3017.

Blamey, R.C. and Reason C.J.C., 2009: Numerical simulation of a mesoscale convective system over the east coast of South Africa. *Tellus,* **61A,** 17–34.

Christensen J.H., B. Hewitson, A. Busuioc, A. Chen, X. Gao, I. Held, R. Jones, R.K. Kolli, W-T. Kwon, R. Laprise, V. Magana Rueda, L. Mearns, C.G. Menendez, J. Raisanen, A. Rinke, A. Sarr and P. Whetton, 2007: Regional climate projections. In:

Solomon S, Qin D, Manning M, Chen Z, Marquis M, Averyt KB, Tignor M Miller HL (eds) Climate change 2007: the physical science basis. Contribution of Working Group I to the Fourth Assessment Report of the Intergovernmental Panel on Climate Change. Cambridge University Press, Cambridge and New York, pp 847–940

Cook K.H., 2000: The South Indian convergence zone and interannual rainfall variability over southern Africa. *J. of Clim.,* **13,** 3789–3804

D'abreton P.C. and P.D. Tyson, 1995: Divergent and non-divergent water vapour transport over southern Africa during wet and dry conditions. *Meteor. Atmos. Phys.,* **55,** 47–59.

D'abreton P.C. and P.D. Tyson, 1996: Three-Dimensional Kinematic Trajectory Modelling of Water Vapour Transport over Southern Africa. *Water SA,* **22,** 297–305.

De Coning E. , S.G. Forbes and E. Poolman, 1998: Heavy precipitation and flooding on 12-14 February 1996 over the summer reainfall regions of South Africa: Synoptic and isentropic analyses. *Nat. Weather. Dig*., **22,** 25-36.

Dinku, T., P. Ceccato, E. Grover-Kopec, M. Lemma, S.J. Connor and C.F. Ropelewski, 2007: Validation of satellite rainfall products over East Africa's complex topography. *Int. J. of Remote Sensing*, **28(7)**, 1503-1526.

Durkee J.D. and T.L. Mote, 2009: Aclimatology of warm-season mesoscale convective complexes in subtropical South America. *Int. J. Climatol.,* **30,** 418–431.

Engelbrecht C.J. and F.A. Engelbrecht, 2015: Shifts in Köppen-Geiger climate zones over southern Africa in relation to key global temperature goals. *Th. and applied climatol.,* DOI 10.1007/s00704-014-1354-1

Engelbrecht F.A., J.L. McGregor and C.J.deW. Rautenbach, 2007: On the development of a new nonhydrostatic atmospheric model in South Africa. *SA J. of Science.*, **103**, 127-134.

Engelbrecht, F.A. and C.J. deW. Rautenbach, 2000: Perspektief vir genestelde klimaatmodellering oor suidelike Afrika. *SA Tydskrif vir Wetenskap en Kuns,* **19**, 47-51.

Engelbrecht, F.A., C.J. deW. Rautenbach, J.L. McGregor and J.J. Katzfey (2002) January and July climate simulations over the SADC region using the limited-area model DARLAM. *Water SA,* **28,** 361-374.

Engelbrecht, F.A., J.L. McGregor and C.J. Engelbrecht, 2009: Dynamics of the Conformal-Cubic Atmospheric Model projected climate-change signal over southern Africa. *Roy. Met. Soc.,* **29,** 1013-1033.

Engelbrecht, F.A., W.A. Landman, C.J. Engelbrecht, S. Landman, M. M. Bopape, B. Roux, J. L. McGregor and M. Thatcher, 2011: Multi-scale climate modelling over Southern Africa using a variable-resolution global model. *Water SA.,* **37,** 637-658.

Garstang, M.B., E. Kelbe, G.D. Emmit and W. B. London, 1987: Generation of convective storms over the escarpment of NE South Africa. *Mon. Weather Rev.,* **115,** 429–443.

Gates, W.L., 1992: AMIP: The Atmospheric Model Intercomparison Project. *Bull. Amer. Meteor. Soc.,* **73,** 1962–1970.

Giorgi, F., 2005: Interdecadal variability of regional climate change: implications for the development of regional climate change scenarios. *Meteor. and Atmos. Physics,* **89(1-4),** 1-15.

Harrison, M.S.J., 1984: Ageneralized classification of SouthAfrican rain-bearing synoptic systems. *Int. J. Climatol*., **4,** 547–560.

Hart, N.C.G., C.J.C. Reason, and N. Fauchereaun, 2010: Tropical-Extratropical Interactions over Southern Africa: Three Cases of Heavy Summer Season Rainfall. *Mo. Weather. Rev*., **138,** 2608-2623.

Hernandez-Diaz, L., R. Laprise, L. Sushama, Martynov, K. Winger and B. Dugas, 2013: Climate simulation over CORDEX Africa domain using the fifth-generation Canadian Regional Climate Model (CRCM5). *Clim. Dyn.,* **40,** 1215-1433.

Hyndman, R.J., and A.B. Koehler, 2006: Another look at the measure of forecast accuracy. *Int. J. of. Forecasting*, 679-888.

Jeong J.H., A. Walther, G. Nikulin, C. Jones and D. Chen, 2011: Diurnal cycle of precipitation amount and frequency in Sweden: observation versus model simulation. *Tellus A*, **63**, DOI: 10.1111/j.1600-0870.2011.00517.x.

Joubert, A.M., J.J. Katzfey, J.L. McGregor and K.C. Nguyen, 1999: Simulating mid-summer climate over southern Africa using a nested regional climate model. *J. Geophys. Res.,* **104** 19015-19025

Jury, M.R., 2012: An intercomparison of model-simulated east-west climate gradient over South Africa. *Water SA*, **38**. ISSN: 1816-7950

Laing A.G. and J.M. Fritsch 1993a: Mesoscale convective complexes in Africa. *Mon. Weather Rev.,* **121,** 2254–2263.

Landman, S., F.A. Engelbrecht, C.J. Engelbrecht, L.L. Dyson and W.A. Landman, 2012: A short-range weather prediction system for South Africa based on a multi-model approach. *Water SA*, **38(5),** 765-774.

Liang X.Z., K.E. Kunkel, G.A. Meehl, R.G. Jones and J.X.L. Wang, 2008: Regional climate models downscaling analysis of general circulation models present climate biases propagation into future change projections. *Geophys. Res. Lett.,* **35,** L08709, doi: 10.1029/2007GL032849

Liang X.Z., L. Li, A. Dai and K.E. Kunkel, 2004: Regional climate model simulation of summer precipitation diurnal cycle over the United States. *Geophys. Res. Lett.,* **31,** doi:10.1029/2004GL021054.

Mason, S.J., and M.R. Jury, 1997: Climatic Change and Variability over Southern Africa: A Reflection on Underlying Processes. *Prog. Phys. Geog.,* **21,** 23–50.

McGregor, J.L., 1996: Semi-Lagrangian advection on conformal-cubic grids. *Mon. Weather Rev*., **124,** 1311-1322.

McGregor, J.L., 2003: A new convection scheme using a simple closure. In: Current Issues in the Parameterization of Convection. *BMRC Research Report*, **93**, 33-36.

McGregor, J.L., 2005: C-CAM: Geometric aspects and dynamical formulation. *CSIRO Atmos. Res. Tech*. **70**, 43 pp.

McGregor, J. L., and M. R. Dix, 2001: The CSIRO conformal-cubic atmospheric GCM. In: Hodnett PF (ed.) *Proc. IUTAM Symposium on Advances in Mathematical Modelling of Atmosphere and Ocean Dynamics*. Kluwer, Dordrecht. 197-202.

McGregor, J.L., J.J. Katzfey, K.C. Nguyen and M.J. Thatcher, 2011: Some recent developments for dynamical downscaling of climate. *Proc. 27th Annual Conference of the South African Society for Atmospheric Sciences*. September 2011, Hartebeeshoek.

Nicholson, S.E., 1986: The nature of rainfall variability in Africa south of the equator. *J. of Climatol*., **6**, 515 530.

Nicholson, S.E., 2000: The nature of rainfall variability over Africa on time scales of decades to millennia. *Glob. And Plan. Change*. **26**, 137-158

Nikulin, G., F. Giorgi, G. Asrar, M. Bushner, R. Cerezo-Mota, O.B. Christensen, M. Deque, J. Fernandez, A. Hansler, and E. van Meijngaard, 2012: Precipitation Climatology in an ensemble of CORDEX-Africa Regional Climate Simulations. *Int. J. Climatol.,* **25,** 6057-6078.

Reason, C.J.C. and H. Mulenga, 1999: Relationships between South African rainfall and SST anomalies in the southwest Indian Ocean. *Int. J. Climatol.*, **19**, 1651-1673.

Reason, C.J.C., W. Landman, and W. Tennant, 2006: Seasonal to decadal prediction of southern African climate and its links with variability of the Atlantic Ocean. *Bull. Amer. Meteor. Soc.,* **87,** 941–955.

Rocha D.A., C.A. Morales, S.V. Cuadra and T. AmbrizziI, 2009: Precipitation diurnal cycle and summer climatology assessmen over South America: An evaluation of Regional Climate Model version 3 simulations. *J. Geophys. Res.* **114**, D10108,doi:10.1029/2008JD010212

Rotstayn, L.D., 1997: A physically based scheme for the treatment of stratiform clouds and precipitation in large-scale models. I: Description and evaluation of the microphysical processes. *Quart. J. R. Meteor. Soc.,* **123,** 1227-1282.

Rouault, M. and Y. Richard, 2003: Intensity and spatial extension of drought in South Africa at different time scales. *Water SA, **29*(4),** 489-500.

Schwarzkopf, M. D. and S. B. Fels, 1991: The simplified exchange method revisited: an accurate, rapid method for computation of infrared cooling rates and fluxes. *J. Geophys. Res*., **96,** 9075-9096.

Shin D.W., S. Cockes and T.E. Larow, 2007: Diurnal cycle of precipitation in a climate model. *J. of Geophys. Res*., **112,** doi:10.1029/2006JD008333.

Sylla M.B.,E. Coppola, L. Mariotti, F. Giorgi, P.M. Ruti, A. Dell'Aquilla, X. Bi, 2010: Multiyear simulations of the African climate using a regional climate model (RegCM3) with the high resolution ERA-interim reanalysis. *Clim. Dyn.,* **35,** 231-247.

Taljaard, J.J., 1986: Change of rainfall distribution and circulation pattern over southern Africa in summer. *J. of Climatol.,* **6,** 579-592.

Thatcher, M. and J.L. McGregor, 2009: Using a scale-selective filter for dynamical downscaling with the conformal cubic atmospheric model. *Mon. Weather Rev*., **137**, 1742-1752.

Thatcher, M. and J.L. McGregor, 2010: A technique for dynamically downscaling daily-averaged GCM datasets over Australia using the Conformal Cubic Atmospheric Model. *Mon. Weather Rev*., **139**, 79-95.

Todd M., R. Washington and P.I. Palmer, 2004: Water vapour transport associated with tropical-temperate trough systems over southern Africa and the southwest Indian Ocean. *Int. J. Climatol.* **24** 555–568.

Tozuka, T., J.A. Babatunde and F.A. Engelbrecht, 2013: Impacts of convection schemes on simulating tropical-temperate troughs over southern Africa. *Clim. Dyn.*, DOI 10.1007/s00382-013-1738-4.

Tyson, P.D., 1986: Climatic Change and Variability over Southern Africa, Oxford University Press, Cape Town, p. 220

Tyson, P.D., and R.A. Whyte, 2000: The Weather and Climate of South Africa. Oxfort University Press Southern Africa, 212-213. ISBN 0 19 571806 2.

Walker N.D. and Lindsay J.A., 1989: Preliminary observations of oceanic influences on the February–March 1988 floods in central South Africa. *SA J. Sci.,* **85,** 164–169.

Wang Y., L.R. Leung, J.L. McGregor, D-K. Lee, W-C. Wang, Y. Ding and F. Kimura, 2004: Regional climate modeling: progress, challenges, and prospects. *J. of the Meteor. Soc. of Japan,* **82,** 1599–1628.

Walsh, K., and J.L. McGregor, 1995: January and July climate simulations over the Australian region using a limited area model. *J. Climatol.,* **8,** 2387-2403.

Zhang Q., H. Kornich and K. Holmgren, 2012: How well do reanalyses represent the southern African precipitation? *Clim. Dyn.* DOI: 10.1007/s00382-012-1423-z

Chapter 4 (Journal Article): High Resolution Modelling over the Eastern Escarpment of South Africa

Authors:

Zane Dedekind

CSIR Natural Resources and the Environment – Climate Studies, Modelling and Environmental Health, Pretoria, 0001, South Africa

Francois A. Engelbrecht

CSIR Natural Resources and the Environment – Climate Studies, Modelling and Environmental Health, Pretoria, 0001, South Africa

High Resolution Rainfall Modelling over the Eastern Escarpment of South Africa

Zane Dedekind[1] and Francois A. Engelbrecht[1]

1. CSIR Natural Resources and the Environment – Climate Studies, Modelling and Environmental Health, Pretoria, 0001, South Africa

4.1 Introduction

Steep gradients in orography are known to induce steep gradients in climate, and the realistic representation of these gradients in climate models require the use of detailed regional climate models (e.g. Giorgi and Mearns, 1991; McGregor, 1997; Engelbrecht *et al.*, 2002). The orography of southern Africa exhibits some particularly steep gradients, which require careful consideration in the design of climate simulations over the region. The country has a pronounced upwelling system along its west coast, generally known as the Benguela current (Andrews and Hutchings, 1980), whilst the fast-flowing narrow Agulhas current has a pronounced influence on the climate of the east coast (Rouault *et al.,* 2002). The coastal plain is generally narrow, with an elevated escarpment (generally reaching altitudes of 1000 – 2000 m) separating the coastal regions from the interior plateau (Van der Beek *et al*, 2002). The eastern escarpment of South Africa and Lesotho (the Drakensberg) are particularly steep and high peaking at altitudes of more than 3000 m. The high altitude of this region influences the local weather and cloud development that produces rainfall. Generally, there exists a positive correlation between altitude and rainfall specifically along the eastern slopes of the eastern mountain ranges in the north eastern Lesotho region (Tyson *et al.*, 1976). However, this relationship seems to break down at altitudes higher than 2100 m (Nel and Sumner, 2006).

Meso-scale convective systems are typically hundreds of kilometres in horizontal dimension at the advanced stages of development and have lifespans in the order of 10 hours. Convective cells, convective lines, gust fronts, meso-lows, meso-highs and tornados are substructures, ranging from 1 to 50 km in horizontal scales, that are embedded within these large systems (Houze *et al.,* 1989). Variations in topography often trigger meso-scale convective systems as already existing convective systems have the potential to create meso-scale convective vortices on the eastern escarpment of South Africa and Lesotho (e.g. Blamey and Reason, 2009). The two prominent rainfall producing systems over the region during summer (Desember-January-February; DJF) are organised line thunderstorms and orographically induced thunderstorms (Tyson *et al.,* 1976). Stations in the Drakensberg record 16 to 18 rain days on average during December and January and the extended

summer period from November to March yield 70 % of the annual rainfall (Tyson *et al.*, 1976). The effects of the eastern escarpment are not limited to localised rainfall effects. However, this region is the primary cause of the well-defined west-east gradient in rainfall totals across South Africa (e.g. Jury, 2012; Engelbrecht *et al.*, 2009). This strong rainfall gradient is diminished by a dry slot (an area of low rainfall) that extends from Namibia, over Botswana and Zimbabwe to over the far north-eastern parts of South Africa that include the Limpopo river basin.

Cumulus convection is the leading rain producing process that contributes to the most rainfall occurring over South Africa. Convective rainfall occurs as a result of the complex interactions between cloud dynamics, cloud microphysical processes, mesoscale forcing, diurnal heating and the synoptic-scale conditions. The occurrence of the thunderstorms over the eastern escarpment of South Africa and Lesotho is mostly found to be later in the day from mid- to late afternoon over the continental interior and during the night in mountainous regions (Schulze, 1965; Rouault *et al.*, 2013). Nel and Sumner (2006) show that the total rainfall measured at Sani Pas and Sentinel, 40.1 % and 30.8 % respectively, fall between 15h00 and 20h00. The diurnal cycle of rainfall is an expression of land surface response to solar radiation and made more complex by a number of dynamical and physical processes (Rouault *et al.*, 2013). A much larger amplitude of the diurnal cycle is experienced by the land rather than the ocean. This is associated with surface heating of land masses, convergence of sea breezes in coastal areas and anabatic flows in valleys and highland areas (McGregor and Nieuwolt, 1998).

Only a few studies where regional climate models have been applied beyond the hydrostatic limit (~ 10 km resolution in the horizontal, see Janjic and Gerrity, (2001) and Engelbrecht *et al.*, (2007)) have been performed for the southern African region to date (e.g. Engelbrecht *et al.*, 2011). At the Council for Scientific and Industrial Research (CSIR) the conformal-cubic atmospheric model (CCAM) has been applied at resolutions of 1 km to simulate the transport of carbon dioxide over the Cape Peninsula (Nickless *et al.*, 2015). In these simulations the domain sizes were relatively small, in the order of 150 x 150 km^2, and the simulations were performed on an 8 km horizontal resolution. The simulations performed spanned only a few years for each of these studies and were nudged within ERA reanalysis data. At the CSIR routine weather forecast systems also exist where numerical weather prediction models are applied at resolutions finer than 10 km. No study has to date, however, verified model simulations beyond the nonhydrostatic limit within the context of the representation of convective rainfall over the region. It is thought that such simulations, that may partially

resolve storm dynamics, may provide a substantial improvement over typical simulations performed at hydrostatic resolutions where convection is parameterised.

Of particular interest with regards to model simulations over the eastern escarpment is the representation of the diurnal cycle in convection and convective rainfall. Generally the simulation of the amplitude and phase of the diurnal cycle provides a valuable test for model parameterizations and for the representation of land-atmosphere feedbacks (e.g. Yang and Slingo, 2001). The verification of model simulations performed at hydrostatic resolutions has indeed revealed systematic errors over the summer rainfall regions. In the simulations of Hernadez-Diaz *et al.* (2012) rainfall peaks too early in the day over the eastern parts of South Africa. General overestimations of rainfall over eastern South Africa has also been reported in the modelling studies of Engelbrecht *et al*. (2002), Engelbrecht *et al*. (2009) and Engelbrecht *et al*. (2011). Along the eastern escarpment of South Africa the diurnal amplitude of surface moisture fluxes has been shown to be important for the diurnal cycle in rainfall as daytime surface latent heat fluxes increase steeply toward the east compared to the almost non-existent night time fluxes that exhibit little to the east-west gradient (Jury, 2012). Tadross *et al.* (2006) analysed the diurnal cycle for 2 seasons, using the MM5 RCM developed at the U.S. National Centre for Atmospheric Research, and found that the amplitudes are roughly comparable to observations, but the noticeable differences are found in the timing of convection within the models. The difference in the diurnal cycle is largely a result of the type of convection scheme used together with the sensitivity to the planetary boundary layer scheme being smaller (Tadross *et al.*, 2006). Correctly simulating all the variables that contribute to the diurnal cycle is of utmost importance, because it influences rainfall on a variety of time scales such as monthly, seasonal, annual, intra-annual and inter-annual rainfall scales.

The key purpose of the paper is to analyse the most extensive model simulations performed to date beyond the hydrostatic limit over eastern South Africa. The model simulations presented are downscaling's of ERA reanalysis data over the steep topography region of the eastern South Africa. The model simulations, of a range of convective rainfall attributes including the diurnal cycle, are verified against observations.

4.2 Data and Methods

The dynamic regional climate model applied in this research is the CCAM of the Commonwealth Scientific and Industrial Research Organisation (CSIRO) in Australia (McGregor, 1996, 2005a, 2005b; McGregor and Dix, 2001; 2008). CCAM is a variable-resolution global atmospheric model that functions as a regional climate model when applied

in stretched-grid mode. A semi-implicit semi-Lagrangian method is used to solve either the hydrostatic primitive equations or the quasi-elastic equations cast in a σ-coordinate based on the full pressure field (e.g. Engelbrecht *et al*., 2007). The GFDL parameterisations for long-wave and short-wave radiation, a stability-dependent boundary layer scheme and a mass-flux cumulus convection scheme are employed. A canopy scheme is included that includes 6 soil temperature layers, 6 soil moisture layers and 3 snow layers.

Towards obtaining the high resolution (8 km resolution in the horizontal) simulations over Lesotho CCAM was applied in stretched-grid mode using a Schmidt transformation factor of 0.133. Each panel of the cube projected onto the sphere contained 160 x 160 grid points. This implies that the high-resolution (8 km in the horizontal) panel occupied a domain of 1300 x 1300 km^2 in the horizontal (with this panel centred over Lesotho). The 8 km resolution simulations were nudged within ERA reanalysis using a digital filter technique to preserve the synoptic-scale atmospheric circulation patterns of the ERA data from 900 hPa upwards (Thatcher and McGregor, 2009; 2010). At its lower boundary the model was forced with sea-surface temperatures and sea-ice from the ERA reanalysis data. The model simulations were performed for the period 1979-2005.

Rainfall station data from South Africa surrounding Lesotho were selected based on completeness of the records. The rainfall stations acquired from the South African Weather Service (SAWS) were required to have more than 80 % complete entries (hourly and daily data, for the case of automatic stations (data record from 1993-2012) and manual stations (data record for 1979-2012)). Additionally, extreme and missing value tests were performed on the 14 daily rainfall stations as well as 5 separate hourly rainfall stations (table 4.1 and table 4.2). The hourly stations are used to create the 6-hourly datasets ranging from 02-08 h, 08-14 h, 14-20 h and 20-02 h. This insight into the diurnal cycle is used to evaluate the 6-hourly CCAM simulations to see if the convection scheme used in CCAM is robust and can describe the diurnal rainfall cycle.

The spatial patterns and magnitude of the simulated monthly and seasonal rainfall totals were verified against rain gauge based data of the Climatic Research Unit (CRU) for the period 1979-2005 (New *et al.*, 1999) and against satellite based sensor data of the Tropical Rainfall Measuring Mission (TRMM) at a resolution of 0.25 ° for the period 1998-2012 (Dinku *et al.,* 2007). The TRMM data was interpolated to 0.5 ° using a box-averaging function within the Gridded Analysis and Display System. From now on the CRU rain gauge based data and the TRMM satellite based data will be referred to as the observational dataset. The CCAM was simulated at an 8 km resolution to show rainfall features against the steep escarpment

of South Africa and Lesotho and was interpolated to fit the TRMM and CRU grids respectively for analysis. No interpolation techniques were used to compare the CCAM simulations against the SAWS station data. The simulations are analysed in the following way:

1) The simulations are subtracted from the TRMM and CRU data to detect systematic over and under estimations of rainfall as a function of space (that is, the model's spatial rainfall biases are identified).
2) The pattern correlation (Walsh and McGregor, 1995) is calculated between the simulations and observed fields as after the simulations were interpolated to the TRMM and CRU fields respectively to inspect the models ability to capture the spatial distribution of rainfall. It is a correlation of two spatial fields, x_i and o_i, at specific time interval as i ranges from 1 to N, where N is the number of grid points in the model domain:

$$\rho = \frac{\sum(x_i - \bar{x})(o_i - \bar{o})}{\sqrt{(\sum(x_i - \bar{x})^2)(\sum(o_i - \bar{o})^2)}} \qquad (1)$$

Here $\bar{x}$ and $\bar{o}$ are the domain averages of x_i and o_i.

3) The Root Mean Square Error (RMSE) is a measure of the accuracy between a specific forecasted variable from a model and the same observed variable since it is scale dependent (Hyndman and Koehler, 2006).
4) The Standard deviation (SD) is calculated as the measurements for the simulations and observed fields as an estimate of average uncertainty of those measured values.
5) South African Weather Service (SAWS) station rainfall is analysed against the simulations as a direct measure of rainfall at a particular point on a monthly, seasonal and annual time-scale.
6) The diurnal cycle is calculated and verified on a 6-hour basis against SAWS rainfall stations that measured hourly rainfall.
7) The Spearman rank correlation (SRC) is applied in the research to determine whether model simulation of inter-annual variability (time series data) has a statistically significant correlation with the corresponding observations. The SRC is calculated on the premise that there are no tied ranks within the data and is then subjected to significance testing.

4.3 Results

Verification of the CCAM simulations against station data

The eastern escarpment of South Africa and Lesotho exhibits steep topographic gradients especially around the Lesotho region. These can induce very large differences in rainfall occurrence over relatively small areas when a weather system moves over the area (Fig. 4.1). For this reason stations were divided into three groups based on location (south, north-west and east of Lesotho). Large differences in annual, seasonal and monthly rainfall totals are evident for the three groups of stations (fig. 4.1 and table 4.1). Stations in the east have annual rainfall totals well above 900 mm, which are severely over estimated by CCAM showing totals above 3000 mm. At the Cathedral Peak and Royal National Park Hotels locations rainfall totals are overestimated by factors of almost 4 times and 2.5, respectively (table 4.1). Over this region the lower tropospheric flow is upslope and surface moisture is advected from the east when ridging anti-cyclones are present to the east of South Africa (Joubert *et al.*, 1999). It is possible that orographic lift and related rainfall are overestimated in the CCAM simulations.

The lower rainfall totals to the south and west of Lesotho is partially due to the rain-shadow effect - the ridging high-pressure cloud bands moving in from the east often do not

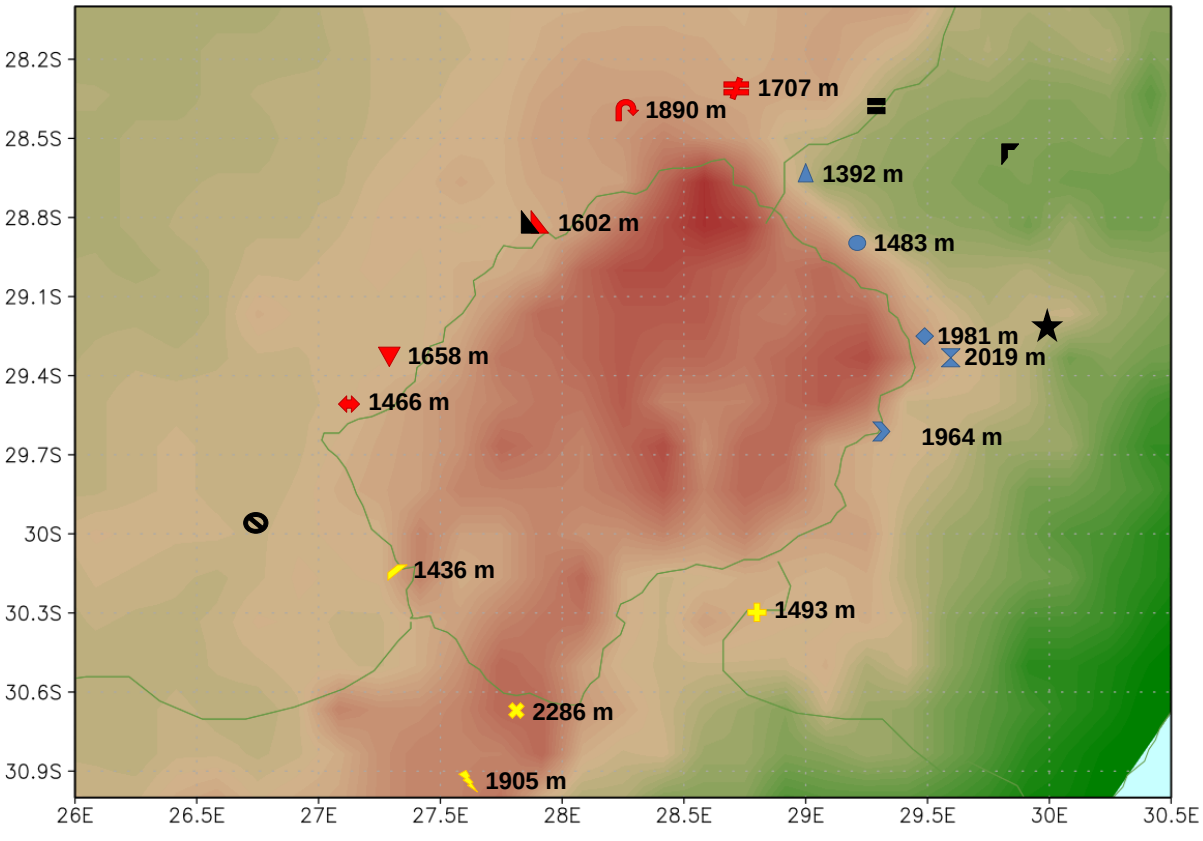

Figure 4.1. Location of South African Weather Service (SAWS) stations around Lesotho measured daily (coloured) and hourly (black)

		CCAM						SR					
	Station	Annual	DJF	Nov	Dec	Jan	Feb	Annual	DJF	Nov	Dec	Jan	Feb
	Cathederal Peak	4237.7	2225.4	460.8	650.6	795.5	761.4	1152.3	586.4	130.6	152.3	209.6	224.4
	Royal National Park	3127.9	1681.6	331.0	477.6	623.0	566.7	1225.7	628.2	145.7	167.7	212.5	235.7
	Ficksburg	1010.5	490.4	127.7	181.6	172.7	139.5	661.0	273.0	81.5	82.2	102.9	89.5
	Giants Castle	2044.4	1163.4	242.8	369.2	410.7	381.9	984.1	498.3	114.8	163.0	179.8	162.8
	Kommissiepoort	937.7	458.4	116.9	159.2	171.7	125.6	642.0	274.9	77.8	81.1	96.4	90.9
	HighMoore	1725.1	937.8	204.4	300.8	337.5	300.4	1233.3	628.8	164.3	196.0	220.6	205.1
	HobHouse	973.0	475.9	119.9	171.2	175.0	128.7	604.1	251.1	80.8	79.6	89.3	89.1
	SaniPass	2030.8	1127.7	227.2	332.2	413.1	390.9	1122.4	571.8	126.9	164.7	208.0	189.4
	FunnyStone	1413.0	591.3	176.5	227.1	216.8	150.1	835.8	329.8	107.0	111.9	111.9	111.9
	BarkleyEast	1236.3	557.9	153.9	218.3	210.2	139.4	601.9	254.1	79.6	81.7	83.7	95.5
	Lille	1030.0	491.9	116.9	186.7	173.7	131.3	698.1	306.7	82.1	98.4	99.5	106.8
	Matatiele	1206.8	589.2	152.6	208.0	203.6	177.0	683.4	318.7	85.0	102.2	119.8	101.2
	HighLands	984.1	468.8	128.3	164.7	170.8	139.1	641.4	281.3	92.0	97.8	92.2	86.6
	Kestell	1043.3	531.7	139.7	179.8	194.4	157.6	684.6	318.4	93.1	103.3	108.9	102.8

Table 4.1. Daily SAWS station rainfall compared to rainfall from CCAM at the points of the SAWS stations. Highlighted blocks show large over estimations (larger than 2x the observed rainfall)

move over the higher eastern escarpment due to the steep topography. Convective clouds that occur in association with easterly winds in the presence of an upper air disturbance typically form in the moist easterly winds on the eastern side of the escarpment and subsequently rain out to the east of the escarpment. This situation is reflected in the lower rainfall amounts, between 600-700 mm, recorded over the eastern Free State showing a strong west-east rainfall gradient over the domain. CCAM correctly simulates the west-east gradient in rainfall, but also overestimates rainfall totals in the west by a factor of two for some locations. The highest simulated rainfall totals for the region occurs during mid-summer (DJF) with lower totals simulated for November when compared to December.

Annual rainfall totals

The distinct west-east rainfall gradient is visible over much of the research domain as the simulated CCAM (CRU) annual rainfall totals in the west are in the range of 800 mm (500 mm) increasing to well over 2000 mm (800mm) in the east (fig. 4.2). Within this strong gradient there are two areas of maximum rainfall on the eastern and western sides of the Lesotho escarpment with the former being the largest (fig. 4.2a). The highest rainfall in the vertical cross-section occurs at 29.25 °S on the eastern side of the Lesotho escarpment around 1450 to 1650 m (fig. 4.2a). Between 26 °E and 27.5 °E, the western side of the mountain, the 8 km CCAM simulations show prominent features of orographic uplift that is not clearly seen in the observations. The high totals are simulated for a region that is not

covered by the SAWS station network and is therefore not available for this study. It is plausible that this local maximum simulated by the model is a real physical feature not present in the 0.5 degree resolution CRU data due to the absence of underlying station data for this region. There is indeed some indication of the existence of western rainfall maxima in the TRMM data although this remotely sensed precipitation data sets are known to have biases in the presence of topography (also see Tian *et al.*, 2007; Condom *et al.*, 2011). It is also noticeable that there is a weak pattern correlation between the TRMM and CCAM datasets whereas the rainfall simulated by CCAM compares better to those depicted by the SAWS station data and CRU gridded station data (fig. 4.2e and 4.2f). The simulated climate is highly variable over the domain (SD = 192) that is not seen in the CRU (SD = 135 mm) or TRMM (SD = 119 mm) datasets. The RMSE for both CCAM-CRU (482 mm) and CCAM-TRMM (572 mm) is very large due to the overestimations seen over the eastern escarpment. Even though the RMSE does not indicate whether it is a wet or dry bias it can clearly be noted as a wet bias (figs. 4.2e and 4.2f).

CCAM generally overestimates rainfall totals across the domain, particularly so over Kwa-Zulu Natal (KZN) and the Lesotho border (fig. 4.2b, 4.2c and 4.2d). These over estimations on the Lesotho border are as large as 800 mm. The SAWS stations situated at a higher altitude like High Moore (2019 m) and Giants Castle (1981 m), on the eastern side of the escarpment, are overestimated by 40 % and 107 % respectively. The correlation between the increase in rainfall, for stations along the eastern side of the escarpment, to an increase in altitude under 2100 m (Nel and Sumner, 2006) is not clearly seen in this paper. Simulations show a rainfall increase up to 1500m (moving east to west) before the rainfall decreases with altitude on the eastern side of the escarpment showing that the relationship between altitude and rainfall breaks down in CCAM above 1500 m (fig. 4.2a). This may be due to the way CCAM incorrectly resolves convection against such steep topography.

Seasonal rainfall totals

Observed summer rainfall patterns over the region closely resemble the annual rainfall pattern depicting that the region is a summer rainfall region. During summer moisture-laden easterly winds frequently flow over the eastern escarpment as low-level high-pressure systems ridge along the South African east coast, thereby inducing high rainfall totals east of the escarpment. In the CCAM simulations large overestimations of summer rainfall totals are evident over KZN and along the Lesotho border. The CCAM simulated rainfall correlates well with that of CRU in space (fig. 4.3), more so than in the case of the TRMM data. The model climate is at least twice as variable as the CRU and TRMM climate. However, the CCAM

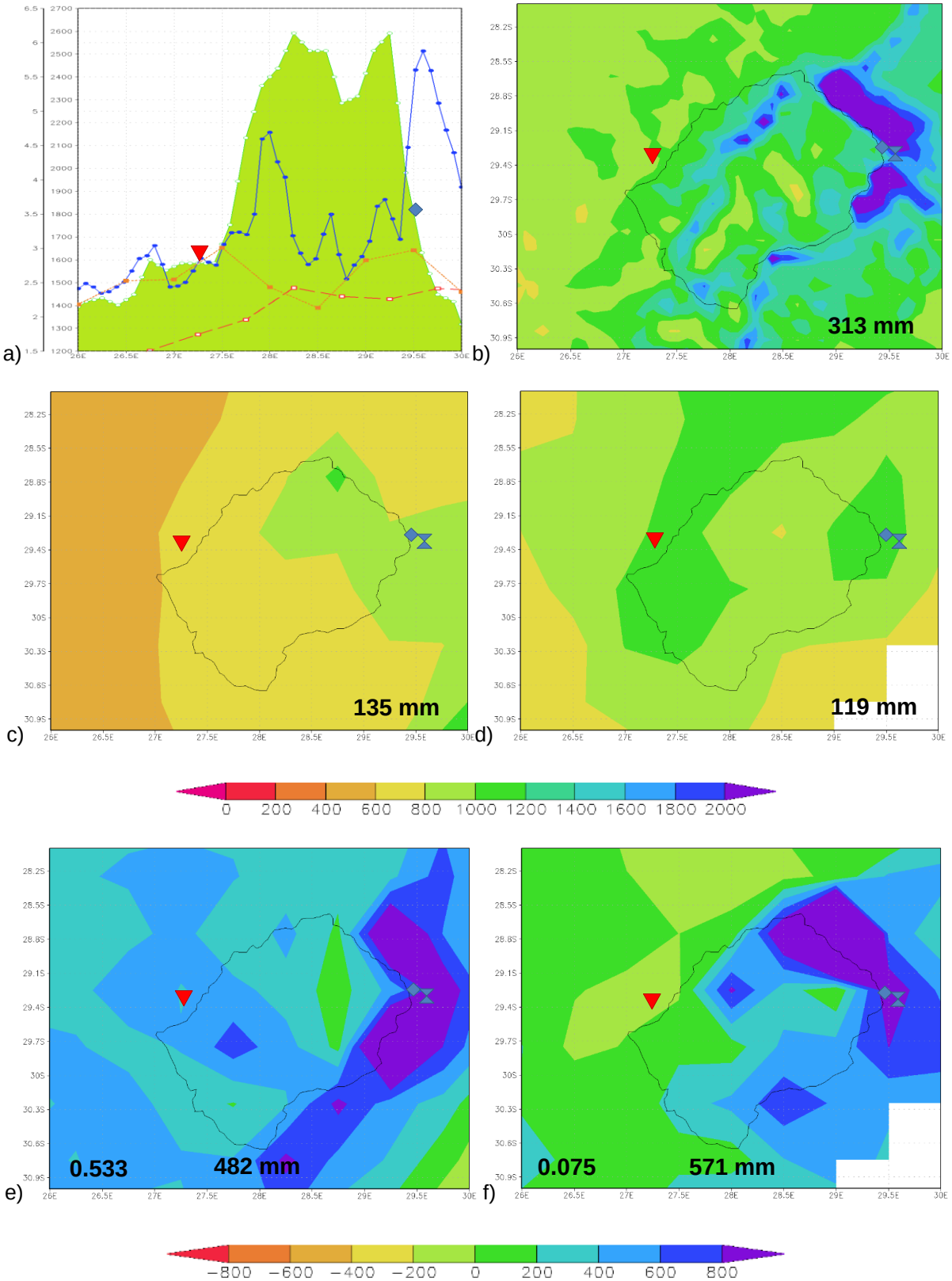

Figure 4.2. a) Vertical cross-section at 29.25 °S for annual rainfall in mm/day (solid line – CCAM; long stripes – CRU; short stripes – TRMM). Annual rainfall totals (mm) for b) CCAM (1979-2005), c) CRU (1979-2005) and d) TRMM (1998-2012). Bias (mm) for e) CCAM-CRU and f) CCAM-TRMM. Also shown is the pattern correlation (bottom left), RMSE (bottom middle) and STDEV (bottom right)

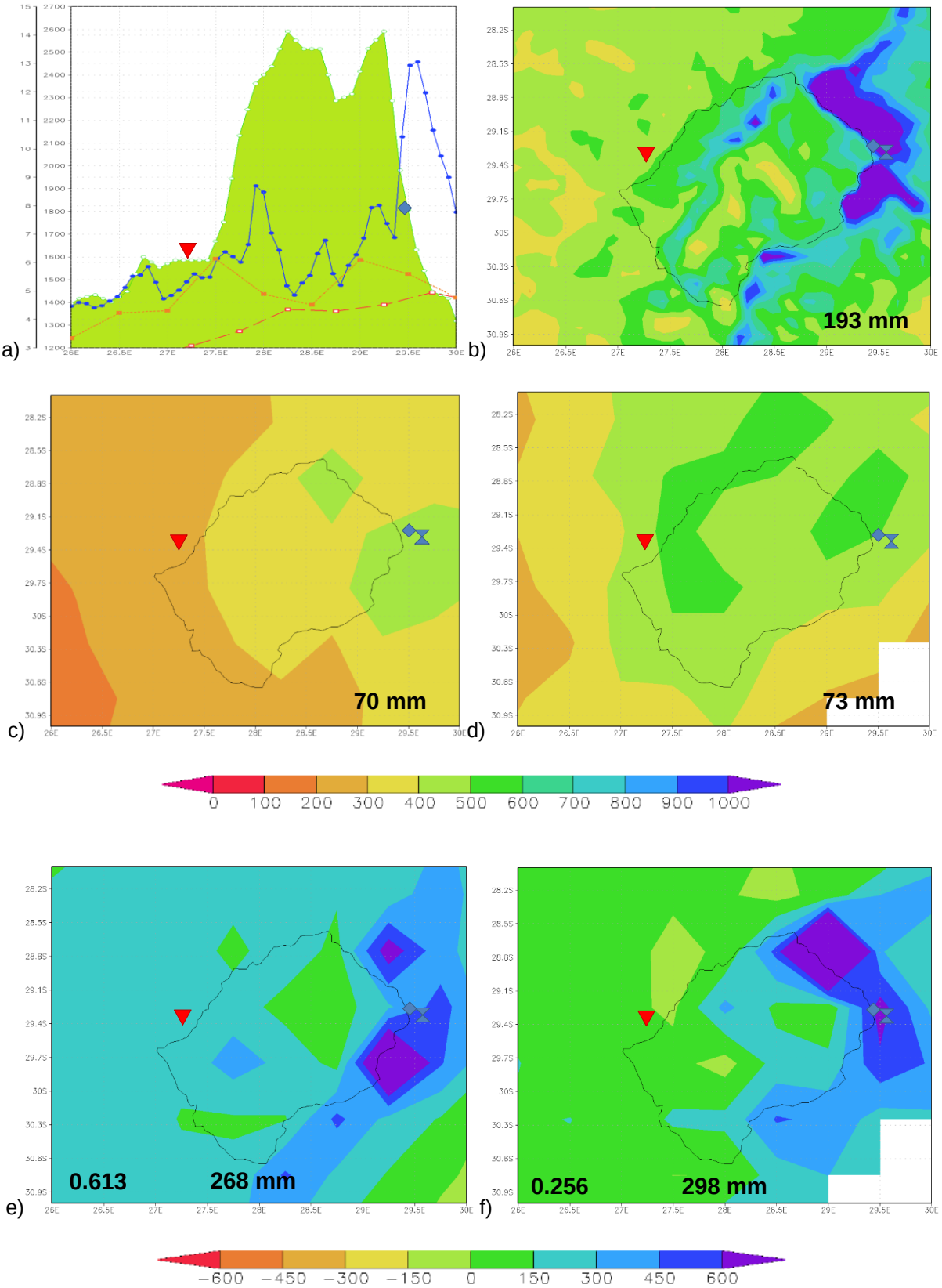

Figure 4.3. a) Vertical cross-section at 29.25 °S for DJF rainfall in mm/day (solid line – CCAM; long stripes – CRU; short stripes – TRMM). DJF rainfall totals (mm) for b) CCAM (1979-2005), c) CRU (1979-2005) and d) TRMM (1998-2012). Bias (mm) for e) CCAM-CRU and f) CCAM-TRMM. Also shown is the pattern correlation (bottom left), RMSE (bottom middle) and STDEV (bottom right)

correlates fairly well spatially with the CRU dataset. The CCAM simulates a western rainfall maximum similar to TRMM at 27.5 °E, but then extends this feature to 28 °E (at 2400 m) as the topography increases on the western side of the mountain. This feature is not present in the TRMM data and implies a wet bias in the model simulations. During the summer season the altitude-rainfall relationship within CCAM does not exist. CCAM shows an increase in rainfall from east to west with altitude up to 1800 m, before decreasing again with the rising mountain (fig. 4.3a).

Monthly rainfall totals

The month by month analysis is an important analysis as previous versions of CCAM incorrectly simulated November as the month of maximum rainfall during summer (Dedekind *et al*., 2015). The early onslaught of the season was a result of the model simulating too strong temperate-trough linkages in November rather than the observed January rainfall maximum (also see Tozuka *et al*., 2013). The newer version of CCAM applied here shows a more realistic seasonal cycle in rainfall with the simulated rainfall peaking during mid-summer rather than in November (fig. 4.4).

TRMM shows relatively large amounts of rainfall on the western side of the Lesotho escarpment when compared to SAWS stations in the vicinity (fig. 4.4d and table 4.1). Kommissiepoort (27.25 °E and 29.4 °S) has an average station rainfall of 2.59 mm/day compared to TRMM having 5.25 mm/day during November. This suggests some apparent biases in the TRMM data in terms of rainfall totals in regions of steep orography (at least when compared to the available station data). CCAM overestimates rainfall totals with respect to both the TRMM and CRU data, with these overestimations most severe on both the western and eastern flanks of the mountain (fig. 4.4a to 4.4f). This can be noted in the large RMSE values obtained for November as well as December and January.

The CCAM simulated wet bias for December over the KZN and Lesotho border is most evident in the TRMM data (fig. 4.5e and 4.5f). The CRU data for December resembles the SAWS station data better than the TRMM data, which points at biases in the TRMM data with respect to the station data. CCAM simulates relatively lower amounts of rainfall above 2200 m compared to November (fig. 4.5a and 4.5b). At Kommissiepoort the rainfall is 2.7 mm/day, a factor of two less than in the CCAM simulations. The Giants Castle (1981 m) and High Moore (2019 m) stations, approximately on the same latitude as Kommissiepoort have simulated (SAWS station) rainfall of 369.2 mm (163 mm) and 300.8 mm (196 mm) respectively. The CCAM rainfall for January increases over the biggest part of the domain

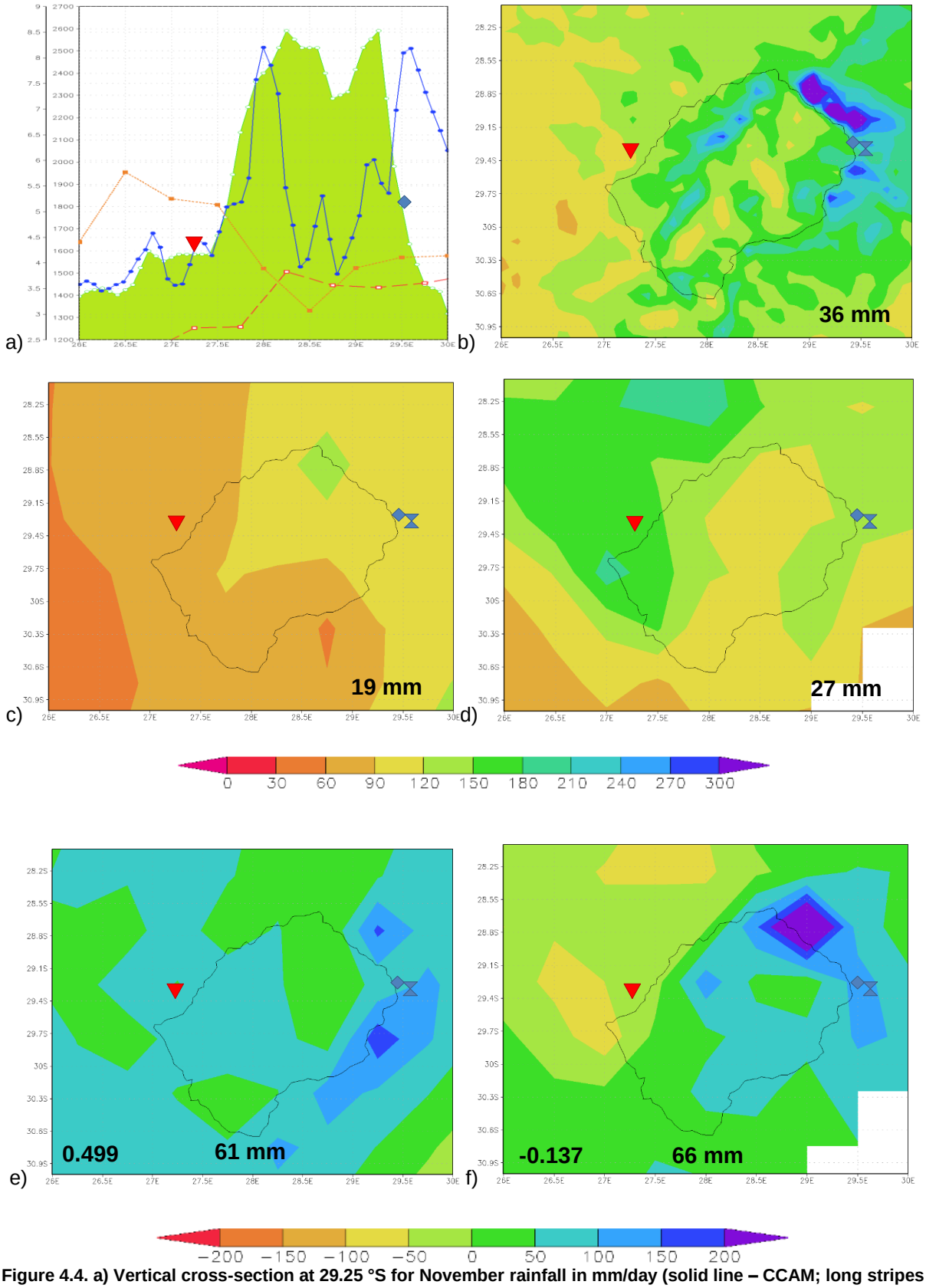

Figure 4.4. a) Vertical cross-section at 29.25 °S for November rainfall in mm/day (solid line – CCAM; long stripes – CRU; short stripes – TRMM). November rainfall totals (mm) for b) CCAM (1979-2005), c) CRU (1979-2005) and d) TRMM (1998-2012). Bias (mm) for e) CCAM-CRU and f) CCAM-TRMM. Also shown is the pattern correlation (bottom left), RMSE (bottom middle) and STDEV (bottom right)

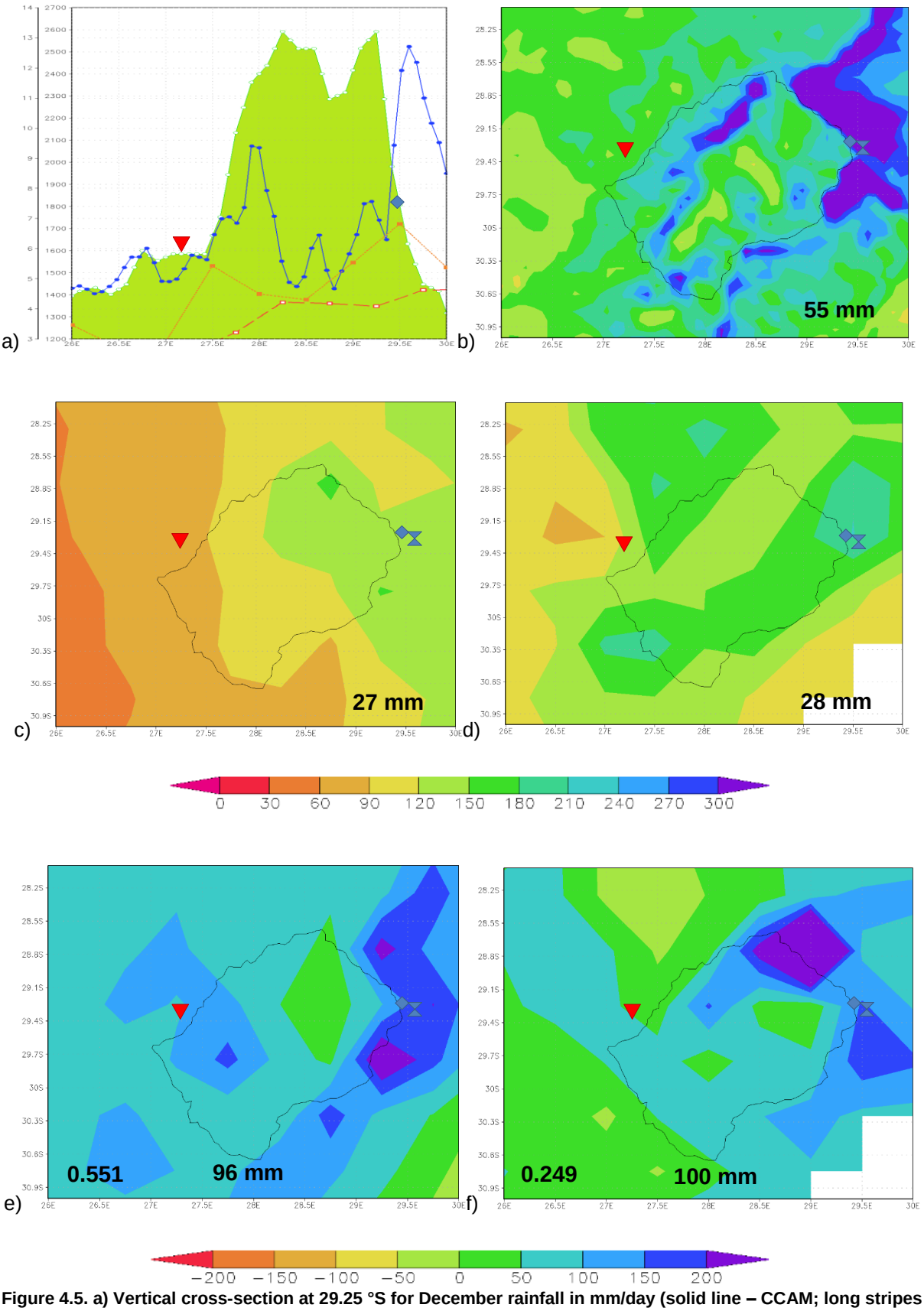

Figure 4.5. a) Vertical cross-section at 29.25 °S for December rainfall in mm/day (solid line – CCAM; long stripes – CRU; short stripes – TRMM). December rainfall totals (mm) for b) CCAM (1979-2005), c) CRU (1979-2005) and d) TRMM (1998-2012). Bias (mm) for e) CCAM-CRU and f) CCAM-TRMM. Also shown is the pattern correlation (bottom left), RMSE (bottom middle) and STDEV (bottom right)

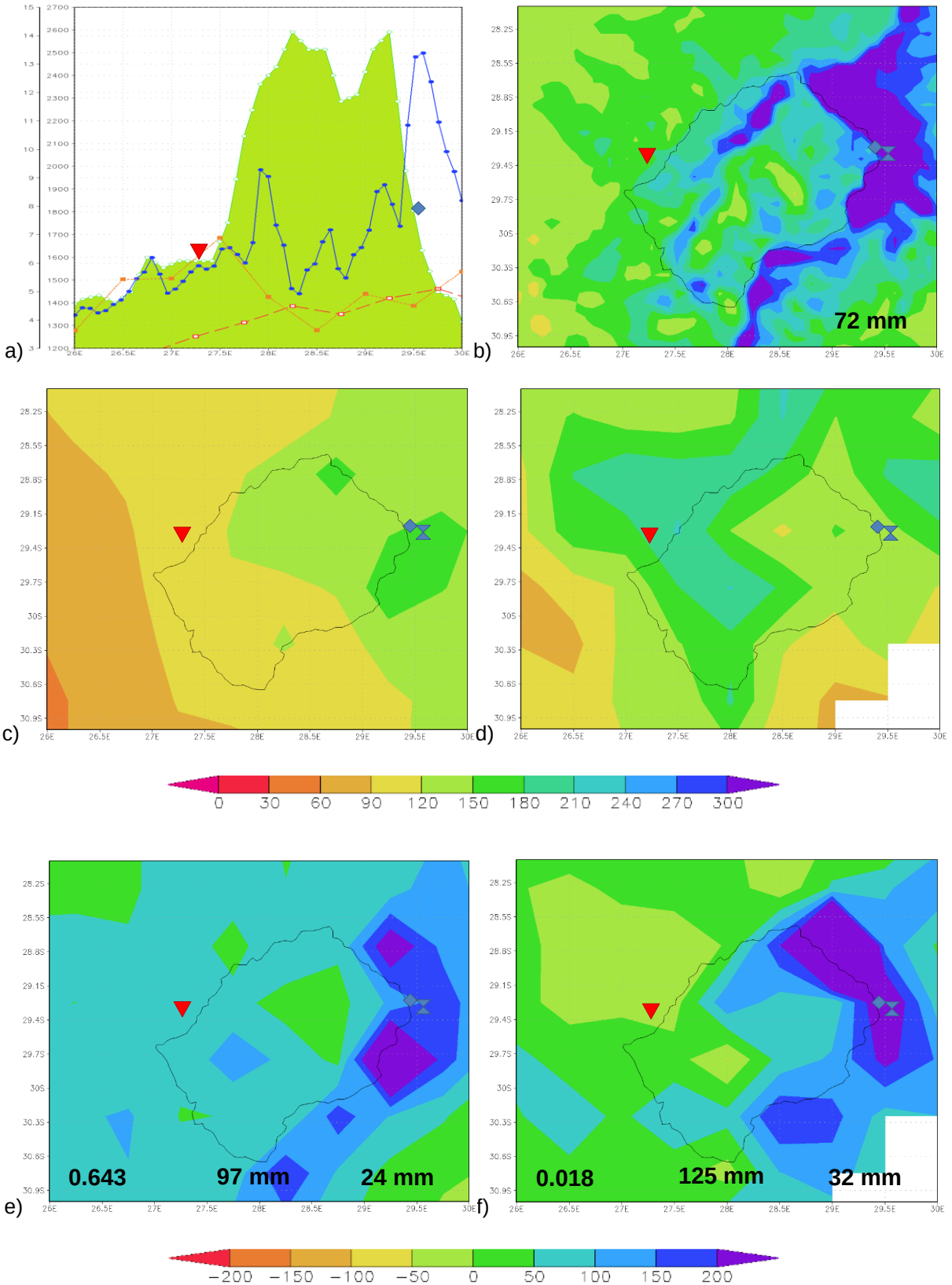

Figure 4.6. a) Vertical cross-section at 29.25 °S for January rainfall in mm/day (solid line – CCAM; long stripes – CRU; short stripes – TRMM). January rainfall totals (mm) for b) CCAM (1979-2005), c) CRU (1979-2005) and d) TRMM (1998-2012). Bias (mm) for e) CCAM-CRU and f) CCAM-TRMM. Also shown is the pattern correlation (bottom left), RMSE (bottom middle) and STDEV (bottom right)

with respect to the December totals, especially on the Eastern Cape - Lesotho border and the KZN - Lesotho border (fig. 4.6b). These local rainfall increases occur consistently with January being the month of highest rainfall over eastern South Africa. The increase occurs in response to a strengthening of the heat low over the central interior aiding in the frequent occurrence of tropical-temperate troughs over the region (Hart *et al.*, 2010). The largest increases from the SAWS stations are on the eastern side of the Lesotho escarpment with the exception of Kommissiepoort having an increase of 17 % on the western side of Lesotho. The TRMM exhibits large increases in rainfall (for January with respect to December) over the Free State that does not correspond to the SAWS data or CCAM simulations (fig. 4.6d). The CRU data displays increased rainfall on the eastern side the escarpment that is similar to CCAM (fig. 4.6c and 4.6e). At Kommissiepoort the station rainfall total is well represented by CRU (gridded station data), but TRMM and CCAM overestimates the rainfall by a factor of 2. The CCAM simulates the west-east rainfall gradient well and captures the increase in rainfall that is caused by the steeper orography at 26.75 °E (fig. 4.6a). In general the CCAM-CRU analyses are for the most part better than for CCAM-TRMM while CCAM-CRU also has a superior spatial correlation (fig. 4.6).

Diurnal rainfall cycle

Representation of the diurnal cycle in convection is known to be problematic in dynamic climate models as most models simulating the peak in rainfall too early in the day (see Tadross *et al.*, 2006). However, these misrepresented maximum rainfall peaks are dependent on the type of convection scheme used in the model. Here the 6-hourly simulated totals of CCAM are analysed to investigate how the model deals with changes in the daily heat balance, moisture distributions during and the influences orographic lift of the diurnal cycle. The effects of the Agulhas current play an important role in the diurnal cycle of adjacent coastal areas (Rouault *et al.*, 2013). Water vapour transfer in the marine boundary layer by the Agulhas current, and a deepening in this layer is a result of intense mixing and unstable atmospheric condition created by colder drier air above the current (Rouault *et al*., 2000; 2003). During anti-cyclonic conditions the water vapour is advected toward land where it interacts with the landmass. Summer rainfall during the night in the vicinity of Durban up to the escarpment can be contributed to the combined effect of orographic effects of the eastern escarpment of South Africa and Lesotho and the warm Agulhas Current (Tyson and Preston-White, 2000). The rainfall producing systems occurring over the area vary from ridging high-pressure systems, cut-off lows, heat thunderstorms that mainly occur late in the afternoon and evenings, cold fronts and tropical - temperate troughs.

	SAWS					CCAM				
		02-08h	08-14h	14-20h	20-02h		02-08h	08-14h	14-20h	20-02h
Ficksburg	Dec	7.6	14.1	36.9	19.5	Dec	37.2	24.7	72.1	53.2
	Jan	14.8	13.4	29.4	20.9	Jan	30.8	22.5	65.1	64.3
	Feb	10.7	13.8	26.6	22.4	Feb	27.1	17.8	51.1	51.5
	DJF	33.0	41.3	92.9	62.8	DJF	95.2	64.9	188.3	169.0
	Annual	89.6	93.4	192.9	142.8	Annual	194.9	209.4	422.3	426.6
Lady Smith	Dec	14.7	6.8	57.3	36.6	Dec	88.0	18.3	39.3	95.9
	Jan	14.1	9.7	57.3	69.7	Jan	119.2	15.1	31.9	117.2
	Feb	7.9	7.1	38.2	38.3	Feb	80.5	19.1	23.3	63.3
	DJF	36.6	23.6	152.8	144.5	DJF	199.7	34.3	55.2	180.5
	Annual	86.5	68.0	283.1	279.0	Annual	551.9	99.4	228.2	386.7
Mooi Rivier	Dec	8.2	8.5	46.2	38.8	Dec	68.6	14.8	33.4	132.9
	Jan	9.5	9.4	50.3	23.4	Jan	60.8	14.2	25.1	142.2
	Feb	6.3	5.0	38.6	14.1	Feb	58.5	16.6	27.6	87.0
	DJF	24.0	22.9	135.0	76.3	DJF	187.9	45.5	86.0	362.1
	Annual	64.3	71.6	294.0	176.7	Annual	593.7	127.9	195.6	730.1
Van Reenen	Dec	19.7	13.4	71.0	51.0	Dec	100.5	31.5	39.4	123.8
	Jan	27.4	21.7	73.7	78.2	Jan	116.6	24.0	40.0	134.1
	Feb	18.2	13.9	66.8	53.0	Feb	99.7	27.5	28.8	118.4
	DJF	65.2	49.0	211.5	182.1	DJF	316.8	83.0	108.2	376.3
	Annual	141.5	111.3	360.1	339.7	Annual	706.9	289.4	241.2	601.2
Wepener	Dec	9.6	10.9	42.2	20.5	Dec	29.5	23.5	61.9	60.1
	Jan	13.1	12.0	42.1	22.1	Jan	21.4	21.7	69.4	56.7
	Feb	13.4	20.4	27.4	23.1	Feb	19.1	11.2	57.8	62.4
	DJF	36.2	43.4	111.7	65.8	DJF	70.0	56.5	189.0	179.2
	Annual	94.9	119.2	226.4	146.3	Annual	104.3	178.6	467.2	495.2

Table 4.2. The diurnal cycle compiled from the South African Weather Service station data compared to CCAM data at the location of the particular station. The location from the stations is marked in Fig. 4.1.

The CCAM simulated diurnal cycle of rainfall is compared to 6-hourly SAWS station data over the domain to analyse the ability to simulate convection and rainfall. The pronounced feature seen in the CCAM simulations on the western side of the escarpment is rainfall peaking between 14h and 20h (fig. 4.7a to 4.7e). Annually the combined afternoon (14-20 h) and evening (20-02 h) rainfall make up 65 % (68 % according to CCAM) and 64 % (77 % according to CCAM) of the total diurnal rainfall cycle at Ficksburg and Wepener respectively

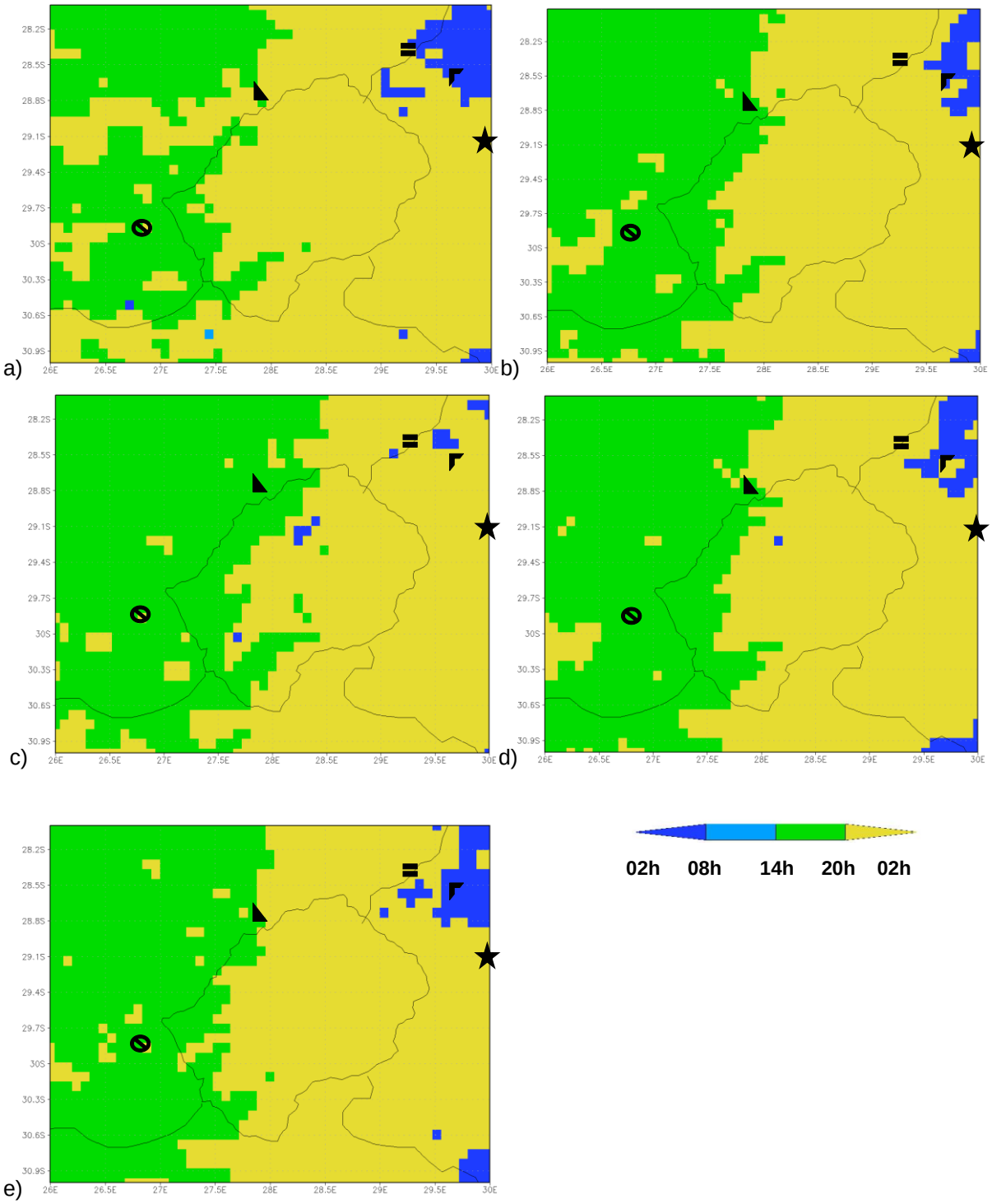

Figure 4.7. 6-Hourly diurnal cycle for CCAM a) annually, b) DJF, c) November, d) December and e) January. Intervals are 02h to 08h (dark blue), 08h-14h (light blue), 14h-20h (green) and 20h-02h (yellow)

(fig. 4.7a and table 4.2). However, CCAM misses the annual and February diurnal rainfall maximum period between 14-20 h for both the stations by simulating the maximum rainfall between 20-02 h. During summer months the afternoon rainfall occurs more frequently than evening showers (fig. 4.7b to 4.7e). CCAM does well in capturing the diurnal cycle on the western side of the escarpment. On the eastern side of the escarpment most weather

stations report the diurnal rainfall cycle to peak between 14-20 h. Over most of this region CCAM simulates rainfall to peak either in the early morning or evening. About 90 % of the SAWS stations rainfall occurs in the second half of the day with the peak between 14-20 h (excluding Lady Smith and Van Reenen). Rouault *et al.* (2013) found that, for stations to the north-east and east of Lesotho (within 150 km), the rainfall peak varied between 18 h and 21 h for the extended South African summer months (November to March). It is clear that CCAM simulates rainfall too late during the day (20-02 h) into the early morning hours (02-08 h) on the eastern side of the escarpment. This is especially true for Lady Smith where the early morning rainfall amount to more than 40 % of the diurnal cycle that is not comparable to the 10 % from SAWS stations (table 4.2). The largest and most unrealistic rainfall station simulations comes from stations on the eastern side of the escarpment with Lady Smith and Van Reenen showing as little as 5 times, and Mooi Rivier 6 times, more rainfall between 02-06 h than the SAWS stations. The CCAM overestimations are higher in the afternoon and evening, when heat convection peaks over the eastern escarpment. Thus, these overestimations can still be ascribed to orographic forcing, although not necessarily to overestimations of the effects of orographic lift.

Intra-annual rainfall

The modelled monthly rainfall totals from the eastern escarpment are compared to the corresponding observed values. The curves are obtained by merely taking rainfall values month to month and plotting it next to each other. Rainfall values are severely overestimated for almost every month except from May-July when rainfall subsides during winter. CCAM simulates the onset of rainfall in September that is comparable to the onset as described by the TRMM and CRU data. The peak of the rainfall season is simulated in January that compares well with the observations. The average rainfall over the domain is 75 mm and 93 mm higher than TRMM and CRU respectively indicating severe overestimations that is unrealistic (fig. 4.7). From January the rainfall reduces gradually until March at which point CCAM simulates the dry conditions that prevail from May to September.

Inter-annual rainfall

The inter-annual rainfall variability for the summer rainfall is analysed for the region over the eastern escarpment of South Africa and Lesotho (26-30 °E and 28-31 °S). The simulated over estimation prevail on a yearly basis with the largest rainfall over estimations occurring between 1985 to 1989 and 1997-2003. Dedekind *et al*. (2015) showed that the same region, at a simulated 50 km resolution, has a SRC of 0.57 that is significant at 99.9 %. The high resolution 8 km simulations, with a newer version of CCAM, performed better obtaining a SRC of 0.69 that is significant at 99.9 % (fig. 4.8). CCAM captures the severe decrease in

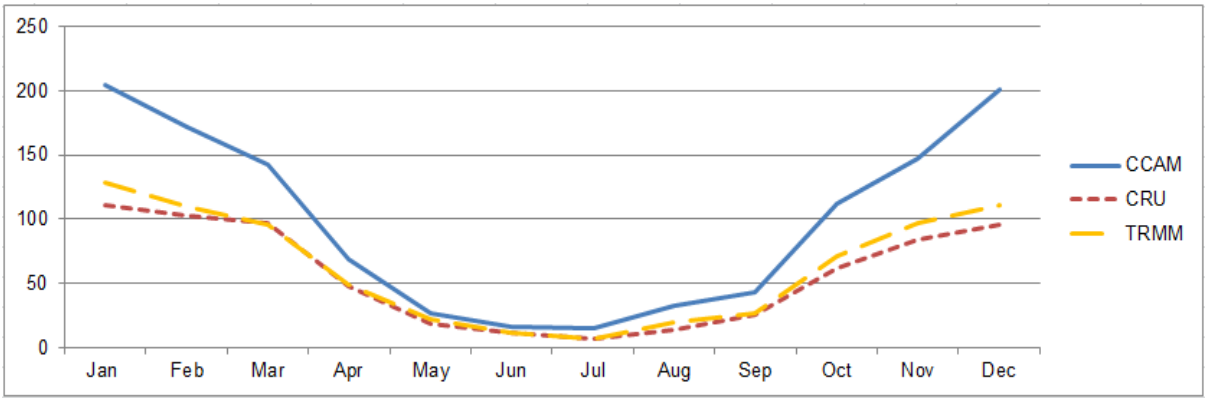

Figure 4.8. Intra-annual rainfall totals (mm) for CCAM (1979-2005), CRU (1979-2005) and TRMM (1998-2012) over Lesotho

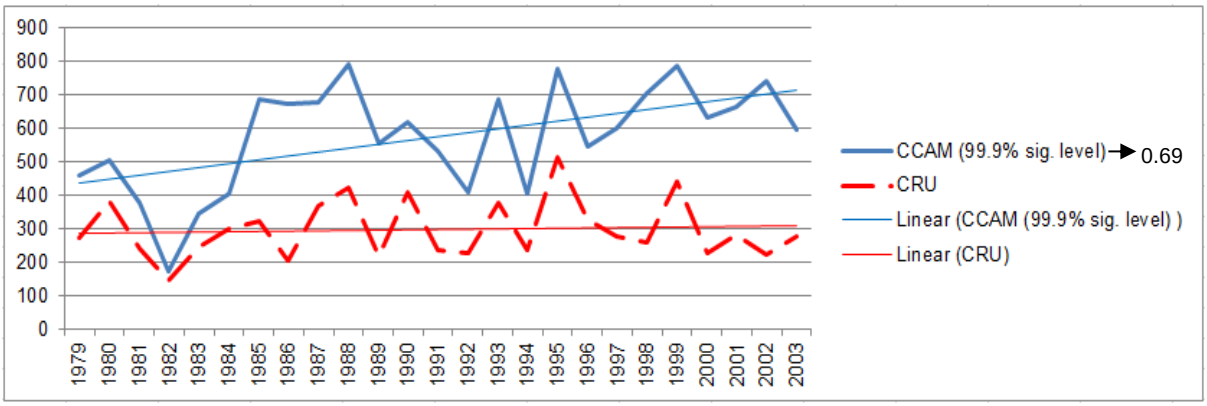

Figure 4.9. Inter-annual DJF rainfall totals (mm) for CCAM (1979-2004) and CRU (1979-2004) over the regions of Lesotho. In brackets is the Spearman rank correlation level of significance and added is the Spearman rank correlation.

rainfall that is associated with the 1982-1983 droughts over southern Africa. The simulated rainfall trend from 1979 to 2004 shows a greater slope indicative of higher rainfall totals over the region in the future, but this is unlikely as this strong positive trend can be explained by the severe droughts that significantly influence the rainfall variability at the start of the period. These CCAM reanalysis simulations are strongly influenced by the nudging in 6-hourly observed circulation patterns. Therefore, it can be stated that the rainfall response to the observed circulation patterns of 1982/83 is simulated correctly (the model correctly simulated drought). There is clear trend in rainfall over the region, but not necessarily a growing bias. The model exhibits large biases for the 1988/89 season, quite similar to the biases observed at the end of the simulation period.

4.4 Conclusions

A Variable resolution Global Circulation Model (CCAM) is used for present-day simulations and measured against observations from CRU, TRMM and SAWS. Rainfall features around Lesotho, the wetter eastern parts of Kwa-Zulu Natal and the drier western parts in the Free

State and Eastern Cape, are captured well by CCAM. However, the model simulations exhibit very large wet biases north east of Lesotho that are at some stations up to 3 times the observed rainfall from SAWS stations. CCAM is able to simulate the well-defined west-east gradient in rainfall over the eastern escarpment of South Africa and Lesotho (e.g. Engelbrecht *et al*., 2009). The strong rainfall gradient in the CCAM rainfall, that is not present in the TRMM rainfall, results in a low pattern correlation between these two fields. The simulated climate from CCAM tends to have a much larger variable climate than the CRU and TRMM climates (CCAM SD > CRU SD and CCAM SD > TRMM SD) for all time scales. The CRU and SAWS data show an increase in rainfall as the longitude increase over the domain. The SAWS data does not show a clear correlation between increases in rainfall as the altitude increase below 2100 m on the eastern side of the escarpment, but CCAM does simulate a large increase in rainfall with elevation in orography below about 1500 m depending on whether annual, seasonal or monthly rainfall were analysed. The intra-annual cycle is also captured, especially the annual rainfall maximum that occurs during January Dedekind *et al*. 2015 showed that an earlier version of CCAM simulated an annual rainfall maximum too early during November. It is important that CCAM can capture the whole cycle with the onset of the season starting in October until January when rainfall subsides for winter months. A significant SRC between CCAM rainfall simulations and observations are indicative of skilfully simulating the inter-annual rainfall variability, but the trend and wet bias are problematic.

Simulating the diurnal cycle is a robust test of how well the dynamics and physics in a model works. CCAM simulates two distinct regions where rainfall occurs between 14-20 h on the western side of the steep Lesotho escarpment and between 20-02 h over the eastern Lesotho escarpment that is not present at the SAWS stations. The observations show that CCAM simulates rainfall too late during the day on the eastern side of the escarpment. Extreme wet biases are also present at Lady Smith, Van Reenen and Mooi Rivier locations. The diurnal cycle for the stations on the western side is reasonably well captured by CCAM. Further investigation is needed to analyse these extreme wet biases occurring over the largest parts of the domain as well as testing another observational dataset, Famine Early Warning Systems Network (FEWS) over such steep topography, over rough terrain. Also, it would be valuable to see whether the high-resolution simulations in the diurnal cycle in rainfall would outperform lower resolutions over the same area.

Acknowledgements

I would like to thank the Applied Centre for Climate and Earth System Studies (ACCESS) for the funding the research, through a bursary allocated to the first author and through its

Thematic Research Area 2. The South African Weather Service is thanked for providing me the stations data used in the paper. The research would not have been possible without the Centre for High Performance Computing (CHPC) providing the computation resources need to perform the high resolution simulations.

4.5 References

Andrews, W.R.H. and L. Hutchings, 1980: Upwelling of the Southern Benguela Current. *Progress in Oceanog.*, **9**, 1-8.

Blamey, R.C. and C.J.C. Reason, 2009: Numerical simulation of a mesoscale convective system over the east coast of South Africa. *Tellus* **61A**, 17–34.

Condom, T., P. Rau and J.C. Espinoza, 2011: Correction of TRMM 3B43 monthly precipitation data over the mountainous areas of Peru during the period 1998–2007. *Hydrol. Proc.*, ***25*(12)**, 1924-1933.

Dedekind, Z., F.A. Engelbrecht and J.H. van der Merwe, 2015: Model simulations of rainfall over southern Africa and its eastern escarpment.

Dinku, T., P. Ceccato, E. Grover-Kopec, M. Lemma, S.J. Connor and C.F. Ropelewski, 2007: Validation of satellite rainfall products over East Africa's complex topography. *Int. J. of Remote Sensing*, **28(7)**, 1503-1526.

Engelbrecht, F. A., C.J. deW. Rautenbach and J. J. Katzfey, 2002. January and July climate simulations over the SADC region using the limitedarea model DARLAM. *Water SA,* **28**, 361–374.

Engelbrecht, F.A., J.L. McGregor and C.J. Engelbrecht, 2009: Dynamics of the Conformal-Cubic Atmospheric Model projected climate-change signal over southern Africa. *Roy. Meteor. Soc.,* **29**, 1013-1033.

Engelbrecht, F.A., J.L. McGregor and C.J. deW. Rautenbach, 2007: On the development of a new nonhydrostatic atmospheric modek in South Africa. *SA J. of Sci.,* **103**, 127-134.

Engelbrecht, F.A., W.A. Landman, C.J. Engelbrecht, S. Landman, M.M. Bopape, B. Roux, J.L. McGregor and M. Thatcher, 2011: Multi-scale climate modelling over Southern Africa using a variable-resolution global model. *Water SA*, **37**, 647-658.

Giorgi, F. and L.O. Mearns, 1991: Approaches to the simulation of regional climate change: a review. *Rev. of Geophys.*, **29(2)**, 191-216.

Hart, N.C.G., C.J.C. Reason, and N. Fauchereaun, 2010: Tropical-Extratropical Interactions over Southern Africa: Three Cases of Heavy Summer Season Rainfall. *Mo. Weather. Rev*., **138,** 2608-2623

Hernandez-Diaz, L., R. Laprise, L. Sushama, Martynov, K. Winger and B. Dugas, 2013: Climate simulation over CORDEX Africa domain using the fifth-generation Canadian Regional Climate Model (CRCM5). *Clim. Dyn.,* **40**, 1215-1433.

Houze, R.A., S.A. Rudledge, M.I. Biggerstaff and B.F. Smull, 1989: Interpretation of Doppler Weather Radar Display of Midlatitude Mesoscle Convective Systems. *American Met. Soc.*, **70**, 608-619.

Hynman, R.J., and A.B. Koehler, 2006: Another look at the measure of forecast accuracy. *Int. J. of. Forecasting*, 679-888.

Janjic, Z.I., J.P. Gerrity Jr and S. Nickovic, 2001: An alternative approach to nonhydrostatic modeling. *Mon Weather Rev*, ***129*(5)**, 1164-1178.

Joubert, A. M., J.J. Katzfey, J.L. McGregor and K.C. Nguyen, 1999: Simulating mid-summer climate over southern Africa using a nested regional climate model. *J. Geophys. Res.,* **104**, 19015-19025

Jury, M.R., 2012: An intercomparison of model-simulated east-west climate gradient over South Africa. *Water SA*, vol. **38**. ISSN: 1816-7950

McGregor, J.L., 1996: Semi-Lagrangian advection on conformal-cubic grids. *Mon. Weather Rev*., **124**, 1311-1322.

McGregor, J.L., 1997: Regional Climate Modelling. *Meteor*. *Atmos. Phys*., **63**, 105-117.

McGregor, J.L., 2005a: Geostrophic adjustment for reversibly staggered grids. *Mon. Weather Rev.,* **133**, 1119-1128.

McGregor, J.L., 2005b: C-CAM: Geometric aspects and dynamical formulation. CSIRO Atmospheric Research Tech. Paper No. **70**. 43 pp.

McGregor, J.L. and M.R. Dix, 2001. The CSIRO conformal-cubic atmospheric GCM. In: Hodnett PF (ed.) *Proc. IUTAM Symposium on Advances in Mathematical Modelling of Atmos. and Ocean Dyn.*. Kluwer, Dordrecht. 197-202.

McGregor, J.L. and M. R. Dix, 2008: An updated description of the Conformal-Cubic Atmospheric Model. In: Hamilton K and Ohfuchi W (eds.) *High Resolution Simulation of the Atmosphere and Ocean*. Springer Verlag. 51-76.

McGregor, G. and S. Nieuwolt, 1998. An introduction to the climates of the low latitudes. *Tropical Climatol.*. 339. John Wiley & Sons. England.

Nel, W. and P. Sumner, 2006: Trends in rainfall total and variability (1970-2000) along the Kwazulu-Natal Drakensberg foothills. *SA Geog. J.,* **88**, 130-137.

New, M., M. Hulme, and P. Jones, 1999: Representing twentieth-century space-time climate variability. Part I: Development of a 1961-90 mean monthly terrestrial climatology. *J. of Clim*, ***12*(3)**, 829-856.

Nickless, A., T. Ziehn, P.J. Rayner, R.J. Scholes and F. Engelbrecht, 2015: Greenhouse gas network design using backward Lagrangian particle dispersion modelling–Part 2: Sensitivity analyses and South African test case. Atmospheric Chemistry and Physics, 15(4), 2051-2069.Pohl, B., M. Rouault and S.S., Roy, 2014: Simulation of the annual and diurnal cycles of rainfall over South Africa by a regional climate model. *Clim. Dyn.*, 1-20.

Rouault M., S.S. Roy and R. C. BALLING Jr., 2013: The diurnal cycle rainfall in South Africa in the austral summer. *Int. J. of Clim.,* **33**, 770-777.

Rouault M., S.A. White, C.J.C. Reason, J.R.E. Lutjharms and I. Jobard, 2002: Ocean–Atmosphere Interaction in the Agulhas Current Region and a South African Extreme Weather Event. *Weather. Forecasting*, **17**, 655–669.

Rouault, M., S.S. Roy R.C. Balling, 2013: The diurnal cycle of rainfall in South Africa in the austral summer. *Int. J. of Climatol.*, **33(3)**, 770-777.

Rouault, M, A.M. Lee-Thorp and J.R.E. Lutjeharms, 2000: Observations of the atmospheric boundary layer above the Agulhas Current during along current winds. *J. of Phys. Oceanog.,* **30,** 70–85.

Rouault, M, C.J.C. Reason, J.R.E. Lutjeharms and A. Beljaars, 2003: NCEP Reanalysis and ECMWF operational model underestimation of latent and sensible heat fluxes above the Agulhas Current. *J. of Clim.,* **16,** 776–782.

Schulze, B.R., 1965: Hail and thunderstorm frequency in South Africa. *Notos*, **14,** 67–71.

Tadross, M.A., W.J. Gutowski Jr, B.C. Hewitson, C. Jack and M. New, 2006: MM5 simulations of interannual change and the diurnal cycle of southern African regional climate. *Theor. and applied climatol.*, **86(1-4)**, 63-80.

Thatcher, M. and J.L. McGregor, 2009: Using a scale-selective filter for dynamical downscaling with the conformal cubic atmospheric model. *Mon. Weather Rev.,* **137**, 1742-1752.

Thatcher, M. and J.L. McGregor, 2010: A technique for dynamically downscaling daily-averaged GCM datasets over Australia using the Conformal Cubic Atmospheric Model. *Mon. Weather Rev.,* **139**, 79-95.

Tian, Y., C.D. Peters-Lidard, B.J. Choudhury and M. Garcia, 2007: Multitemporal analysis of TRMM-based satellite precipitation products for land data assimilation applications. *J. of Hydromet.*, ***8*(6)**, 1165-1183.

Tozuka, T., B.J. Abiodun and F.A. Engelbrecht, 2014: Impacts of convection schemes on simulating tropical-temperate troughs over southern Africa. *Clim. Dyn.*, ***42*(1-2)**, 433-451.

Triegaardt, D.O., 1965a: Experimental barotropic forecasting over subtropical regions. *Notos* **14**, 3–15.

Tyson, P.D., R.A. Preston-Whyte and R. E. Schulze, 1976: The climate of the Drakensberg. Natal Town and regional planning commission: Pietermaritzburg.

van der Beek, P., M.A. Summerfield, J. Braun, R.W. Brown and A. Fleming ,2002:. Modeling postbreakup landscape development and denudational history across the southeast African (Drakensberg Escarpment) margin. *J. of Geoph. Research: Solid Earth (1978–2012)*, **107(B12)**, ETG-11.

Walsh, K., and J.L. McGregor, 1995: January and July climate simulations over the Australian region using a limited area model. *J. of Clim.,* **8**, 2387-2403.

Yang, G.Y. and J. Slingo, 2001: The diurnal cycle in the Tropics. *Mon. Weather Rev*., **129**, 784–801

Chapter 5: Conclusions

GCMs are based on the physical laws applied to the atmosphere, ocean and land surface, including the feedbacks between these systems. GCMs applied at climate change timescales have relatively low horizontal resolutions – in the order of 200 km. As a consequence, certain mesoscale-weather systems and orographic forcing, including steep topography, are not adequately resolved and treated within GCMs. RCMs are used to obtain high resolution simulations over selected areas of interest. CCAM is a variable-resolution atmospheric model that can be applied at quasi-uniform resolution globally or in stretched-grid mode over an area of interest (using the Schmidt transformation) to function as an RCM. Its stretched-grid capability implies that CCAM is a flexible downscaling tool that can function across a multitude of resolutions. For example, the model has been applied in stretched-grid mode to provide simulations of 60 km resolution over southern Africa and 1 km resolution over the False Bay region of South Africa (Engelbrecht *et al.*, 2011). Moreover, CCAM is applied over across a range of time scales, that us, for short-range weather forecasting, seasonal forecasrting and the projection of future climate change (e.g. Engelbrecht *et al.*, 2011). Applying a model that is normally used for the projection of future climate change across a range of spatial and time scales provides the opportunity to test the models ability to simulate important atmospheric features such as convection and the ENSO teleconnection to southern Africa (Engelbrecht *et al.*, 2011).

The main purpose of this study is to apply CCAM across a range of different spatial resolutions, to determine how well the model represents rainfall features over southern Africa in the various configurations. Of particular interest is the model's ability to simulate rainfall attributes over the eastern escarpment region of South Africa. CCAM was applied at resolutions typical of GCMs (200 km), RCMs (50 km) and at meso-scale resolutions of 8 km in the horizontal. All the simulations were performed for several decades in length, towards identifying systematic errors.

As part of research objective 1, verifying the ability of CCAM to simulate synoptic-scale pattern over southern Africa, the present day CCAM-AMIP (200 km resolution) and CCAM-NCEP (50 km resolution) simulations of southern Africa climate were performed using CCAM. The model was set up on the CHPC where all the model simulations were performed. In the AMIP simulations, the model was forced at its lower boundary with observed sea-surface temperatures (SSTs) and sea-ice, with the model atmosphere free to respond to this forcing. In the NCEP simulations, the model was similarly forced at its lower boundary with SSTs and sea-ice patterns, but with additional synoptic-scale atmospheric

forcing applied every six hours. That is, in these simulations the atmospheric circulation patterns closely resembles the observed patterns at the synoptic-scale which provides an opportunity to examine how well the model simulates the convective rainfall patterns that occur in association with these circulation fields i.e.:

- The meridional movement of the ITCZ-induced rainfall bands over southern Africa are captured realistically;
- The observed dry slot that extends eastward at 20 °S from eastern Botswana to Limpopo and southern Zimbabwe during summer is realistically represented in the simulations;
- The west-east rainfall gradient that exists over South Africa annually and during summer is present in the CCAM simulations;
- The presence of the observed rainfall band linking southern Africa to the tropics that is indicative of the occurrence of TTT induced cloud bands is present in the CCAM simulations;
- The climate variability, SD, from CCAM-NCEP and CCAM-AMIP is well captured;
- The pattern correlation for all time scales between the simulations and observations is high, especially for CCAM-NCEP that for the most part outperforms CCAM-AMIP.

The second objective is to evaluate the CCAM simulations of rainfall over complex orography. The following is evident from the CCAM-AMIP 200 km resolution and CCAM-NCEP 50 km resolution simulations when compared to the observational data:

- The onslaught of the rainfall season seen in the intra-annual rainfall cycle is captured well over eastern and north eastern South Africa. However, observations show the rainfall maximum for LES, ESA and NESA to be in January compared to the December maximum in the simulations;
- The CCAM-NCEP rainfall simulations display skill in representing the observed inter-annual variability in rainfall over eastern and north eastern South Africa.

However, a few shortcomings have also been identified in that:

- Rainfall totals are severely overestimated over the eastern escarpment of southern Africa indicating inadequate parameterisation of deep convection that occurs over the mountains;
- The influence topography has on the circulation patterns, such as the strong ascent of moist air influences rainfall over the eastern escarpment of South Africa and Lesotho, are not fully captured;

- The simulated rainfall over LES, ESA and NESA peaks in November (CCAM-AMIP) and December (CCAM-NCEP) which is not the case in the observed rainfall maximum in January;
- The intra-annual cycle in rainfall is overestimated, from May to December, especially over LES where the orography is at its steepest.

The results do show that CCAM is able to simulate different synoptic-scale rainfall regimes over SAT realistically. However, rainfall over the escarpment of Lesotho was found to be problematic to portray realistically. Large simulated positive rainfall biases are associated with the steep orography that induces rainfall over the eastern escarpment regions including Lesotho. This result prompted performing high resolution simulations over Lesotho (research objectives 3 and 4).

For research objective 3, use the CCAM to perform high resolution (8 km) rainfall simulations over the eastern escarpment of South Africa, ERA reanalysis data was downscaled to an 8 km resolution over the eastern escarpment of South Africa and Lesotho, using CCAM in stretched grid mode. The model was set up on the CHPC where all the model simulations were performed for the period 1979-2005. The simulations (research objective 4) show:

- That the eastern parts of the escarpment in Kwa-Zulu Natal are generally wetter than the western parts of the escarpment over the Free State. This result is in strong agreement with what is seen with the observations – the model does well in portraying the meso-scale gradients in rainfall over Lesotho. However, there are very large biases north-east of Lesotho with rainfall totals overestimated by a factor of three compared to the observed totals from SAWS rainfall stations;
- A noteworthy feature in the simulated rainfall over Lesotho is the occurrence of a strip of high rainfall totals, stretching from the north of Lesotho to the central parts. The TRMM data suggest that this feature may be real, but the station network does not resolve the feature. Further work is needed to establish whether this feature is real, if so, to explore the underlying circulation dynamics;
- A well-defined west-east gradient in rainfall is present over the eastern escarpment of South Africa even though this gradient is not present in the TRMM data. That raises questions about the validity of the observed dataset over steep orography. The simulations capture the west-east rainfall gradient remarkably well;
- An increase in rainfall with altitude is not present in the SAWS or CRU data above 2100 m on the eastern side of the escarpment whereas CCAM show large increases in rainfall above 1700 m up to 2400 m Jury (2012) show that the overestimation found on

the eastern escarpment is due to too strong uplift that consequently creates higher simulated rainfall totals and this might very well be a factor within CCAM;

- A very low pattern correlation compared to TRMM for all time scales whereas there exist a clear pattern correlation with CRU;
- The model climate to be too variable over all the time scales (SD at least a factor of 2 larger than the observations);
- The diurnal cycles from CCAM to have a clear distinction between the time of day and the location where rainfall occurs. Rainfall on the western side of the escarpment is mostly simulated to fall in the afternoon and early evening (14h-20h) whereas rainfall on the eastern escarpment fall in the evening over a bigger area of the domain and in the early parts of the morning. The simulated diurnal rainfall cycle on the eastern side of the escarpment does, however, not compare well with SAWS stations that show the rainfall maximum to be in the afternoon and early evening. It is also on this side of the escarpment that rainfall is unrealistically represented with overestimation in the order of five to six times that of the SAWS stations. Overall CCAM does well in simulating rainfall at such a high resolutions over the eastern escarpment of South Africa that has proven to be problematic at lower resolutions. CCAM simulates too strong convection that can be a result of exaggerated uplift in the model's convection scheme that influences all the time scales especially on the eastern side of the escarpment. Further investigation into the analysis of different types of convection schemes is needed to understand how rainfall is simulated over steep orography and which dynamical and physical processes is the cause for the overestimations.

References

Andrews, W. R. H. and L. Hutchings, 1980: Upwelling in the southern Benguela Current. *Prog. in Oceanog.*, ***9*(1)**, 1-81.

Blamey, R.C., and C.J.C. Reason, 2009: Numerical simulation of a mesoscale convective system over the east coast of South Africa. *Tellus* **61A,** 17–34.

Bopape, M.J., F.A. Engelbrecht, D.A. Randall and W.A. Landman, 2013: Simulating suppressed and active convection periods during TOGA COARE.

Bopape, M.J., F.A. Engelbrecht, D.A. Randall and W.A. Landman, 2014: Simulations of an isolated two-dimensional thunderstorm: Sensitivity to cloud droplet size and the presence of graupel. *Asia-Pacific J. of Atmos. Sci.*, **50(2)**, 139-151.

Cerlini, P.B., K.A. Emanuel and E. Todini, 2005: Orographic effects on convective precipitation and space-time rainfall variability: preliminary results. *Hyd. and Earth System Sci. Disc.*, ***9*(4)**, 285-299.

Cook, K.H., 2000: The south Indian convergence zone and in-terannual rainfall variability over southern Africa. *J. of Clim.*, **13**, 3789–3804.

D'Abreton, P.C., and P.D. Tyson, 1995: Divergent and non-divergent water vapour transport over southern Africa during wet and dry conditions. *Meteor. Atmos. Phys.,* **55,** 47–59.

D'Abreton, P.C., and P.D. Tyson, 1996: Three-Dimensional Kinematic Trajectory Modelling of Water Vapour Transport over Southern Africa. *Water SA,* **22,** 297–305.

Dai, A., K.E. Trenberth, 2004: The diurnal cycle and its depiction in the community climate system model. *J. of Clim,* **17**, 930–951.

Davies, T., M.J.P. Cullen, A.J. Malcolm, M.H. Mawson, A. Staniforth, A. A. White, and N. Wood, 2005: A new dynamical core for the Met Office's global and regional modelling of the atmosphere. *Roy. Meteorol. Soc.*, **131**, 1759-1782.

Dinku, T., P. Ceccato, E. Grover-Kopec, M. Lemma, S.J. Connor and C.F. Ropelewski, 2007: Validation of satellite rainfall products over East Africa's complex topography. *Int. J. of Remote Sensing*, **28(7)**, 1503-1526.

Engelbrecht, F.A., 2005: Simulations of climate and climate change over southern and tropical Africa with the conformal-cubic atmospheric model. In *Clim. Change and Water Res. in SA*: *Studies on scenarios, impacts, vulnerabilities and adaptation,* ed. R.E. Schulze, chap. 4, pp. 57–74. WRC Report 1430/1/05. Water Research Commission, Pretoria.

Engelbrecht, F.A., 2006: Theory and application of quasi-elastic equations in terrain-following coordinates based on the full pressure field. Ph.D. thesis, University of Pretoria, South Africa.

Engelbrecht, F.A., C.J. deW. Rautenbach, and J.J. Katzfey, 2002: January and July climate simulations over the SADC region using the limitedarea model DARLAM. *Water SA,* **28**, 361–374.

Engelbrecht, F.A., J.L. McGregor, and C.J. Engelbrecht, 2009: Dynamics of the Conformal-Cubic Atmospheric Model projected climate-change signal over southern Africa. *Roy. Meteorol. Soc.,* **29,** 1013-1033

Engelbrecht, F.A., J.L. McGregor and C. J. deW. Rautenbach, 2007: On the development of a new nonhydrostatic atmospheric model in South Africa. *SA J. of Sci.,* **103**, 127-134.

Engelbrecht, F.A., W.A. Landman, C.J. Engelbrecht, S. Landman, M.M. Bopape, B. Roux, J.L. McGregor, and M. Thatcher, 2011: Multi-scale climate modelling over Southern Africa using a variable-resolution global model. *Water SA*, **37**, 647-658.

Garstang, M., B.E. Kelbe, G.D. Emmitt and W.B. London, 1987: Generation of convective storms over the escarpment of northeastern South Africa. *Mon. Weather Rev.*, **115,** 429–443.

Gates, W.L., 1992: AMIP: The atmospheric model intercomparison project. *Bulletin of the American Meteorol. Soc.*, ***73*(12)**, 1962-1970.

Giorgi, F.and X. Bi, 2000: A study of internal variability of a regional climate model. *J. of Geophys. Res.: Atmos. (1984–2012)*, **105(D24)**, 29503-29521.

Giorgi, F. and L.O. Mearns, 1991: Approaches to the simulation of regional climate change: a review. *Rev. of Geophys.*, ***29*(2)**, 191-216.

Harrison M.S.J., 1984: A generalized classification of South African summer rain-bearing synoptic systems. *Int. J. of Clim*, **4,** 547–560.

Hart, N.C.G., C.J.C. Reason, and N. Fauchereaun, 2010: Tropical-Extratropical Interactions over Southern Africa: Three Cases of Heavy Summer Season Rainfall. *Mon. Weather Rev*., **138,** 2608-2623

Hernandez-Diaz, L., R. Laprise, L. Sushama, Martynov, K. Winger, and B. Dugas, 2013: Climate simulation over CORDEX Africa domain using the fifth-generation Canadian Regional Climate Model (CRCM5). *Clim. Dyn.,* **40,** 1215-1433.

Hewitson, B., C. Lennard, G. Nikulin and C. Jones, 2012: CORDEX-Africa: a unique opportunity for science and capacity building. CLIVAR Exchanges 60, International CLIVAR project office, Southampton, UK, 6-7

Hohenegger, C., L. Schlemmer and L. Silvers, 2015: Coupling of convection and circulation at various resolutions. *Tellus A*, **67**.

Houze, R.A., S.A. Rudledge, M.I. Biggerstaff, and B.F. Smull, 1989: Interpretation of Doppler Weather Radar Display of Midlatitude Mesoscle Convective Systems. *American Met. Soc.*, **70**, 608-619.

Hynman, R.J., and A.B. Koehler, 2006: Another look at the measure of forecast accuracy. *Int. J. of. Forecasting*, 679-888.

IPCC, 2013: Climate Change 2013. The Physical Science Basis. http://www.ipcc.ch/report/ar5/wg1

Janjic, Z.I., J.P. Gerrity Jr and S. Nickovic, 2001: An alternative approach to nonhydrostatic modeling. *Mon. Weather Rev.*, ***129*(5)**, 1164-1178.

Jury, M.R., 2012: An intercomparison of model-simulated east-west climate gradient over South Africa. *Water SA*, vol. **38**. ISSN: 1816-7950

Kalognomou, E-A, C. Lennard, M. Shongwe, I. Pinto, A. Favre, M. Kent, B. Hewitson, A. Dosio, G. Nikulin, H-J. Panitz and M. Büchner, 2013: A diagnostic evaluation of precipitation in CORDEX models over Southern Africa. *Int. J. of Climatol, doi*: 10.1175/jcli-d-12-00703.1

Kim, J., D.E. Waliser, C. Mattmann, C.Goodale, A. Hart, P. Zimdars, D. Crichton, C. Jones, G. Nikulin, B. Hewitson, C. Jack, C. Lennard and A. Favre, 2014: Evaluation of the CORDEX-Africa multi-RCM hindcast: systematic model errors. *Clim. Dyn.*, ***42***, 1189-1202

Landman, S., F.A. Engelbrecht, C.J. Engelbrecht, L.L. Dyson and W.A. Landman, 2012: A short-range weather prediction system for South Africa based on a multi-model approach. *Water SA*, **38(5),** 765-774.

Landman, W.A. and A. Beraki, 2012: Multi-model forecast skill for mid-summer rainfall over southern Africa. *Int. J. of Climatol*, ***32***, 303-314.

Landman, W.A., D. DeWitt, D-E. Lee, A. Beraki and D. Lotter, 2012: Seasonal rainfall prediction skill over South Africa: 1- vs. 2-tiered forecasting systems. *Weather Forecast.* **27,** 489-501.

Lennard, C., 2014: Simulating an Extreme Wind Event in a Topographically Complex Region. Boun. Layer Meteorol., **153(2)**, 237-250.

Lyons, S.W., 1991: Origins of convective variability over equatorial southern Africa during austral summer. *Int. J. Climatol*, **4**, 23–39.

Malherbe, J., F.A. Engelbrecht and W.A. Landman, 2013: Projected changes in tropical cyclone climatology and landfall in the Southwest Indian Ocean region under enhanced anthropogenic forcing. *Climate dynamics*, ***40***, 2867-2886.

Mason, S.J., 1995: Sea-surface temperature – South African rainfall associations, 1910–1989. *Int. J. of Climatol.,* **15**,119–135.

Mason, S.J., and M.R. Jury, 1997: Climatic Change and Variability over Southern Africa: A Reflection on Underlying Processes. *Prog. Phys. Geog,.* **21,** 23–50.

Mavume, A.F., L. Rydberg, M. Rouault, J.R.E. Lutjeharms, 2009: Climatology and landfall of tropical cyclones in the southwest Indian Ocean. *WIO J. of Mar. Sci.*, **8(1)**,15–36.

McGregor, J.L., 1996: Semi-Lagrangian advection on conformal-cubic grids. *Mon. Weather Rev*., **124,** 1311-1322.

McGregor, J.L., 1997: Regional Climate Modelling. *Meteorol. Atmos. Phys*., **63**, 105-117.

McGregor, J.L., 2005a: Geostrophic adjustment for reversibly staggered grids. *Mon. Weather Rev.,* **133,** 1119-1128.

McGregor , J.L., 2005b: C-CAM: Geometric aspects and dynamical formulation. CSIRO Atmospheric Research Tech. Paper No. 70. 43 pp.

McGregor, J.L., and M.R. Dix, 2001: The CSIRO conformal-cubic atmospheric GCM. In: Hodnett PF (ed.) *Proc. IUTAM Symposium on Advances in Mathematical Modelling of Atmos. and Ocean Dyn.*. Kluwer, Dordrecht. 197-202.

McGregor, J.L., and M.R. Dix, 2008: An updated description of the Conformal-Cubic Atmospheric Model. In: Hamilton K and Ohfuchi W (eds.) *High Resolution Simulation of the Atmos. and Ocean*. Springer Verlag. 51-76.

McGregor, G.R. and S. Nieuwolt, 1998: Tropical climatology: an introduction to the climates of the low latitudes (No. Ed. 2). John Wiley & Sons Ltd.

New, M., M. Hulme, and P. Jones, 1999: Representing twentieth-century space-time climate variability. Part I: Development of a 1961-90 mean monthly terrestrial climatology. *J. of Clim.*, ***12*****(3)**, 829-856.

Nicholson, S.E. and J. Kim, 1997: The relationship of the El Nino-Southern oscillation to African rainfall. *Int. J. of Climatol.*, **17(2)**, 117-135.

Nickless, A., T. Ziehn, P.J. Rayner, R.J. Scholes and F. Engelbrecht, 2015: Greenhouse gas network design using backward Lagrangian particle dispersion modelling–Part 2: Sensitivity analyses and South African test case. *Atmos. Chemistry and Phys.*, ***15*****(4)**, 2051-2069.

Nikulin, G., F. Giorgi, G. Asrar, M. Bushner, R. Cerezo-Mota, O.B. Christensen, M. Deque, J. Fernandez, A. Hansler, and E. van Meijngaard, 2012: Precipitation Climatology in an ensemble of CORDEX-Africa Regional Climate Simulations. *Int. J. Clim,* **25,** 6057-6078.

Ohfuchi, W., H. Sasaki, Y. Masumoto and H. Nakamura, 2005: Mesoscale resolving simulations of the global atmosphere and ocean on the Earth Simulator. *EOS Trans. AGU,* **86**, 45–46.

Palmer, P.I., E. Heifetz, M.C. Todd and R. Washington, 2004: The meridional flux of angular momentum during major tropical–temperate rainfall events over southern Africa. *Clim. Dyn*.

Pearson, K. J., G.M.S. Lister, C.E. Birch, R.P. Allan, R.J. Hogan and S.J. Woolnough, 2014: Modelling the diurnal cycle of tropical convection across the 'grey zone'. *Q. J. of Roy. Met. Soc.*, **140**, 491-499.

Pohl, B., M. Rouault and S.S. Roy, 2014: Simulation of the annual and diurnal cycles of rainfall over South Africa by a regional climate model. *Clim. Dyn.*, ***43*(7-8)**, 2207-2226.

Ratna, S.B., J.V. Ratnam, S.K. Behera, C.J. Rautenbach, T. Ndarana, K. Takahashi and T. Yamagata, 2013: Performance assessment of three convective parameterization schemes in WRF for downscaling summer rainfall over South Africa. *Clim, Dyn*., (on line). doi:10.1007/s00382-013-1918-2

Reason, C.J.C., S. Hachigonta and R.F. Phaladi, 2005: Interannual variability in rainy season characteristics over the Limpopo region of southern Africa. *Int. J. of Climatol.*, ***25*(14)**, 1835-1853.

Reason, C.J.C. and D. Jagadheesha, 2005: A model investigation of recent ENSO impacts over southern Africa. *Meteor. and Atmos. Phys.*, ***89*(1-4)**, 181-205.

Reason, C.J.C., W. Landman, and W. Tennant, 2006: Seasonal to decadal prediction of southern African climate and its links with variability of the Atlantic Ocean. *Bull. Amer. Meteor. Soc.,* **87,** 941–955.

Reason, C.J.C. and H. Mulenga, 1999: Relationships between South African rainfall and SST anomalies in the southwest Indian Ocean. *Int. J. of Climatol.*, ***19*(15)**, 1651-1673.

Rouault, M. and Y. Richard, 2003: Intensity and spatial extension of drought in South Africa at different time scales. W*ater SA*, ***29*(4)**, 489-500.

Rouault, M., S.S. Roy and R.C. Balling, 2013: The diurnal cycle of rainfall in South Africa in the austral summer. *Int. J. of Climatol.*, **33(3)**, 770-777.

Rouault, M., S.A. White, C.J.C. Reason, J.R.E. Lutjeharms and I. Jobard, 2002: Ocean-atmosphere interaction in the Agulhas Current region and a South African extreme weather event. *Weather and Forecasting*, ***17*(4)**, 655-669.

Riphagen, H.A., 1984: *The implementation of a split explicit weather prediction model for the Southern Hemisphere.* M.Sc. dissertation, University of Pretoria, South Africa.

Riphagen, H.A., and J. Van Heerden, 1986: Comparative trials of a semi-Lagrangian advection scheme in a numerical weather prediction model. In *Proc. 12th SA Symposium on Numerical Mathematics, Umhlanga Rocks,* pp. 139–153.

Singleton, A.T. and C.J.C. Reason, 2007: A numerical model study of an intense cutoff low pressure system over South Africa. *Mon. Weather Rev.*, ***135*(3)**, 1128-1150.

Shen, B.W., R. Atlas, J.D. Chern, Q. Reale, S. J. Lin, T. Lee and J. Chang, 2006: The 0.125 degree finite-volume general circulation model on the NASA Columbia supercomputer: preliminary simulations of mesoscale vortices. *Geophys. Res. Lett.,* **33**, L05801, doi:10.1029/2005GL024594.

Tadross, M.A., W.J. Gutowski Jr, B.C. Hewitson, C. Jack and M. New, 2006: MM5 simulations of interannual change and the diurnal cycle of southern African regional climate. *Theor. and applied climatol.*, **86(1-4)**, 63-80.

Taljaard, J.J., 1986: Change of rainfall distribution and circulation pattern over southern Africa in summer. *J. of Clim.,* **6,** 579-592.

Thatcher, M., and J.L. McGregor, 2009: Using a scale-selective filter for dynamical downscaling with the conformal cubic atmospheric model. *Mon. Weather Rev.,* **137,** 1742-1752.

Thatcher, M., and J.L. McGregor, 2010: A technique for dynamically downscaling daily-averaged GCM datasets over Australia using the Conformal Cubic Atmospheric Model. *Mon. Weather Rev.,* **139,** 79-95.

Thatcher, M., and McGregor, J.L. 2011: A technique for dynamically downscaling daily-averaged GCM datasets using the conformal cubic atmospheric model. *Mon. Weather Rev.,* ***139*****(1)**, 79-95.

Todd, M., and R. Washington, 1999: Circulation anomalies associated with tropical-temperate troughs in southern Africa and the south west Indian Ocean. *Clim. Dyn.*, ***15*****(12)**, 937-951.

Todd, M. C., R. Washington and P.I. Palmer, 2004: Water vapour transport associated with tropical–temperate trough systems over southern Africa and the southwest Indian Ocean. *Int. J. of Climatol.*, ***24*****(5)**, 555-568.

Triegaardt, D.O., 1965a: Experimental barotropic forecasting over subtropical regions. *Notos* **14**, 3–15.

Triegaardt, D.O., 1965b: The application of dynamic methods of weather prediction to the South African forecasting problem: a progress report. *SA Weather Bureau News Lett.,* **201**, 187–188.

Tyson, P.D. and R.A. Preston-Whyte, 2000: weather and climate of southern Africa. Oxford University Press.

Tyson, P.D., 1986: Climatic Change and Variability over Southern Africa, Oxford University Press, Cape Town, p. 220

Tyson, P.D., and R.A. Preston-Whyte, 2000: The Weather and Climate of South Africa. Oxfort University Press

van der Beek, P., M.A. Summerfield, J. Braun, R.W. Brown and A. Fleming, 2002: Modeling postbreakup landscape development and denudational history across the southeast African (Drakensberg Escarpment) margin. *J. of Geophys. Res.: Solid Earth (1978–2012)*, **107**, ETG-11.

Walsh, K., and J.L. McGregor, 1995: January and July climate simulations over the Australian region using a limited area model. *J. of Clim.,* **8,** 2387-2403.

Wang, Y., L. Zhou and K. Hamilton, 2007: Effect of convective entrainment/detrainment on the simulation of the tropical precipitation diurnal cycle*. *Mon. Weather Rev.*, ***135*****(2)**, 567-585.

Washington, R. and A. Preston, 2006: Extreme wet years over southern Africa: Role of Indian Ocean sea surface temperatures. *J. of Geophys. Res.: Atmos (1984–2012)*, **111**.

White, A.A., and R.A. Bromley, 1995: Dynamically consistent, quasi-hydrostatic equations for global models with a complete epresentation of the Coriolis force. *Q. J. Roy. Met. Soc.* **121**, 399–418.

Yang, G.Y., and J. Slingo, 2001: The diurnal cycle in the Tropics. *Mon. Weather Rev*., **129,** 784–801.

Yuan, C., T. Tozuka, W.A. Landman and T. Yamagata, 2014: Dynamical seasonal prediction of Southern African summer precipitation. *Clim. Dyn.*, **42**, 3357-3374.

Addendums

Permission that manuscript can be submitted for degree purposes

February 9, 2015

To whom it may concern

Dear Sir/Mam

I, Jacobus van der Merwe, the undersigned, co-author of the manuscript,

> **Dedekind, Z, F.A. Engelbrecht and J. van der Merwe, 2014:** Model simulations of rainfall over southern Africa and its eastern escarpment

herewith give permission that this manuscript can be submitted as part of Zane Dedekind's MSc thesis. Zane Dedekind's contributions to this manuscript include:

1. Research into convective rainfall over southern Africa;
2. Design of the CCAM model runs;
3. Running the model at the CHPC;
4. Design of the statistical methods and;
5. Write-up of the paper

Sincerely,

Jacobus van der Merwe

jhvdmerwe@csir.co.za